8-2011

Magnetic Field Dependent Electroluminescence and Charge Transport in Organic Semiconductors

Ming Shao
mshao2@utk.edu

To the Graduate Council:

I am submitting herewith a dissertation written by Ming Shao entitled "Magnetic Field Dependent Electroluminescence and Charge Transport in Organic Semiconductors." I have examined the final electronic copy of this dissertation for form and content and recommend that it be accepted in partial fulfillment of the requirements for the degree of Doctor of Philosophy, with a major in Materials Science and Engineering.

Bin Hu, Major Professor

We have read this dissertation and recommend its acceptance:

Roberto S. Benson, Syed Islam, Shanfeng Wang, Ilia N. Ivanov

Accepted for the Council:
Dixie L. Thompson

Vice Provost and Dean of the Graduate School

(Original signatures are on file with official student records.)

Magnetic Field Dependent Electroluminescence and Charge Transport in Organic Semiconductors

A Dissertation Presented for
the Doctor of Philosophy Degree
The University of Tennessee, Knoxville

Ming Shao
August 2011

Dedication To My Parents

&

My Wife Huiming Yu

I dedicate my work to you.

ACKNOWLEDGEMENTS

First, I am deeply thankful to my advisor, Dr. Bin Hu for his five years guidance and valuable suggestions about my research work and dissertation. I acquired my theoretical and practical laboratory knowledge from him. Without his guidance and support, I could not finish my thesis. Also I would like to thank my committee members, Dr. Roberto Benson, Dr. Shanfeng Wang, Dr. Syed Islam and Dr. Ilia N. Ivanov, for their instructive advice and great support.

I must thank my collaborators at the Oak Ridge National Laboratory (ORNL) for their help in providing facilities and many helpful discussions. They are Dr. David B. Geohegan, Dr. Ilia Ivanov, Dr. Kai Xiao, Dr. Matthew Gartett, Dr. Chengjun Sun.

I would also like to thank my present and former colleagues in our lab. Liang Yan , Huidong Zang, Lili Wu, Jaime Sullivan, Dr. Yue Wu, Dr. Zhihua Xu, Dr. Youzhi Wu, Dr. Tho Nguyen, Dr. Xinjun Xu and Dr. Lianbin Niu have given numerous contributions and help to my research work.

Finally, I particularly thank my wife Huiming Yu, my parents and parents in law for their great understanding, support and encouragements to me during these years.

ABSTRACT

It has been found that a small magnetic field (<300 mT) can substantial change the electroluminescence, photoluminescence, photocurrent, electrical injection current in nonmagnetic organic semiconductors. It is generally believed that these magnetic field effects (MFE) are related to the spin dependent processes in organic semiconductor. However, the origin of MFE is still not well understood. In this dissertation, we investigate the underlying mechanism for magnetic field effects on electroluminescence (MFE_{EL}) and magnetoresistance (MR) and demonstrate the complete tuning of MFE_{EL} and MR based on our theoretical understanding.

We consider MFE arising from magnetic field sensitive intersystem crossing (ISC) and triplet charge reaction. Magnetic field can increase the singlet ratios through ISC, accounting for positive $MFE_{EL.}$ Magnetic field modulated ISC strongly depends on the electron-hole pair separation distance. MFE can be enhanced by increasing the electron hole pair distance through material mixing and interplaying the electric dipole-dipole interaction. Meanwhile, two possible mechanisms corresponding for negative MFE_{EL}: triplet-triplet annihilation and triplet charge reaction are also discussed. The negative MFE_{EL} is achieved through adjusting triplet density charge confinement and exciton/charge ratio, which indicates that triplet charge reaction is a dominate process accountable for negative $MFE_{EL.}$

Significant MR and MFE_{EL} are observed in strong spin orbital coupling iridium complex based OLED device after introducing the non-magnetic insulating blocking PVA layer. A possible mechanism for this new interface induced MR and MFE_{EL} is

proposed based on magnetic field perturbed spin-spin interaction at short capture distance of inter-charge carriers. The comparative study of two strong spin orbital coupling materials $Ir(ppy)_3$ and $Ir(ppy)_2(acac)$ with different electrical dipole moments indicate the electric dipole-dipole interaction can change MR and MFE_{EL} from short distance capture based regime to long distance intersystem-crossing regime.

At last, we demonstrate the fully tuning sign of magnetic field effect on the fluorescence (MFE_{FEL}) and phosphorescence (MFE_{PEL}) by using the ISC, energy transfer and spin-spin interaction. In addition, we demonstrate a giant MFE_{EL} (400%) in electrochemical cells and attribute this giant MFE_{EL} to Lorentz force driven ion transport and Lorentz force dependent diffusion layer thickness through convection.

TABLE OF CONTENTS

LIST OF FIGURES

CHAPTER1 INTRODUCTION

1.1 Organic semiconductor

Organic materials, such as plastic and rubber, are usually considered as electrical insulating materials due to a wide band gap. However, this traditional view point was totally challenged by the discovery of the conducting polymer. A. J. Heeger, Alan MacDiarm and Hideki Shirakawa changed the conductivity of polymer over the full range from insulator to metal by chemical doping or by electrochemical doping on 1970s and thus won the Nobel prize in Chemistry 2000. In general, organic semiconducting materials can be divided into two categories based on its molecular weight, namely small molecular and conjugated polymer. Both small molecular and polymer contain the conjugated structure.

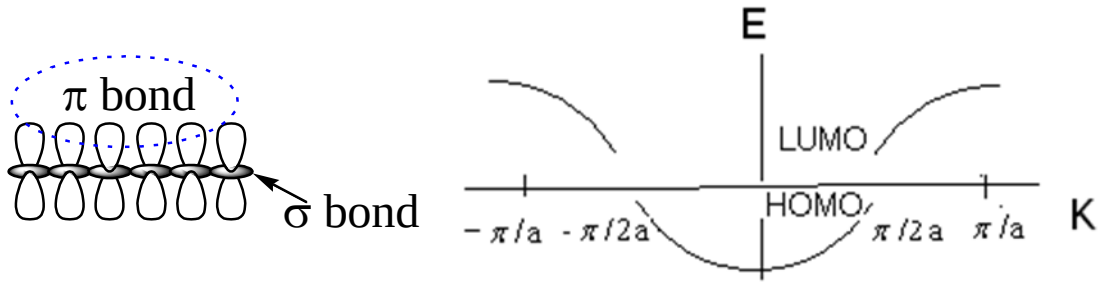

Figure 1.1 (a) Schematic view of electronic orbital of conjugated polymer backbone (b) Band structure of organic semiconductor

Due to the configuration of alternating single and double bonds along the backbone of organic molecular, the P_z orbital of each carbon atom, which is perpendicular to the backbone, will overlap each other and form π bond, leading to the delocalized electron

cloud with a periodic alternating density over the whole molecule. The overlap of P_z orbital forms the bonding π orbitals and antibonding π^* orbitals, namely the highest occupied molecular orbitals (HOMO) and lowest unoccupied orbitals (LUMO)[1,2].

To analog with traditional inorganic semiconductor, the HOMO and LUMO are also named as low-energy valence band (VB) and high energy conduction bands (CB). The new generation of organic semiconducting materials do not only exhibit the electrical and optical properties of metals or semiconductors but also keep the advantage of organic material such as light weight and flexible. Therefore, the discovery and development of organic semiconductor opens a new area for organic electronics and organic optoelectronics, aiming to produce low cost, large scale, flexible semiconductor device, such as the organic light emitting diode (OLED)[3,4], organic photovoltaic (OPV)[5,6] and organic thin film transistor (OTFT)[7,8]etc al.

1.2 Organic light emitting diode (OLED)

OLED was one of the extensive studied organic semiconductor devices and the first successful commercialized organic semiconductor device in flat panel display. Many companies such as Kodak, Dupont, Philips, SONY, LG, Samsung et al have demonstrated their OLED applications in mobile phone and TV. Recently, Samsung has claimed that the OLED will be the trend of next generation display technology. First, let us briefly review the history of OLED development. Organic electroluminescence phenomenon was first observed in organic single crystal in 1960s. The OLED research was initially stimulated by the pioneer work of C. W. Tang[3] in Kodak, who first achieved

the low voltage driving and luminescence efficiency by evaporating appropriate small molecules to introduce a novel double-layer structure. Short after, the Cambridge group of Friend also demonstrate the first semiconducting polymer: poly (p-phenylene vinylene) (PPV) based OLED in 1990[9]. To overcome the insolubility issue of PPV, the Heeger group synthesized the soluble PPV derivative, poly (2-methoxy-5-(2'-ethyl-hexoxy)-p-phenylene vinylene) (MEH-PPV), and form the polymer based OLED by using the solution based spin-coating method[10].

1.2.1 Device structure of OLED

Next, we introduce the basic device structure of OLED as shown in Figure 1.2. The simplest OLED has a sandwiched structure: a light emitting layer suited between two electrodes. The transparent indium tin oxide (ITO) film is used as anode for the hole injection and light output. Different low work function metals or alloy such as Ca, LiF/Al, Mg/Ag are employed as cathode to facilitate the electron injection into light emission layer. However, the single layer OLED usually do not exhibit high efficiency. The reason is due to the unbalanced electron and hole injection and transport. Therefore, people usually construct multilayer device structures to facilitate the electron and hole injection, and balance the electron hole recombination, aiming to improve the device efficiency.

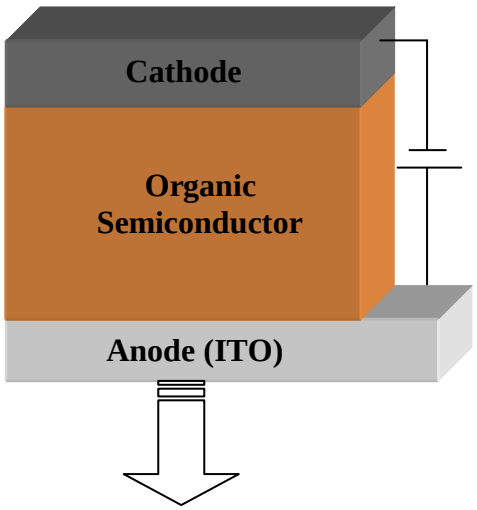

Figure 1.2 Device structure of a typical OLED

1.2.2 Working principle of OLED

In general, the working mechanism of OLED can be divided into four separate steps shown in Figure 1.3: (1) charge carrier injection from the electrode (2) charge carrier transport under the applied voltage (3) the recombination of electron and hole followed by radiative and non-radiative decay of excited states.

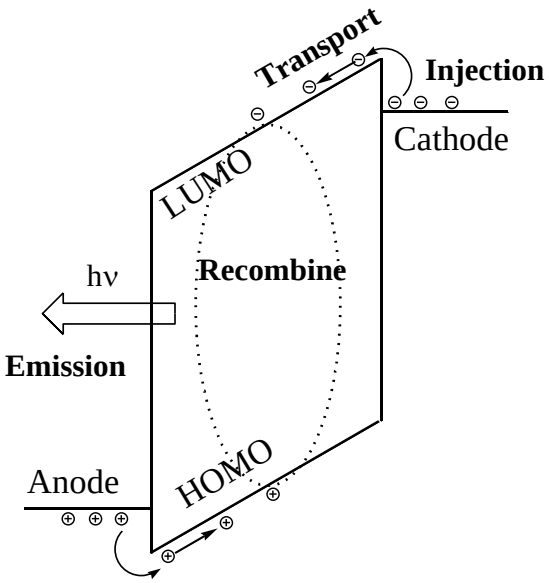

Figure 1.3 The working principles of OLED. Three different steps: charge injection, charge transport and charge recombination

1.2.2.1 Charge injection

The typical thickness of OLED is on the order of 100 hundred nm. The electric field across the OLED is very high ~10^6 V/cm even applying several volts bias. Under this high electrical field, the holes can overcome the energy barrier between the workfunction of ITO and the HOMO of the organic semiconductor, and inject into the HOMO of middle organic semiconductor. Similarly, the electron can overcome the energy barrier near the cathode and inject into the LUMO of the organic semiconductor material. In general, the thermionic injection model or Fowler Nordheim tunneling theory are used to quantitively describe the charge injection in OLED. In thermionic injection, the injected current can be expressed by Equation 1.1[11].

$$J = J_0(e^{\frac{qV_F}{nK_bT}} - 1) \qquad \text{(Equation 1.1)}$$

Where q is the electron charge, V applied voltage, n the ideality factor, and k_b the Boltzman constant. In Fowler Nordheim tunneling theory, the injection current can be calculated by Equation 1.2[12]

$$J = \left(\frac{c}{\phi_B}\right)\left(\frac{V}{d}\right)\exp\left[\frac{-B\Phi_B^{1.5}}{V/d}\right] \qquad \text{(Equation 1.2)}$$

Where $C=q^3/8\pi h$, $B=8\pi(2m^*)^{1/2}/3hq$, m^* is the relative effective mass, V is applied voltage and d is the thickness of the organic film. However, neither thermionic injection or Fowler Nordheim tunneling injection are sufficient to describe the current-voltage characteristics in OLED. Thus, we still need to consider the charge carrier transport process in organic semiconductor film.

1.2.2.2 Charge transport

After injection, the injected electron and hole will drift under the applied electrical field along the HOMO and LUMO of organic light emitting molecules, separately. In contrast to the inorganic semiconductor, the mobility of organic semiconductor is usually low <20 $cm^2V^{-1}s^{-1}$. [13] The reason for the low mobility of organic material is due to the distinct charge transport mechanism. In inorganic semiconductor, the electron and hole can freely move in the conducting band (CB) and valence band (VB) according to band theory. However, the charge carriers in organic semiconductor are not free but localized. Charge carriers can only consecutively hops among small molecule sites or polymer segment in organic semiconductor. Besides, the chemical impurities and structural defects in the

organic film can introduce additional energy level and act as different types of charge traps, which further reduce the charge carrier mobility in organic film. In disordered small molecular systems and polymers, the mobilities are typically between 10^{-5} to 10^{-3} $cm^2V^{-1}s^{-1}$. Due to the low mobility of organic semiconductor, the current in OLED is space charge limited current (SCLC). According to Mott-Gurney principle, the current density can be proportional to the square of the applied voltage shown in Equation 1.3[14]

$$J = \frac{9}{8}\varepsilon\varepsilon_0\mu\frac{V^2}{d^3} \qquad \text{(Equation 1.3)}$$

Where ε and ε_o are the relative and absolute permittivity, μ is overall effective charge carrier mobility, V is the applied voltage and d is the thickness of the device.

1.2.2.3 Charge recombination

Among various types of recombination process, the Langevin type bimolecular recombination is dominant in low mobility organic materials. It occurs when the mean free path for optical phonon emission λ is much smaller than $r_C = (e^2/4\pi\varepsilon\varepsilon_0 kT)$ Coulombic capture radius. The Langevin bimolecular recombination coefficient can be calculated by Equation 1.4[2]

$$\gamma = \frac{q(\mu_n + \mu_p)}{\varepsilon\varepsilon_0} \qquad \text{(Equation 1.4)}$$

where q is the electron charge, μ_n and μ_p are the respective mobility of electron and hole, ε and ε_o are the relative and absolute permittivity. Due to the Coulombic attraction, the electron and hole will first capture together to form a neutral bounded electron hole pair, also namely polaron pair. When the electron and hole are getting closer and locate in a

same molecule, they will eventually form a closely bound electron hole pair, namely exciton. Due to the larger e-h separation distance, the polaron pairs usually have lower binding energy than exciton. It should be noted that the each polaron (electron or hole) has a half integer spin, either spin up or spin down. Therefore, there are four possible spin configurations for a bounded polaron pair and exciton: S_0 (↑↓), T_1(↑↑), T_0(↑↓), T_{-1}(↓↓).

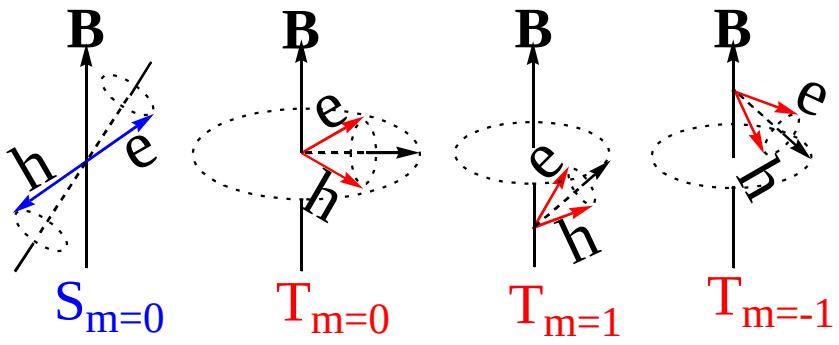

Figure 1.4 Schematic representation of the singlet and triplet states

From the above schematic, we can see the singlet exciton has an anti-parallel spin configuration while the triplet has a parallel configuration. In most stable organic molecules, the HOMO is complete filled and consequently have the singlet character (spin 0) in the ground state. Thus, only the transition from the singlet excited states to singlet ground state is spin allowed according to the Pauli exclude principle, while the transition from triplet excited states to singlet ground state is spin forbidden. The relaxation of singlet exciton from high energy excited states to the low energy ground state will give the radiative emission and generate the fluorescence. Meanwhile, the triplet excitons decay non-radiatively and the released energy will convert into heat

instead of light emission. According to simple spin statistic, it is generally accepted the singlet and triplet exciton ratio is 1:3 under electrical excitation[2,15]. However, the singlet triplet ratio is still in controversy since theoretical and experimental studies suggest that the singlet/triplet ratio may be beyond 1:3 in some conjugate polymer based OLEDs[16,17,18,19].

1.2.3 Efficiency of OLED

Based on above discussed light emission processes, the internal and external quantum efficiency of OLED can be given by Equation 1.5 and Equation 1.6

$$\eta_{\text{int}} = \gamma \chi_{st} q \qquad \text{(Equation 1.5)}$$

$$\eta_{ext} = \eta_{\text{int}} \eta_c \qquad \text{(Equation 1.6)}$$

Where γ is exciton formation fraction of electron hole recombination, χ_{st} is the singlet exciton fraction, q is the efficiency of radiative emission from the singlet exciton and η_c is the light outcoupling fraction. Therefore, the internal quantum efficiency η_{int} of fluorescence based OLED is less than 25% limited by spin conservation. Without the use of any light out-coupling structure, the η_c is around 20% estimated by Fresenl loss($1/2n^2$), assuming reflect indices of organic materials n is 1.6. By multiplying all the factor together, the external quantum efficiency of fluorescence OLED is no more than 5%. Based on the equation, it should be noted that singlet fraction is the most critical factor to limit the final efficiency of OLED. In order to get high efficiency OLED, researchers are trying to make full use of the 75% triplet, which is usually wasted by the non-radiative emission due to strong exciton-phonon coupling. As we pointed out before, the decay of a triplet exciton is generally spin forbidden because of the spin conservation requirement.

However, this spin forbidden transition is partially allowed by introducing heavy metal complex due to its strong spin orbital coupling strength. In this case, although the decay of the triplet state is still slow, the triplet can emit the phosphorescence. Baldo et al. successfully use this concept and demonstrated the high efficiency phosphorescence based OLED by doping the heavy metal complex PtOEP into a charge transport host[20]. Further studies shows that the internal quantum efficiency of phosphorescence OLED can reach nearly 100% with balanced electron hole injection and exciton confinement structure[21,22]. Except utilizing phosphorescent materials, investigators are trying to use alternative methods to control the singlet and triplet ratio in OLED. One exciting idea is to inject spin polarized electrons and holes from ferromagnetic electrodes to form singlet or triplet preferentially, which expect to get 50 % singlet excitons compared to 25% in a normal OLED[23].

1.3 Organic spintronics and magnetic field effects in organic semiconductors

In fact, how to control spin injection and spin transport is also the fundamental issues for spintronics. In comparison with traditional electrons, spintronics do not only control the charge to store or transport information, but also manipulate the electron spin degree of freedom.

1.3.1 Spin orbital coupling and hyperfine interaction

In general, there are two important spin flipping mechanisms to change the electron spin configuration in solid state films. One is the spin orbital coupling (SOC). SOC describes

the interaction between the electron's spin and its orbital motion around the nucleus shown as in Figure 1.5. The magnetic moment μ can interact with the magnetic field B generated by the orbital motion.

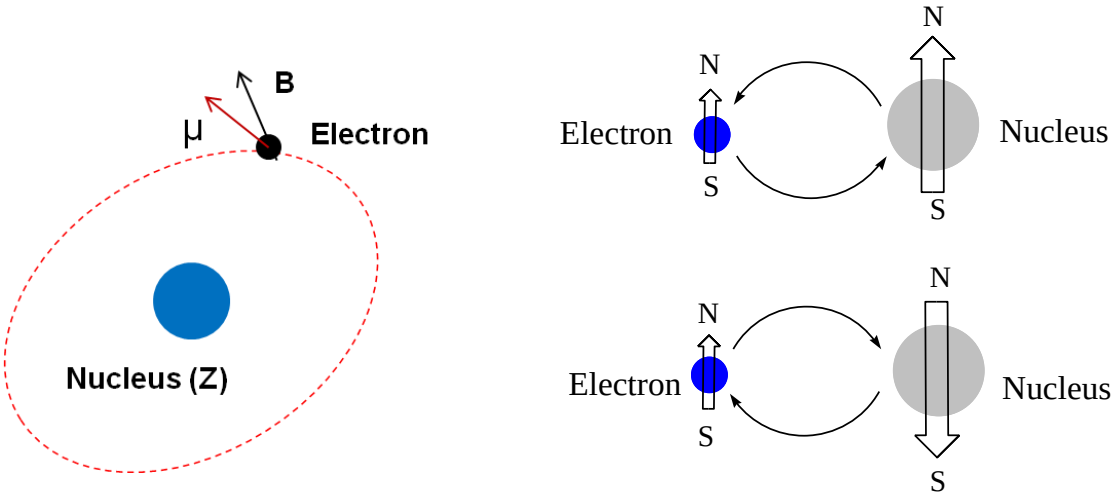

Spin orbital coupling Hyperfine interaction

Figure 1.5 Schematic representation of the spin orbital coupling and hyperfine interaction

The spin orbital Hamiltonian can be expressed by Equation 1.7

$$H_{SOC} = \frac{1}{2m_e c^2 r}\left(\frac{\partial V}{\partial r}\right)\hat{L}\hat{S} = \xi_{n,l}\hat{L}\hat{S} = 2\beta_B\left\langle\frac{Z}{r^3}\right\rangle_{n.l}\hat{L}\hat{S} \qquad \text{(Equation 1.7)}$$

Where $\xi_{n,l}$ is the SOC constant, n is the principle quantum number, l is the orbital angular momentum, L is the orbital momentum operator, S is the electron spin operator, β_e is the Bohr magneton, Z is the nuclear charge and r is the radius between electron and nucleus

It should be noted that SOC strength is proportional to the power 4 of atomic number of the nucleus in hydrogen like atoms. Therefore, the heavy atom can lead to strong SOC.

The other spin flip channel is hyperfine interaction as shown in Figure 1.5. Hyperfine interaction is the interaction between proton nuclear spin and electron spin. The hyper fine Hamiltonian is defined as Equation 1.8:

$$H_{HFI} = a \hat{I} \hat{S} \qquad \text{(Equation 1.8)}$$

Where a is the hyperfine interaction constant, I is the nuclear spin operator and S is the electron spin operator. Many efforts have been put into seeking new materials for spintronics. Compared with commonly used inorganic materials in spintronics, organic semiconductor material appeals to be a promising candidate because the organic material theoretically has long spin relaxation times and long spin diffusion length compared with other semiconductor materials. The reason for this long spin diffusion length is because most organic materials are composed of light weight atoms such as H, O with weak spin orbital coupling (SOC) strength. Lighter atoms have weaker spin orbital coupling. Consequently, the electron spin orientation can be sustained in organic semiconductor material. The combination of organic electronics and spintronics also open a new research field: organic spintronics[24,25].

1.3.2 Magnetic field effect in device with magnetic electrode

Organic spintronics normally employ ferromagnetic electrodes for spin-injection. Xiong et al first demonstrated the giant magnetoresistance (GMR) in vertical organic spin valves device[26]. They employed two ferromagnetic electrodes $La_{0.67}Sr_{0.33}MnO_3$ (LSMO), Cobalt and organic material Alq_3 as space layer. The thickness of middle organic spacer is over 100 nm. They observed the large device resistance change when switching the orientation

of the magnetization of two ferroelectrodes. The GMR result gives direct experimental evidence that the organic semiconductor materials have long spin diffusion length.

1.3.3 Magnetic field effects in device with nonmagnetic electrode

In fact, even before using ferromagnetic electrodes to inject spin polarized charge carriers into organic semiconductors, investigators have already carried a lot of studies on magnetic field effects on kinetics of chemical reactions[27,28]. Recently, there are growing interests in the magnetic field effects in organic semiconductor devices with nonmagnetic electrodes. Frankevich found that the photocurrent in PPV can be enhanced to a few percentages under an external magnetic field[29,30]. Ito studied the magnetic field effects on the charge transfer transient photocurrent and fluorescence in a doped photoconductive polymer films[31]. Kalinowski reported that the electroluminescence intensity and current of tris-(8-hydroxyquinolinato) aluminum (III) (Alq_3) based OLED can be increased up to 5% and 3% respectively by increasing the magnetic field to 300 mT[32]. Almost at the same time, Wohlgenannt group discovered a new large room temperature magnetoresistance phenomenon, namely as organic magnetoresistance (OMAR), both in the polymer and small molecule based organic semiconductor[33,34,35]. Further extensive studies show that OMAR is controlled by the voltage, temperature, the thickness of the semiconducting layer and the device structure[36,37]. Different with the organic spin valve device, OMAR does not require the ferromagnetic electrode and can be easily observed at room temperature and high voltage bias. The question naturally arises “why a low magnetic field can change the photocurrent, photoluminescence, electroluminescence and electrical injection current in nonmagnetic organic semiconducting materials with

nonmagnetic electrode." It is generally believed that these magnetic field effects (MFE) are related to the spin dependent processes in organic semiconductor. However, there are still many controversies about the origin of these magnetic field effects. Many different models have been proposed to explain these MFE results.

1.4 Possible mechanisms of magnetic field effects

In general, there are three major models for the observed MFE. The first one is magnetic field sensitive intersystem crossing (ISC) in the polaron pair before the exciton formation[32,37,38]. The second model considers the spin dependent exciton reaction after the exciton formation. These magnetic field sensitive processes include the exciton exciton reaction and exciton charge reaction[39,40,41]. It should be noted both magnetic field sensitive ISC and reaction occurs at the excited states. The third model is bipolaron model[42,43,44]. In contrast to other two models, the bipolaron model attribute the MFE to the spin dependent transport, which does not necessarily require the presence of the excited states.

1.4.1 Magnetic field sensitive ISC

First, we introduce magnetic sensitive intersystem crossing process. When injected electron and hole reach the Coulombic capture radius, the free electron and hole first proceed through a Coulombic correlated polaron pair. Both spin orbital coupling (SOC) and the hyperfine interaction (HFI) can flip the electron spin orientation, and causes the ISC between singlet state and triplet polaron pair. At zero magnetic field, the singlet and triplet polaron pairs are degenerate because of the negligible exchange energy between

the singlet and triplet polaron pair due to large electron hole separation distance. When an external magnetic field is comparable to the internal magnetic interaction (SOC and hyperfine interaction) strength, triplet polaron pair can be split into three states($^3PP_+$, $^3PP_0$, $^3PP_0$) due to the external Zeeman effect. In this case, only $^3PP_0$ is convertible with singlet $^1PP_0$, and consequently reduce the spin mixing between singlet states and triplet states. Since the conversion from the singlet to triplet polaron pair is partially blocked, magnetic field can enhance the singlet / triplet polaron pair ratio and subsequent final singlet exciton population, leading to a positive magnetic field on the electroluminescence (MFE_{EL})[32]. Furthermore, this positive MFE_{EL} also indicates a new method to improve the fluorescence efficiency of OLED.

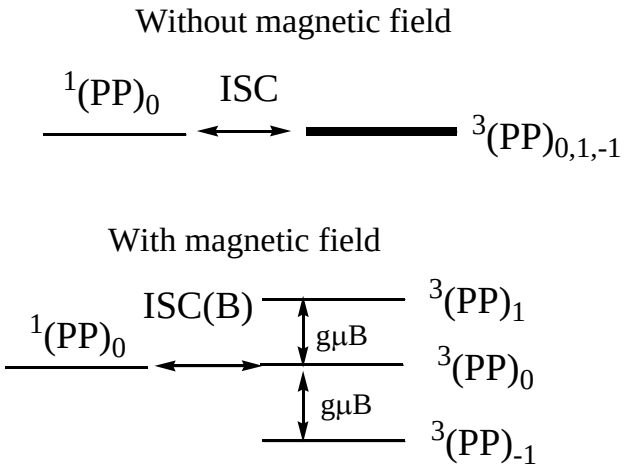

Figure 1.6 Magnetic field sensitive ISC at the polaron pair state

It has been also known that singlet states have larger dissociation rate compared to triplet states because of its ionic nature[19,32,45]. Therefore, the increased singlet state density, caused by the magnetic field modulated ISC, will lead to the increase of device current,

generating negative (- MR). Similarly, magnetic field sensitive ISC can also explain the enhancement of photocurrent very well, namely MFP.

1.4.2 Spin dependent exciton reaction

Next, we discuss the spin dependent exciton reaction. After electrons and holes condense into tightly bounded exciton, exciton will migrate in organic semiconductor describe by a diffusion controlled process. During this process, Exciton will evitably collide with each other, or with the free electron and trapped charge, leading to exciton-exciton interaction and exciton charge interaction. In principle, both singlet and triplet can be involved in the exciton reaction. Due to the longer lifetime of triplet exciton, the triplet-triplet annihilation (TTA) and triplet charge reaction (TCR) are dominant processes in organic semiconductor. In fact, these two annihilation mechanisms are known as major energy loss channels in limiting the final efficiency of OLED and organic laser working at high excitation densities. Moreover, it was reported that TTA and TCR are spin dependent processes in which the reaction constant can be modulated by the external magnetic field[46-49]. TTA can be described by the following Equation 1.9:

$$T + T \underset{k_{-1}}{\overset{k_1}{\rightleftharpoons}} (T..T) \underset{k_{-2}}{\overset{k_2}{\rightleftharpoons}} S + S_0 + h\nu \qquad \text{(Equation 1.9)}$$

Two triplet exciton collide with each other, and fuse into a singlet S at the excited states and a S_0 in ground state. Experimentally, the creation of singlet S will exhibit delayed fluorescence. Here, k_1 is the formation rate of a intermediate (T..T) pair state and k_2 is the TTA rate generating delayed fluorescence. Accordingly, k_{-1} and k_{-2} are their dissociation rates. Depending on the relative spin orientation, intermediate pair state (T..T) will have

nine possible spin states, a pure singlet, two triplet and five quintet. An external magnetic field can mix or split these possible spin states, and consequently change the annihilation rate constant. Since delayed fluorescence is proportional to $\gamma_{TTA,}$ this magnetic field modulated rate constant can be well reflected from the intensity change of delayed fluorescence. Recently, Belaid and Xiong et al use this theory the explain the observed magnetic field effect on electroluminescence in OLED[50,51].

Similarly, triplet charge reaction can be expressed by Equation 1.10 as follows:

$$T + D_{\pm 1/2} \underset{k_{-1}}{\overset{k_1}{\rightleftharpoons}} (T..D_{\pm 1/2}) \xrightarrow{k_2} S_0^{*} + D_{\pm 1/2} \qquad \text{(Equation 1.10)}$$

Triplet can interact with paramagnetic centers with spin $\pm 1/2$ (doublet) such as free charge or trapped charge to annihilate a singlet (S_0) at the ground state and releasing a new free charge from trapped charge. Here, k_1 is the formation rate of a intermediate singlet doublet (T..D) pair complex, k_2 is the dissociation rate into a new singlet doublet pair and k_{-1} is the dissociation rate back into original singlet doublet pair. Only the intermediate pair with doublet spin configuration can undergo this reaction. An external magnetic field can modify the singlet fraction in the intermediate pair, and consequently change the overall reaction constant. The reaction constant is suppressed with the increasing magnetic field. This theory was first proposed by Merrifield[47]. Recently, Desai et al use this model to explain the OMAR in organic semiconductor[39]. He considered the quenching of the triplet states or scattering of the free carrier caused by triplet charge reaction can lead to the reduction of carrier mobility, and consequently generate positive(+MR). Combined with magnetic field sensitive ISC theory, magnetic field can

reduce the triplet concentration and thus increase the mobility of charge carriers, generating negative (-MR).

1.4.3 Bipolaron model

The last bipolaron theory is proposed by the Bobbert and Wohlgenannt[42,43]. When charge carriers hops form site to site in disordered organic semiconductor, the electron and hole can also form the same polarity electron-electron (e-e) pair or hole-hole (h-h) pair, namely bipolaron, because of strong electron-phonon coupling and energy penalty for having a doubly occupied sites. If two charges have the same spin, they can not occupy the same site due to strong on-site exchange effects, which is also called as spin blocking. Oppositely, two charges with different spins can form bipolaron, allowing carrier to pass as shown in Figure 1.7.

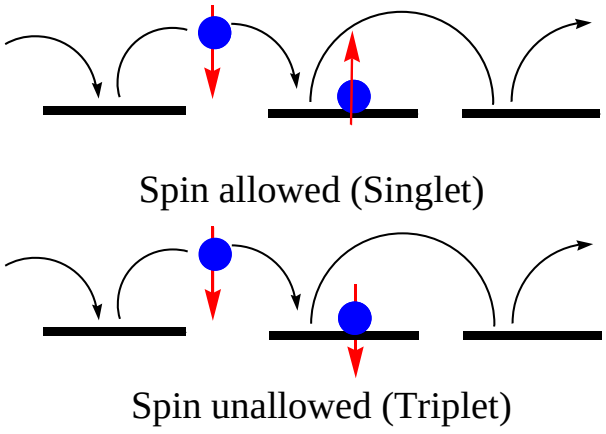

Figure 1.7 Schematic representation of bipolaron model

In the absence of magnetic field, the bipolaron with triplet configuration can partially mix the singlet character induced by the local hyperfine interaction. As an external magnetic

field is applied, the triplet pair is spilted into three different states (T_0, T_+, T_-) due to larger Zeeman energy compared to hyperfine interaction. In this case, the spin blocking is increased, which gives positive (+MR). On the other hand, when the bipolarons are formed, there are less free charges to carry the current. The reduction of bipolaron can correspond to a increase in the charge carrier mobility, which gives a negative (-MR). Whether MR shows positive or negative depends on the density of free electrons and holes and the branching ratio, which describe the ability of a charge go through the blocking site.

1.5 Outline of this dissertation

So far, no one existing theory can explain all the observed magnetic field effects very well. For example, the origin of magnetic field effects on resistance is still highly debated. Therefore, it needs re-examine these magnetic field sensitive processes and indentify the underlying mechanism of magnetic field effect on the electroluminescence and magnetoresistance. Moreover, the observed magnetic field effects may be composed of multiple components, which come from different contributions from separate mechanisms[52]. My research will further elucidate the critical factors that determine the magnetic field effect on the electroluminescence and current in non-magnetic OLED. Understanding these magnetic effects can form a unique experimental tool to investigate various excitonic processes, the charge injection and transport involved in the OLED and organic photovoltaic, which delivers the critical understanding to develop advanced OLED, solar cell materials and devices. Furthermore, based on the understanding of

magnetic field phenomenon, we can intentionally control the amplitude and sign of MFE_{EL} and MR, leading to a new branch of organic spintronics: organic magneto-optoelectronics with nonmagnetic active material and nonmagnetic electrode.

Based on the research progress in this field, my work will focus on the following issues. (1) Examining the e-h pair role in magnetic field effects on photoluminescence (MFE_{PL}) and electroluminescence (MFE_{EL}) (2) Investigating the origin of negative magnetic field effect on the electroluminescence in OLED (3) Studying interface related MFE_{EL} and MR (4) Electrical dipole-dipole interaction effect on MFE_{EL} and MR (5) Simultaneously tuning the magnetic field effect on the fluorescence and phosphorescence (6) Exploring the large magnetic field effect in organic semiconductors.

This dissertation includes eight chapters. Chapter 1 introduces the fundamentals for organic semiconductor materials and organic light emitting diodes devices, organic spintronics, various magnetic field effects in organic semiconductors and the review on existing major models for these magnetic field effects. Chapter 2 covers the organic semiconductor devices fabrication and magnetic field measurement on the photoluminescence (MFE_{PL}), electroluminescence (MFE_{EL}), injection current (MR or MC) and photocurrent (MFP) in detail. Chapter 3 presents our new understanding of MFE_{PL} and MFE_{EL} on a selected exciplex system based on magnetic field dependent intersystem crossing (ISC). The relationship between positive magnetic field effect and electron-hole pair separation distance will be addressed. Based on the theoretical prediction of magnetic field sensitive ISC, we experimental enhance the positive MFE_{PL} and MFE_{EL} by increasing the electron-hole pair separation distance. Chapter 4 explores

the possible mechanism for negative MFE_{EL} observed in organic semiconductor devices. There are two existing mechanisms: triplet-triplet annihilation (TTA) and triplet charge reaction (TCR) to explain negative $MFE_{EL.}$ MFE_{EL} can be tuned to negative by increasing the triplet density, confining the charge carrier and adjusting the balance degree of bipolar injection. Our experimental results and theoretical calculation support that TCR accounts for negative MFE_{EL}. Chapter 5 reports the significant interface induced MFE_{EL} and MR in strong spin orbital coupling iridium complex based OLED devices by introducing the non-magnetic insulating PVA layer. A possible model will be proposed to explain this interface based MC and MFE_{EL} based on magnetic field perturbed spin-spin interaction of inter-charge carriers at short capture distance. Chapter 6 compares the distinct MFE_{EL} and MR from two heavy metal complex $Ir(ppy)_3$ and $Ir(ppy)_2(acac)$, which have strong spin-orbital coupling but different electrical dipole moments. The electrical dipole-dipole interaction effect on the MFE_{EL} and MR will be further investigated in this chapter. Chapter 7 presents the tuning of magnetic field effect on the fluorescence (MFE_{FEL}) and phosphorescence (MFE_{PEL}) simultaneously by adjusting the device structures. The sign of MFE_{FEL} and MFE_{PEL} can be either in the same direction or in the opposite direction, which is against previous proposed formation based MFE. The possible mechanism to explain the relative sign of MFE_{FEL} and MFE_{PEL} will be discussed. Chapter 8 reports the giant magnetic field effects (400 %) on the electroluminescence in electrochemical cells. The mechanism correspond to this giant magnetic field effect will be elucidated. Chapter 9 will summarize the whole dissertation.

CHAPTER 2

DEVICE FABRIACTION AND MAGNETIC FIELD EFFECTS MEASUREMENT

In this chapter, we introduce the detailed fabrication procedures of organic semiconductor devices. The magnetic field effects measurement on the device injection current, photoluminescence, electroluminescence and photocurrent were also described in detail. At last, we show a series of universal magnetic field effects curves from a widely used semiconductor polymer: polyfluorene (PFO) system.

2.1 Device fabrication

The organic semiconductor materials used in our experimental are purchased commercially and used as received. All organic materials were carefully sealed in the desiccators to avoid the degration caused by the oxygen and humidity. Before the every experiment, we weigh the materials by using high precision balance (Ohas Analytical plus) and store them in clean vials. Our magnetic field sensitive organic semiconductor devices have the similar sandwiched structures like normal OLED. The device fabrication follows the standard procedures of OLED device fabrication including the substrate cleaning, organic active film formation and electrode deposition.

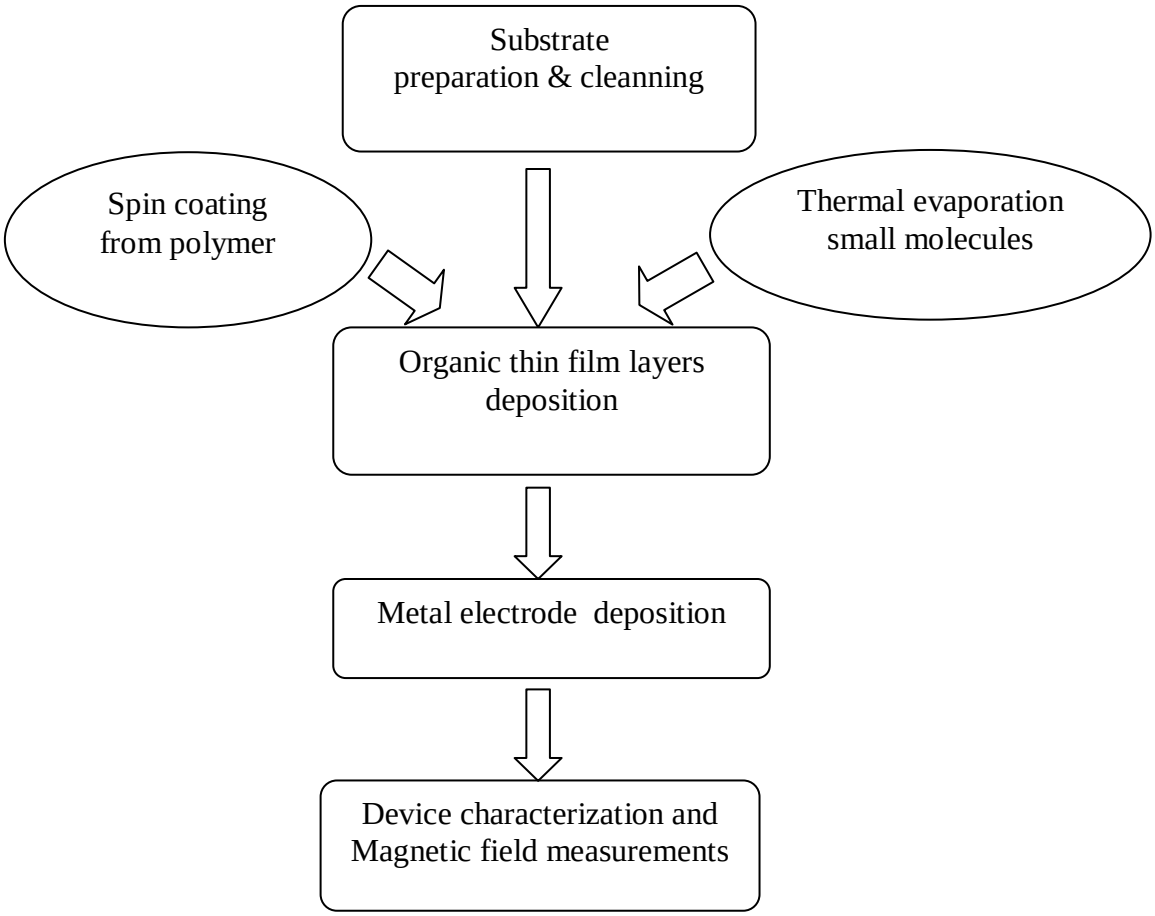

Figure 2.1 Procedures for device fabrication and characterization

2.1.1 ITO substrate preparation and cleaning

We used the customized patterned ITO glass substrate with the dimension 15 mm × 15 mm in our experiment. ITO glass is a layer of transparent conductive indium tin oxide film (In_2O_3 90%:$SnO_2$10%) coated on the thin glass, which is normally used as the device anode. The thickness of ITO film is around 200 nm with the average roughness 2 nm. The electrical and optical measurement shows the electrical square resistance is about 15

Ω/□ and the optical transmission is over 85 %. To facilitate electrical connection in further magnetic field measurement, we first bond the copper wires to the ITO substrate with the thermosetting silver paste after heating the substrate 20 minutes at 160 ℃. The prepared ITO substrate is shown in Figure 2.2 (a)

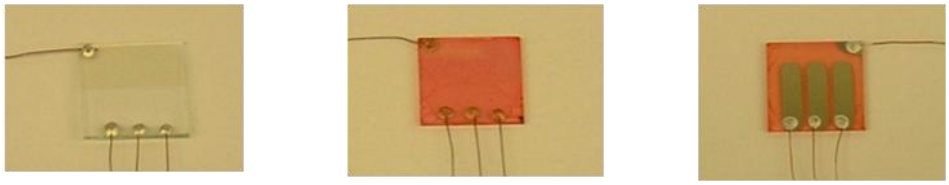

(a) **(b)** **(c)**

Figure 2.2 (a) ITO substrate with copper wiring (b) ITO coated with organic thin film (c) A completed device with metal electrode

Next, ITO substrate is cleaned by detergent for 15 minutes ultrasonic bath, followed by deionized water, acetone, 2-Propanol and Chloroform ultrasonic cleaning for 15 minutes for every step. After the solvent cleaning, the ITO was dried in the vacuum oven. UV-Ozone surface treatment is performed to clean the substrate from the remaining organic solvent. Careful ITO cleaning and surface treatment is very critical to the device performance. If the ITO substrate is not clean, the device is very easy to be electrical short circuit due to the formation of pinholes and filaments in the film.

2.1.2 Active organic thin film formation

We deposited functional polymeric thin film and small molecular thin film by spin coating and vacuum thermal evaporation, respectively. First, we weighed the semiconductor polymer based on designed solution concentration. Then, polymer materials were dissolved in chosen organic solvent to form uniform solution. Figure 2.3 shows the different semiconductor polymer solutions used in our experiments.

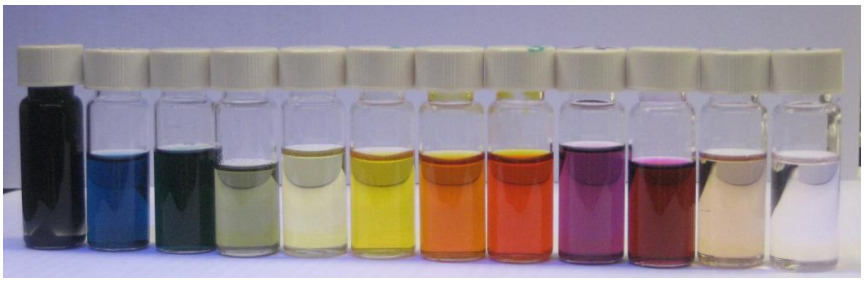

Figure 2.3 Semiconductor polymer solutions with different energy bandgap

Further, the solution was dropped on the pre-cleaned ITO substrate. When we start the spin coating recipe, the spin coater will rotate at high speed and the solution will spread to form a uniform thin film due to centrifugal force. The formed organic thin film was shown as Figure 2.2 (b). Depending on the solution concentration, acceleration time, spin speed, spin time and solvent selected, we can get desired thickness organic thin films. In general, the higher concentration of solution, the shorter accelerate time and spin time, the lower spin speed, lower boiling point solvent will give thicker film. The film thicknesses were measured by utilizing Veeco diCaliber (004-1001-000) Atomic Force Microscope (AFM). The whole spin coating process was done in a glove box under nitrogen protection.

Small molecular materials cannot be directly spin cast as normal polymer materials due to its low viscosity. We either blend small molecular materials into some inert polymer, and then do the spin coating as well as polymer materials. Or, we directly put the small molecular powers in the evaporation boat and transferred into the vacuum chamber of evaporating system for thermal evaporation. The ITO substrates were fixed on the substrate holder, which is above the evaporation boat. When the vacuum of chamber was pumped below 2×10^{-6} Torr, we gradually increase the current driven through the boat slowly while monitoring the thickness monitors. As a steady evaporation rate (1-3 Angstroms/s) is achieved, we open the substrate shutter and start deposition process. After the desired thickness is achieved, we close the shutter and shut off the current. We repeat this step until finish multi-layer organic films evaporation.

2.1.3 Deposition metal electrodes

After we finished active organic film deposition, we use a shadow mask to define the electrode pattern. The defined device area is 0.05 cm^2. We transfer assembled substrates holder and put the high purity metals (aluminum wires, calcium power) into the evaporator boat for thermal evaporation. The thermal evaporation of electrode is similar to the organic film deposition, except that much higher temperatures are required. A typical 50 nm thick of aluminum electrode was capped on top of the electrode to finish the whole device fabrication processes. A completed device is shown as Figure 2.2 (c).

2.2 Magnetic field effect measurements

After the device fabrication is finished, we need to take a series of measurement to test optical, electrical, magnetic properties of devices. Except the normal characterizations of organic semiconductors such as absorption, spectra, current-voltage-light intensity and efficiency measurements, we build the novel magnetic field measurement setup. With this setup, we are able to investigate the magnetic field sensitive photoluminescence, photocurrent, electroluminescence and current in organic semiconductor devices such as OLED and organic photovoltaic (OPV). The setup of magnetic field measurement is shown in Figure 2.4.

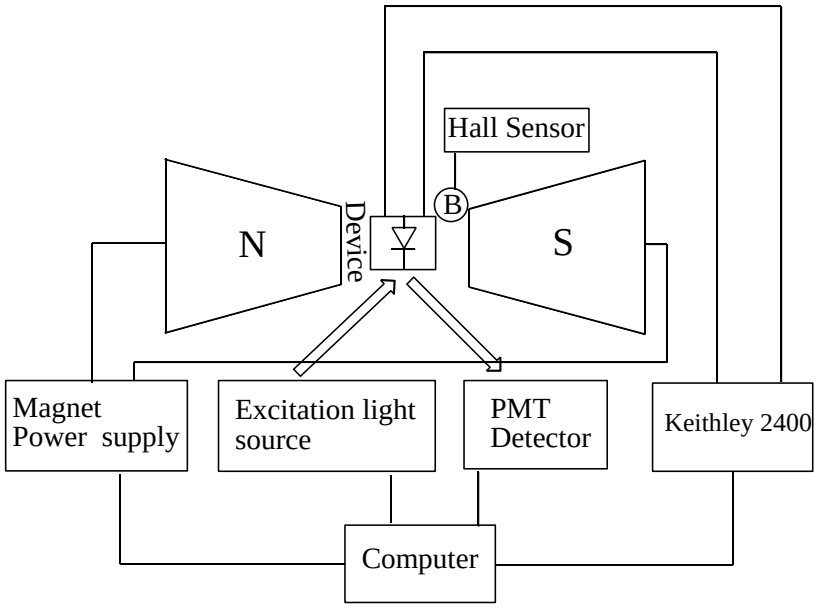

Figure 2.4 A schematic of magnetic field effects measurement setup

The devices were positioned in the middle of two poles of an electrical magnet for magnetic measurement. The magnetic field direction was parallel to the device plane. The

magnetic field strength was controlled by the current driven by a Sorensen DLM80-7.5 power supply. The magnetic field strength is proportional to the provided current and the exact value was measured by a Hall gaussmeter placed close to the sample.

In this thesis, the magnetic field effect on the photoluminescence, electroluminescence, injection current and photocurrent is defined as MFE_{PL}, MFE_{EL}, MR (also namely MC) and MFP, respectively, shown in Equation 2.1-2.4.

$$MFE_{EL} = \frac{EL(B) - EL(0)}{EL(0)} \quad \text{(Equation 2.1)}$$

$$MFE_{PL} = \frac{PL(B) - PL(0)}{PL(0)} \quad \text{(Equation 2.2)}$$

$$MR = \frac{R(B) - R(0)}{R(0)} = \frac{\frac{U}{I(B)} - \frac{U}{I(0)}}{\frac{U}{I(0)}} = \frac{I(0) - I(B)}{I(B)} \approx -MC \quad \text{(Equation 2.3)}$$

$$MFP = \frac{PC(B) - PC(0)}{PC} \quad \text{(Equation 2.4)}$$

Where EL, PL, R, I, PC are electroluminescence intensity, photoluminescence intensity, resistance, injection current, photocurrent, respectively. B and 0 represent with and without an external magnetic field.

In MFE_{EL} measurement, we operate the device at constant current mode in which a constant current was applied on the device by a Keithley 2400 Source meter. The electroluminescence was conducted through an optical fiber to a SPEX Fluorog 3 PMT detector when both the intensities and spectra can be recorded. We monitor the electroluminescence intensity change of organic semiconductor devices under different magnetic field. In MFE_{PL} and MFP measurement, the mono wavelength excitation light

was supplied by the SPEX Fluorog 3 spectrometer. Meanwhile, we recorded the photoluminescence intensity by using the PMT detector and measured the photocurrent by using the Keithley 2400 Source meter. For MR or MC measurement, the devices were measured at dark condition which can remove the potential MFP influence. MR or MC measurement was usually operated at constant voltage mode in which a constant voltage was applied on the device. Similar to MFE_{EL} measurement, we use the Keithley 2400 to monitor the current change under different magnetic field.

We investigated magnetic field responses for many widely used non- magnetic organic semiconductor materials including both polymers and small molecules. Most of organic semiconductors show the significant magnetic field response, which indicates that magnetic field response is a universal phenomenon, not limited to a specific material. As an example, Figure 2.5 shows the magnetic field effects on a polyfluorene (PFO) polymer.

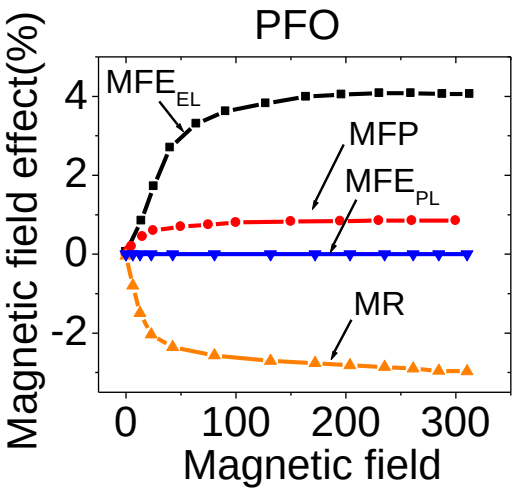

Figure 2.5 Magnetic field response of ITO/PEDOT/PFO/Al OLED

MFE_{EL} was measured at constant current density (20 mA/cm^2) and MR was measured at constant voltage 12 V targeting at 20 mA/cm^2. We note that the electroluminescence intensity increases dramatically at low magnetic field (<50 mT) and then slowly saturates after the 50 mT. Meanwhile, MR decreases at low magnetic field followed by the slow saturation at higher magnetic field. Similarly, the MFP exhibits the same trend as well. Therefore, it is natural to consider that these magnetic field responses may share the same origin. Meanwhile, we should also note the difference between them. In investigated systems, positive MFE_{EL} were frequently found. No sign change was observed when we adjust the applied voltages. While, MR can easily change its sign from the negative and positive value, depending on the driving voltage, measurement temperatures and device structures. In addition, it should be noted that the photoluminescence intensity is not sensitive to applied magnetic field shown in Figure 2.5. We will further discuss the reason for this negligible MFE_{PL} in next chapter.

CHAPTER 3

THE ROLE OF ELECTRON-HOLE PAIR IN MAGNETIC FIELD EFFECTS

3.1 Abstract

In this chapter, we investigate the magnetic field effect on the photoluminescence (MFE_{PL}) and electroluminescence (MFE_{EL}) in a TPD/BBOT exciplex system. The TPD/BBOT exciplex show the significant MFE_{PL} , while pristine organic semiconductor materials normally exhibit negligible MFE_{PL}. The experimental results indicate the electron-hole pair distance is crucial to the magnetic field effects through magnetic field sensitive intersystem crossing. Moreover, MFE_{PL} and MFE_{EL} can be enhanced by increasing the electron-hole separation distance through convenient materials mixing and adjusting the electrical dipole-dipole interaction in the organic semiconductor films.

3.2 Introduction

Although different models have been proposed to explain newly observed organic magnetoresistance (MR) phenomenon, the origin of MR is still in puzzle. The key difference between e-h pair, exciton reaction and bipolaron model is first two models require the formation of singlet and triplet electron-hole pair and subsequent exciton formation, while, the bipolaron model is a single carrier model in nature, which doesn't require the formation of e-h pair. Thus, indentifying the e-h pair role in magnetic field effects is necessary to distinguish the different MR models.

In order to distinguish the bipolaron with other two models, a straightforward way is to construct single carrier device by modifying the device architecture. Gärditz et al. built the Alq_3 based electron only device in which no significant MR is observed[53]. Further,

Desai also found that the MR was only observed above the light turn on voltage of the Alq_3 based device[40]. Before the light turn on voltage, the device can be regarded as unipolar in which only one type of carrier exists. After the turn on voltage, bipolar injection occurs in the device and injected electron hole will recombine into exciton indicated by the light emission. Recently, Yusoff built the single carrier device for electron only and holy only device, making use of the n-type silicon and p-type silicon to filter the electron and hole, respectively[54]. MR was absent in those two single carrier devices. Those experiment results strongly support that the recombination of electron-hole pair is the necessary condition for the presence of MR. However, Nguyen also built the single carrier device by modifying the injection electrodes of the device[55]. No MR was observed in electron only device, but a clear MR is observed in hole only device with Au as the cathode. Meanwhile, the largest MR is observed in the well balanced bipolar injection device. The experiment results from different groups seem contradict to each other, which makes it difficult to draw a convincing conclusion. The question behind these results is whether these devices are true single carrier devices as expected. Due to the electrode surface energy reduction caused by surface dipole moment, some minority carriers can still be unexpected injected into device.

Except for constructing the unipolar device, another alternative way is to use magnetic field effect on the photoluminescence (MFE_{PL}) to investigate the electron-hole pair role in the magnetic field effects. Under photoillumination, the singlet exciton is directly formed followed by the various decay channels such as the intersystem crossing between singlet and triplet state, dissociation into free electron and hole, radiative and non-

radiative emission to the ground state. In contrast to electroluminescence process, photoluminescence process do not experience charge transport process and lacks the evolution from loosely bounded electron hole pair state to the final closely bounded exciton state, which can exclude the influence of charge transport. We have investigated the MFE_{PL} for a variety of pure organic semiconductor materials. In all these systems, no significant MFE_{PL} was observed compared to the significant magnetic field effect on the electroluminescence (MFE_{EL}). This experimental result gives us an intuitional hint that magnetic field effect is closely correlated to the electron hole pair. In order to test this assumption, we introduce a specific type of inter-molecular excited states: exciplex. Unlike the Frenkel exciton that electron and hole are located in the same molecular, an exciplex is formed by inter-molecular electron transfer between ground donor (D) and excited acceptor (A) located at different molecular sites.

3.3 Experimental

Organic semiconductor materials N, N'-diphenyl- N, N'-bis (3-methylphenyl) -1, 1'-biphenyl-4,4'- diamine (TPD) and 2,5-bis(5-tertbutyl-2-benzoxazolyl) thiophene (BBOT) are selected to serve as donor (D) and acceptor (A). TPD is a commonly used hole transporting material in OLED, with the LUMO 2.2 eV and HOMO 5.4 eV. BBOT is a green emitter with good electron transport ability with the LUMO 3 eV and HOMO 5.8 eV. The insulating polymers poly(methyl methacrylate) (PMMA) and polystyrene (PS)are used as a matrix to facilitate the formation of the thin film. High polar camphoric anhydride (CA) molecule with permanent dipole moment of 11D is used to introduce

intermolecular dipole-dipole interaction. All molecular structures of TPD and BBOT are shown in Figure 3. 1. Those materials TPD, BBOT, CA and PMMA or PS are blended in desired molar ratio and then dissolved in chloroform solvent. Subsequently, blended solutions are spin cast on the precleaned ITO glass to form the films about 100 nm thicknness. Final Al electrode of 40 nm was deposited by using high-vacuum thermal evaporation (10^{-6} Torr).The photoluminescence and electroluminescence of organic films ware characterized by a Jobin Yvon Fluorolog-3 spectrometer with an optical fiber connection to the OLED placed in a magnetic field generated by an electromagnet. The MFE_{EL} was measured at constant current condition 20 mA/cm^2.

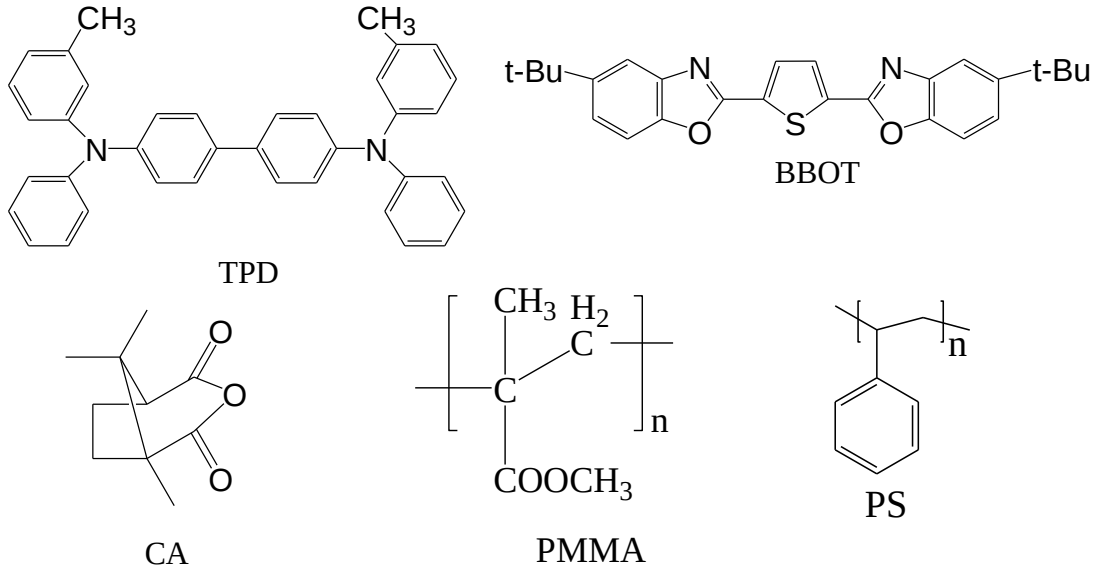

Figure 3.1 Chemical structures of materials used in the experiment

3.4 Results and Discussions

3.4.1 Magnetic field effect on the photoluminescence (MFE_{PL}) of Exciplex

We measure the photoluminescence spectra of TPD, BBOT and TPD:BBOT composite film as shown in Figure 3.2. The photoluminescence from TPD and BBOT is located at 400 nm and 440 nm, respectively. However, the TPD: BBOT composite film shows a new broad spectrum with the peak emission at 525 nm, which is apparently different with the emission from TPD and BBOT single component.

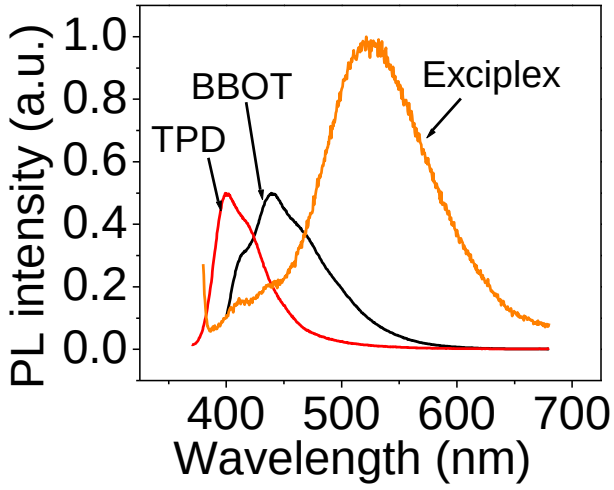

Figure 3.2 (a) Photoluminescence spectra of TPD, BBOT, and TPD/BBOT exciplex

In addition, this new emission peak is consistent with the energy difference between the LUMO (3 eV) of BBOT and HOMO (5.4 eV) of TPD as shown in of Figure 3.3. Therefore, this new red shifted peak indicates the formation of exciplex between TPD

and BBOT[56]. The formation mechanism of exciplex can be understood by the energy diagram shown in the Figure 3.3.

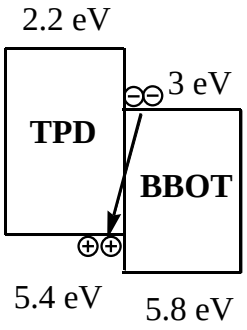

Figure 3.3 (a) Energy band diagram and TPD/BBOT exciplex formation at the interface

The injected electron is blocked by the high LUMO of TPD at TPD/BBOT interface. The exited BBOT molecule will interact with the ground TPD molecule to form intermolecular excited states: exciplex. Furthermore, we show the magnetic field measurement on the photoluminescence of exciplex in Figure 3.4. Interestingly, the TPD:BBOT exciplex system shows a clear positive MFE_{PL} with the amplitude of 1.5 %. In contrast, both TPD and BBOT pristine film show a negligible $MFE_{PL.}$ The question naturally arises why MFE_{PL} can only be observed in exciplex system. It should be noted that the exciplex is one type of intermolecular excited states. In this case, the electron and hole are located in two neighboring molecules and consequently the electron-hole separation distance is larger than the intramolecular excited states, in which the electron and hole are located in a single molecule.

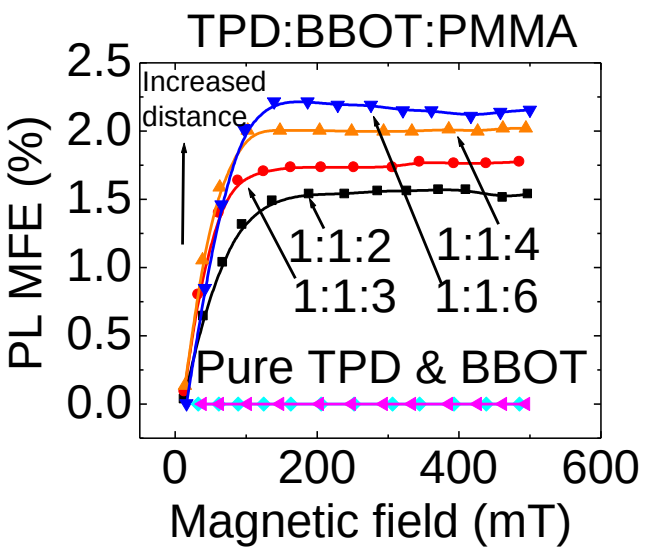

Figure 3.4 Magnetic field effect on the photoluminescence intensity (MFE_{PL}) of pure TPD, BBOT and TPD/BBOT exciplex with different blend ratio

As shown in Figure 3.4, the MFE_{PL} of exciplex (TPD: BBOT 1:1) can be further increased from 1.5 % to 2% by reducing the exciplex:PMMA ratio from 1:1:2 to 1:1:4. Here, PMMA also act as a spacer to separate the TPD and BBOT molecules. Reducing the exciplex concentration in PMMA matrix is equivalent to increase the intermolecular distance of exciplex. Therefore, we can consider that the large electron hole separation distance is helpful to generate magnetic field effect in organic semiconductor.

3.4.2 Electron hole separation distance dependent ISC crossing

Next, we investigate why adjusting the electron-hole separation distance can significantly impact the magnetic field response from organic semiconductor. In principal, polaron pair, exciplex (or charge transfer state) and exciton can be treated as the electron hole pairs with different electron hole separation distance. In exciton state, the electron and hole is usually located in a single molecule with the smallest electron hole separation distance, typical less than 1 nm. The electron and hole is closely bounded together through strong Coulombic attraction. In exciplex state, the electron hole is located at neighboring molecules and can be took as close contact pair with medium electron hole separation distance. In polaron pair state, the electron and hole is usually located in different molecules. Electron hole separation distance can be several times the nearest-neighbor intermolecular distance (4nm-10nm). Therefore, different electron-hole separation distance can lead to two major differences in molecular interaction. The first one is the binding energy generated by long range Coulombic attraction . The Coulombic attraction is expressed by $e^2/4\pi\varepsilon r$, which is reciprocal proportional to the electron hole separation distance. Therefore, the exciton has typical large binding energy around 1 eV [57], compared to small binding energy 0.1 eV[58] of polaron pair. The second is the energy difference ΔE_{ST} between singlet and triplet state caused by short range spin exchange interaction. Spin exchange interaction J [59]is defined as equation 3.1

$$J = J_0 e^{\frac{-r}{2L}} \qquad \text{(Equation 3.1)}$$

where J_0 is the coupling matrix, r and L are electron-hole separation distance and charge location radius, respectively. Spin exchange interaction exponentially decays with the

increasing electron-hole separation distance. In excition state, ΔE_{ST} can be as large as 0.7 eV[60] when electron and hole are closely located in a single molecule. In polaron pair state, ΔE_{ST} becomes negligible with the increasing electron-hole separation distance[29].

It has already been known that an external magnetic field can change the singlet and triplet ratio by modifying intersystem crossing (ISC). In order to make magnetic field sensitive ISC happen, two necessary conditions [61]should be satisfied shown in Figure 3.5.

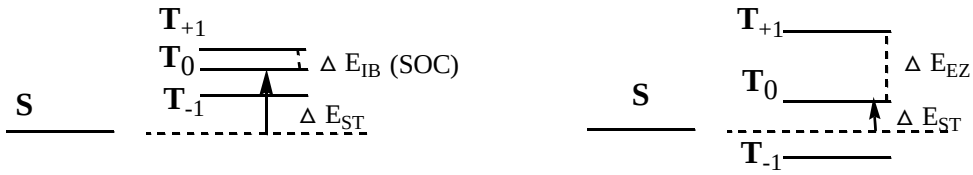

Without applied magnetic field **With applied magnetic field**

Figure 3.5 Schematic representation two preconditions of magnetic field dependent Intersystem crossing (ISC)

First, applied external magnetic field should be larger than the internal magnetic field generated by the hyperfine interaction and spin orbital coupling. Second, the external Zeeman splitting caused by applied external magnetic field should be comparable to the singlet-triplet energy difference ΔE_{ST}, which strongly depends on the electron-hole separation distance. Most organic fluorescent materials have the weak spin orbital coupling strength and their hyperfine interaction is usually smaller than the applied magnetic field (300 mT). Thus, the first condition is usually easy to satisfy. Considering

the second condition, an external magnetic field is larger than negligible ΔE_{ST} in polaron pair state, but much smaller than the large ΔE_{ST} in excitonic state. Consequently, an external magnetic field can change the ISC in polaron pair state, while has little influence on the ISC in excitonic state. This theoretical prediction is consistent with our experimental observation that significant magnetic field effect on electroluminescence (MFE_{EL}) is easily observed in many organic semiconductors, while it is difficult to observe MFE_{PL} because polaron pair state with negligible ΔE_{ST} is absent under photo excitation. Moreover, magnetic field sensitive ISC also explains well why we can observe clear MFE_{PL} in exciplex system. The electron-hole separation distance in the exciplex is larger than that of the exciton, and consequently has smaller $\Delta E_{ST.}$ In this case, a sufficient external magnetic field is able to reduce the energy gap between singlet and triplet, and initiate the ISC. Specifically, reducing the singlet and triplet energy gap ΔE_{ST} will facilitate the transition from triplet to singlet state, and consequently increases the singlet ratio. Correspondingly, the increased singlet excited states density will contribute to more fluorescence emission. As a result, magnetic field sensitive ISC can increase the photoluminescence intensity, exhibiting a positive MFE_{PL} of exciplex.

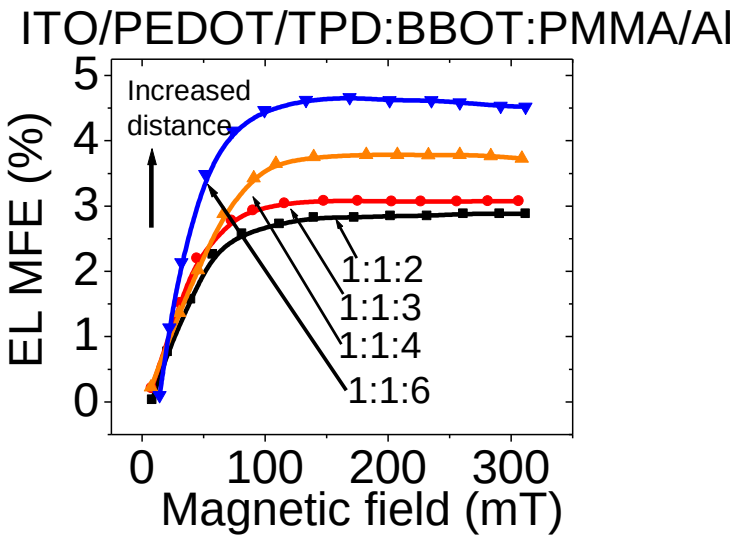

Figure 3.6 Magnetic field effect on the electroluminescence intensity (MFE_{EL}) of ITO/PEDOT/TPD:BBOT:PMMA/Al at different exciplex blend ratio

Similarly as we observed in Figure 3.4 that the MFE_{PL} can be enhanced with the increasing electron-hole separation distance. Figure 3.6 shows the positive magnetic field effect on the electroluminescence intensity (MFE_{EL}) of the exciplex can be enhanced from 2.8 % to 4.6 % as well as we increase the exciplex to inert PMMA spacer ratio from 1:1:2 to 1:1:6. Both increased MFE_{PL} and MFE_{EL} strongly support that the electron-hole separation distance dependent ISC is crucial to the observed positive magnetic field response.

3.4.3 Electrical Dipole-dipole interaction on the MFE

We have already demonstrated that adjusting the electron-hole separation distance through material mixing as a convenient method to tune the MFE of photoluminescence. We further consider other alternative ways to tune the magnetic field response. In principal, the Columbic attraction between intermolecular excited states arises from intermolecular electrical dipole-dipole interaction. The internal electrical polarization field can significantly influence the formation of exciplex by perturbing the intermolecular Columbic attraction. More importantly, the intermolecular dipole-dipole interaction can change the electron-hole capture distance through local field, and consequently provide an effective method to modify the magnetic field response. Previous photochemistry studies of radical-ion pair formation in liquid solution have found that the distance between donor and acceptor is very critical to influence the magnetic field effects on the fluorescence emission of exciplex. This conclusion is experimentally supported by changing the distance of donor and acceptor in chain linked electron donor (N-N-dimethylanilin) DMA and electron acceptor pyrene system[62,63]. In liquid solution, the donor and acceptor distance of radical-ion pair strongly depends on the solvent polarity. A maximum magnetic field effect on the fluorescence intensity of an intermolecular DMA/pyrene exciplex can be achieved by optimizing the dielectric constant solvent [64] . Similarly, we want to apply this concept into solid organic semiconductor thin film to tune the magnetic field responses in solid film. In order to investigate the electrical dipole-dipole interaction, we dispersed the high polar camphoric anhydride (CA) molecules, which has a large ground state dipole moment (μ=6 D)[65], into

the TPD/BBOT exciplex system to increase the local electrical field around the intermolecular exciplex. Figure 3.7 (a) shows the photoluminescence (PL) spectra after doping different concentration CA molecules. Dispersing polar CA molecules can largely quench the intensity of exciplex emission. High polar CA can induce molecular polarization by interacting with molecular dipoles, generating local electric fields in organic materials. When an intermolecular exciplex is considered as an electrical dipole, the strong local electric field induced by the high polar CA molecules can dissociate the intermolecular excited states and consequently quenches the PL intensity of exciplex. It is further noted that dispersing the polar CA molecules causes a significant red shift on the PL of TPD/BBOT exciplex emission as shown in Figure 3.7 (b). The PL red shift reaches 30 nm at the CA concentration of 30 %.

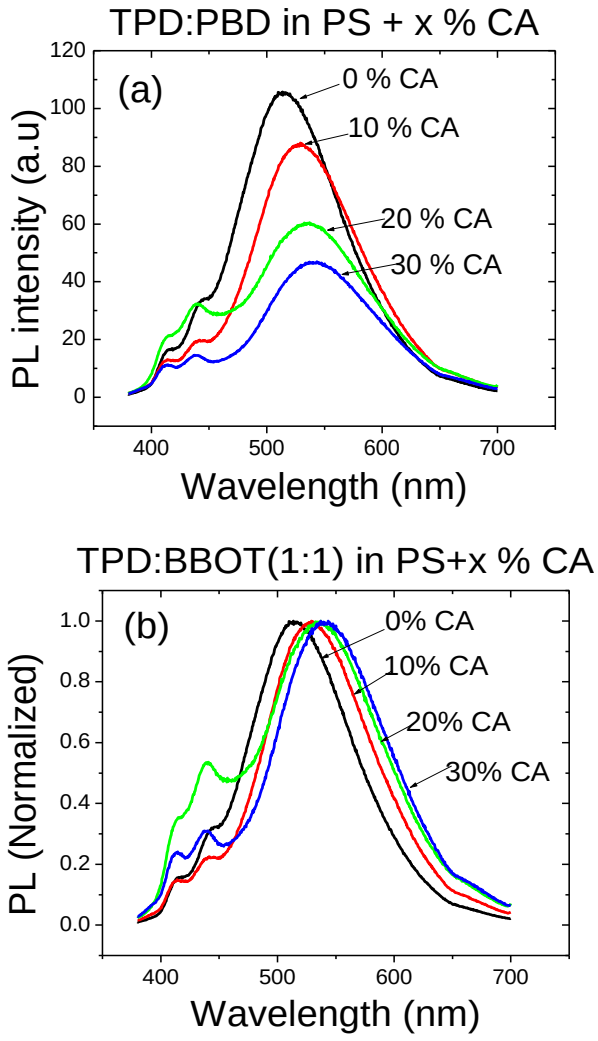

Figure 3.7 (a) Photoluminescence quenching of TPD/BBOT exciplex film with different CA concentration (b) Photoluminescence spectra shift of TPD/BBOT exciplex with different CA concentration.

Increasing the CA concentration increased the strength of the local electric fields in the film. Through dipole-dipole interaction, the excited state molecules will appropriate orient and alter the energy difference between excited states and ground state, which is

known as solid state solvation. Therefore, this PL spectra shift further indicates that the inter-molecular dipole-dipole interaction indeed occurs between the light-emitting inter molecules TPD/BBOT exciplex and the polar CA molecules in the TPD/BBOT:CA: PS composite.

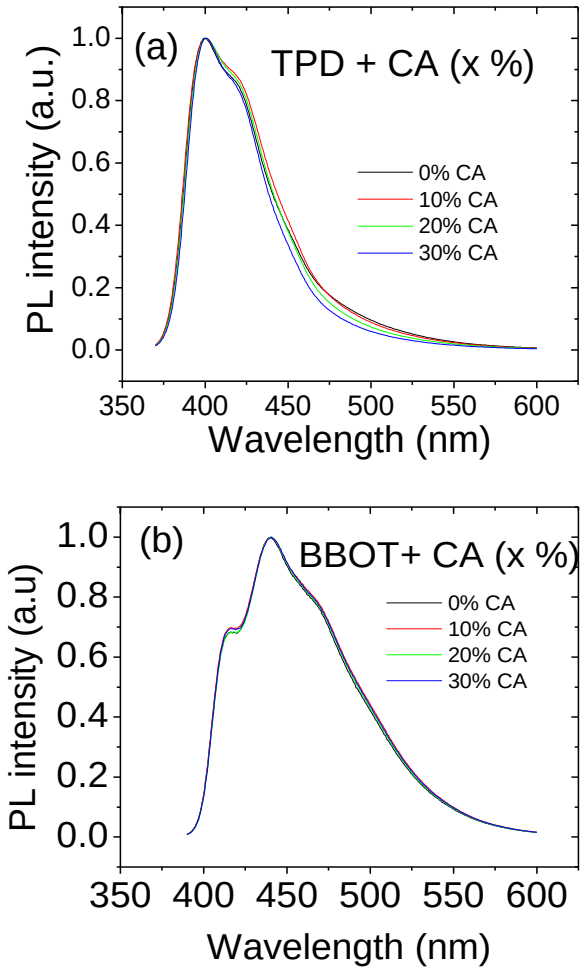

Figure 3.8 Photoluminescence spectra of TPD (a) and BBOT (b) with different CA doping concentration

On contrast, we also investigate the PL spectra of single component TPD and BBOT with different CA concentration, respectively. In Figure 3.8 (a) and (b), no significant PL spectra shift is observed. These experiment results clearly indicate that there is no strong electric dipole-dipole interaction between TPD or BBOT and CA molecules. Intramolecular excited state like Frenkel exciton has strong binding energy[57]because of its small electron-hole separation distance. The local electrical field generated by the CA molecules cannot affect the strong Columbic attraction in exciton, but is sufficient to destroy the comparable smaller Columbic attraction in exciplex through dipole-dipole interaction. Thus, we cannot observe the clear spectra shift in pure TPD film by increasing the CA concentration.

We now discuss the effects of inter-molecular dipole-dipole interaction on MFE_{EL} in organic semiconducting materials. In general, an external magnetic field can change the singlet and triplet ratios from two different ways either by perturbing the inter-charge spin-spin interaction during electron-hole capture at short distance, or by modifying the intersystem crossing (ISC) after electron-hole capture at long distance through intersystem crossing. Because the singlets and triplets have different lifetimes, spin configurations, and ionic natures, changing singlet and triplet ratios can affect the electroluminescence, electrical current, photocurrent, and photoluminescence based on charge recombination and dissociation, generating capture-based MFE and intersystem crossing (ISC)-based MFE in organic semiconducting materials. Specifically, in capture-based MFE, the electron-hole capture experiences inter-charge spin-spin interaction at short distance. When this spin-spin interaction exists, the electron-hole capture favors the

formation of singlet states due to strong exchange energy. An external magnetic field can perturb this spin-spin interaction and consequently changes the inter-charge spin configuration, leading to a decrease in singlet formation and an increase in triplet formation during the capture at short distance. Reflected from the electroluminescence, we will observe a negative MFE_{EL}. On contrast, in ISC-based MFE, the electron-hole capture experiences negligible spin interaction at long distance and undergoes a spin-random formation of singlet and triplet states with the ratio of 1:3. In this case, an external magnetic field can not perturb the singlet and triplet ratio through the capture. However, at long electron-hole capture distance, the Zeeman splitting induced by external magnetic field is comparable to the singlet-triplet energy difference caused by exchange interaction in polaron pair states. As a consequence, an external magnetic field can increase singlet ratio but decrease the triplet ratio by modifying the intersystem crossing based on Zeeman splitting, generating a positive MFE_{EL}. Increasing the electron-hole separation distance can shift the MFE from capture-based MFE occurring at short capture distance to ISC based MFE occurring at long capture distance.

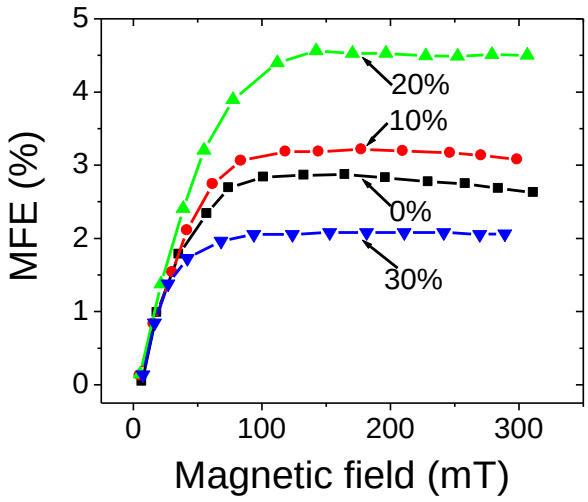

Figure 3.9 Magnetic field effect on the electroluminescence of ITO/PEDOT/TPD:BBOT:PS +CA(x wt %)/Al at different CA concentration

Figure 3.9 shows the magnetic field effect on the electroluminescence (MFE_{EL}) of the TPD:BBOT exciplex. When we disperse 10% CA into TPD/BBOT:PS composite, the MFE_{EL} increase from the initial 2.8% to 3.2%. The maximum MFE_{EL} around 4.5% is achieved at 20% CA doping. Further increasing the CA concentration up to 30%, MFE_{EL} of exciplex emission decreases to 2%. It is known that electric dipole-dipole interaction can enhance molecular electrical polarization and consequently increase the electron-hole separation distance, which will change the MFE_{EL} from capture based regime to ISC based regime. Increasing the CA molecule concentration up to 20% can essentially increase the electron-hole capture distance, and consequently enhance the $MFE_{EL.}$ Similar to the finding in liquid radical-ion solution, the maximum MFE_{EL} on the exciplex is only observed when the separation distance between donor and acceptor is in an optimum

range, not too small or not too long. At the optimum electron-hole separation distance, the singlet and triplet energy difference caused by exchange interaction should be small enough to allow hyperfine interaction inducing spin mixing and ISC. If the electron-hole separation distance is too small, the external Zeeman splitting caused by applied magnetic field is negligible compared to large singlet and triplet energy and consequently cannot change the ISC, leading to negligible MFE. On the other hand, as the electron-hole separation distance enlarges too much, the electron hole pairs can easily dissociate into free charge carriers through Onsager process. In this case, the coherence between electron and hole will get lost, and consequently magnetic field effect will be reduced. This is consistent with the experimental finding that MFE_{EL} decreases at the heavy 30 % CA loading.

3.5 Conclusion

In conclusion, most organic semiconductor materials show the negligible $MFE_{PL,}$ however, the significant MFE_{PL} is observed in the intermolecular excited state: TPD/BBOT exciplex. After comparing the distinct MFE_{PL} of intramolecular and intermolecular excited states, and different magnetic field response under photoexcitation and electrical excitation, we consider that electron-hole separation distance is critical to determine the magnetic field response in organic semiconductor. Therefore, we propose the electron-hole distance dependent ISC crossing mechanism to explain our experiment findings. Moreover, we experimentally tune the MFE_{PL} and MFE_{EL} by modifying the electron-hole separation distance through the simply material mixing and electrical

dipole-dipole interaction, respectively. This find has both theoretical and practical impotance. On one hand, our experiment results further support that magnetic field sensitive ISC corresponds to the magnetic response of organic semiconductor. On the other hand, changing the electron-hole capture distance through materials mixing and inter-molecular dipole-dipole interaction presents a new methodology to tune the magnetic responses of organic semiconductor devices.

CHAPTER 4

NEGATIVE MAGNETIC FIELD EFFECTS ON ELECTROLUMINESCENCE GENERATED BY TRIPLET-CHARGE ANNIHILATION IN ORGANIC SEMICONDUCTORS

4.1 Abstract

A magnetic field can usually increase electroluminescence intensity by perturbing singlet-triplet intersystem crossing in polaron-pair states through spin-momentum conservation, leading to positive magnetic field effects on electroluminescence (MFE_{EL}) in organic semiconductors. Recent studies have found that a magnetic field can also decrease electroluminescence intensity and generates negative MFE_{EL}. However, the origin of negative MFE_{EL} has been a controversial issue between triplet-charge annihilation (TCA) and triplet-triplet annihilation (TTA). Here, we demonstrate that the TCA is a dominant process accountable for negative MFE_{EL} by adjusting triplet density, charge confinement, and exciton/charge ratio in organic light-emitting diodes with dual electro-fluorescence and electro-phosphorescence. Specifically, the electro-fluorescence can clearly show negative MFE_{EL} when both interfacial confinement and unbalanced exciton/charge ratio exist to enhance the TCA. However, the electro-fluorescence only exhibits positive MFE_{EL} when interfacial confinement exists without unbalanced exciton/charge ratio to enhance the TTA. As a result, it can be concluded that negative MFE_{EL} comes from the TCA but not the TTA in organic semiconductors due to their different Coulomb interaction radii. Clearly, our experimental studies of negative MFE_{EL} indicate the TCA is a major process that forms non-useful and useful processes in organic light-emitting diodes and solar cells.

4.2 Introduction

It has been found that an external magnetic field can substantially change the electroluminescence intensity in organic semiconductors, leading to MFE_{EL} in organic light-emitting diodes (OLEDs)[32,33,36,39,66]. Elucidating the MFE_{EL} has become a high interest based on following two possible impacts. First, the MFE_{EL} can form effective mechanism for organic semiconductors to be used in magneto-optoelectronic devices[67]. Second, the MFE_{EL} can be used as a powerful tool to reveal spin-dependent useful and non-useful processes in organic light-emitting and photovoltaic systems[50,68,69]. In general, the MFE_{EL} can include both positive and negative components in a low magnetic field (< 100 mT). Obviously, the positive and negative MFE_{EL} reflect the increase and decrease in singlet/triplet ratio, respectively, in an organic semiconductor upon applying magnetic field. It should be noted that the increase in singlet/triplet ratio responsible for the positive MFE_{EL} has been commonly attributed to the magnetic field-sensitive intersystem crossing (ISC) in polaron-pair states[32,38,39,70]. Specifically, the ISC must undergo both energy and spin-momentum conservations. The relatively large electron-hole separation distance leads to small singlet-triplet energy difference and weak spin interaction in polaron pairs[29,32,59], which can be easily compensated by a low magnetic field through energy and spin-momentum conservations. As a result, the ISC in polaron-pair states becomes sensitive to a low magnetic field. Specifically, through energy conservation the Zeeman splitting from a low magnetic field can be comparable to the singlet-triplet energy difference in polaron-pair states, increasing the ISC rate by contributing to the energy conservation. Through spin-momentum conservation a low magnetic field can

compete with weak spin interaction in polaron-pair states, increasing the ISC rate by contributing to the spin-momentum conservation[37, 61]. As a consequence, a low magnetic field can increase the ISC from triplets to singlets in polaron-pair states and then boosts the ratio of singlet polaron pairs. The increase in singlet polaron pairs can essentially reflect as an increase in singlet excitons after the polaron pairs relax into excitons, generating positive MFE_{EL} in electro-fluorescence through magnetic field-dependent ISC. However, the magnetic field-dependent ISC in polaron pairs can not decrease singlet ratio to generate negative MFE_{EL} in electro-fluorescence. In general, there are two possibilities: triplet-charge annihilation: TCA and triplet-triplet annihilation: TTA that can be responsible for the decrease in the singlet ratio when applied magnetic field decreases TCA and TTA rate-constants[46-49]. The TCA can dissociate the triplet excitons through Coulomb scattering and generate free charge carriers[49,37]. The dissociated charge carriers can recombine into singlet and triplet excitons with the statistic ratio of 1:3 through a random capture[1,15]. On contrast, the TTA can directly generate singlet excitons in organic materials[46,71,72]. Therefore, when a low magnetic field decreases the singlet ratio by reducing the TCA and TTA rate constants, negative MFE_{EL} in electro-fluorescence can then be observed. It should be pointed out that the TCA and TTA have been proposed based on different experiments: chemical dynamics and delayed fluorescence. However, whether the negative MFE_{EL} comes from TCA or TTA is still a controversial issue[50,73,74]. Clearly, clarifying the origin of negative MFE_{EL} can not only increase the understanding on the mechanisms of magnetic field effects but also forms effective experimental tool to study triplet-related useful and non-useful processes

involved in light-emitting and photovoltaic responses. In this work we use dual electro-fluorescence and electro-phosphorescence to investigate the mechanisms of negative MFE_{EL} by controlling triplet density, charge confinement, and exciton/charge ratio.

4.3 Experimental

The organic semiconducting materials used here include PFO, PEDOT:PSS, $Ir(mppy)_{3,}$ $Alq_{3,}$ CBP, and BCP. The chemical structures of materials are shown in figure 4.1.

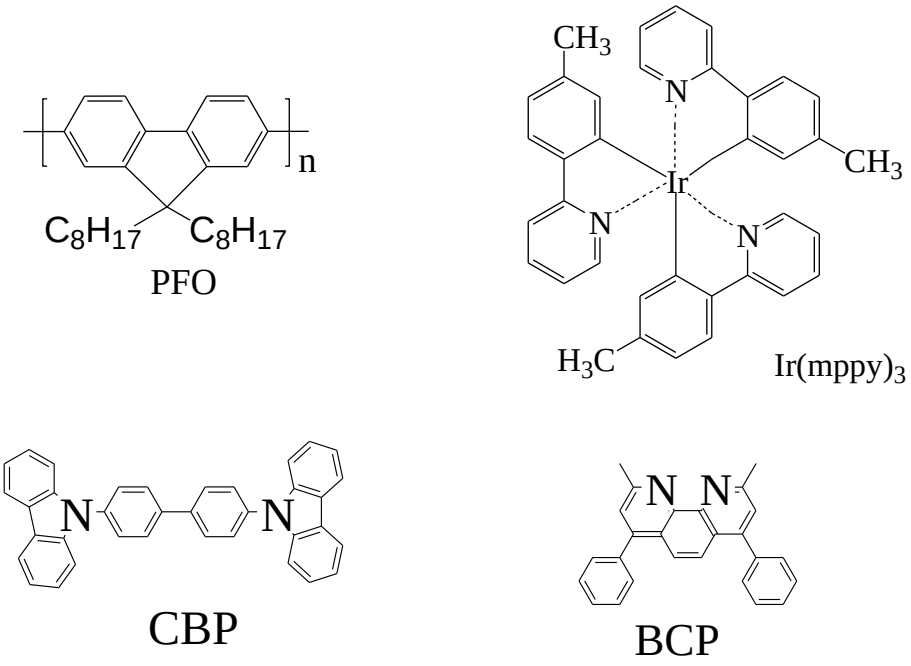

Figure 4.1 Chemical structures of materials used in the experiment

The low weight ratio Alq_3 and $Ir(mppy)_3$ are mixed with PFO polymer in chloroform solvent. The 90 nm thick polymer thin fims were spin cast from the composite solution in a nitrogen atmosphere. The metal Al electrodes were deposited under the vaccum 2×10^{-6} Torr. The double layer PFO/PMMA OLEDs were fabricated by using

nitromethane to spin casting the insulating PMMA layer on the PFO underlayer. The double layer PFO/CBP and PFO/BCP OLEDs were prepared by spin coating PFO underlayer followed by high vacuum thermal evaporation of CBP and BCP as the blocking layer. The thickness of the films was measured by a DekTek surface profiler. The magnetic field effects were measured by positioning the OLEDs in an electromagnet. The electroluminescence was characterized by a Jobin Yvon Fluorolog-3 spectrometer with an optical fiber connection. The magnetic effect on electroluminescence (MFE_{EL}) is defined as the electroluminescence change $\frac{(EL_B - EL_0)}{EL_0}$ under the influence of a magnetic field. The EL_B and EL_0 are the electroluminescence with and without an applied magnetic field, respectively.

4.4 Results and Discussion

4.4.1 Introducing triplet charge reaction by adjusting triplet density

Figure 4.2 (a) shows that increasing triplet exciton density can lead to a negative component in the electro-fluorescence based MFE_{EL} when the heavy-metal complex $Ir(mppy)_3$ molecules are dispersed into fluorescent polyfluorene (PFO) matrix.

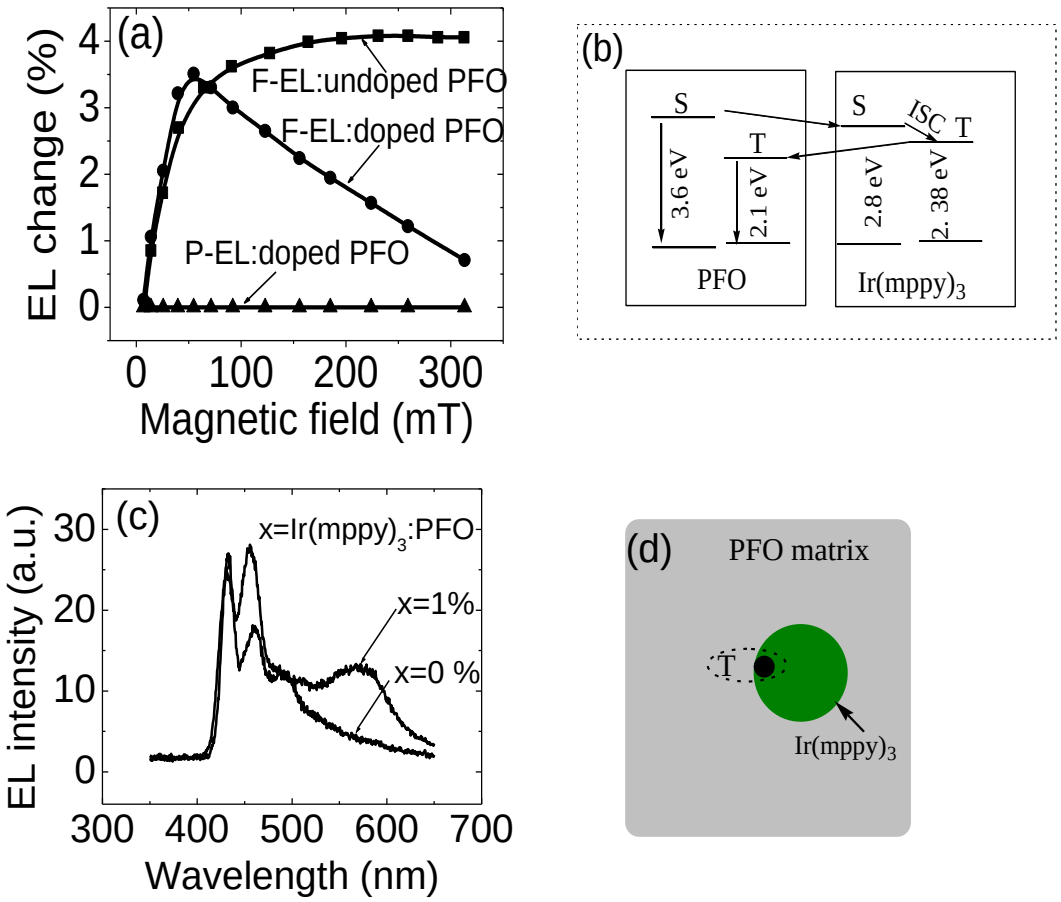

Figure 4.2 (a) MFE_{EL} for both electro-fluorescence (F-EL) and electro-phosphorescence (P-EL) observed from the PFO matrix in ITO/PFO+$Ir(mppy)_3$ (1wt%)/Al OLED. (b) Schematic energy-transfer processes between dispersed $Ir(mppy)_3$ molecules and PFO matrix in $Ir(mppy)_3$:PFO composite. (c) EL spectra from ITO/PFO/Al and ITO/PFO+$Ir(mppy)_3$ (1wt%)/Al OLEDs. (d) Schematic diagram for TCA occurring at molecule/chain interface in $Ir(mppy)_3$:PFO composite.

We should note that the $Ir(mppy)_3$:PFO composite can exhibit dual electro-fluorescence and electro-phosphorescence from the PFO matrix due to introduced inter-molecular SOC between $Ir(mppy)_3$ and PFO chains. Specifically, the dispersed $Ir(mppy)_3$ molecules can function as traps for charge carriers to form high-density triplet excitons with almost 100 % fraction[75] in the dispersed $Ir(mppy)_3$ molecules. The high-density triplet excitons formed in the dispersed $Ir(mppy)_3$ molecules can efficiently transfer to the PFO matrix through Dexter process [76,77](schematically shown in Figure 4.2 (b)). As a result, the PFO matrix can have high-density triplet excitons in the $Ir(mppy)_3$:PFO composite. On the other hand, theoretical studies have shown that delocalized π electrons can enter the magnetic field generated by adjacent orbital current and consequently enhances the SOC in organic materials[78]. As a result, the inter-molecular SOC can be introduced between the $Ir(mppy)_3$ molecules and the PFO chains in the PFO:$Ir(mppy)_3$ composite[79,80]. In particular, the introduced inter-molecular SOC can generate electro-phosphorescence from the PFO matrix. It can be seen in Figure 4.2 (c) that the electroluminescence (EL) from the $Ir(mppy)_3$:PFO composite consists of the short-wavelength portion peaked at 420 nm and the long-wavelength portion peaked at 590 nm. The short-wavelength EL peaked at 420 nm is known as the electro-fluorescence from the PFO[81]. Obviously, the long-wavelength EL peaked at 590 nm is different from the phosphorescence (510 nm[82]) of $Ir(mppy)_3$ molecules but matches the triplet energy (2.15 eV[83]) of PFO. Therefore, the long-wave-length EL peaked at 590 nm can be attributed to the electro-phosphorescence from the PFO matrix in the $Ir(mppy)_3$:PFO composite. This electro-phosphorescence implies that the dispersed $Ir(mppy)_3$ molecules can largely increase the SOC of PFO

matrix through inter-molecular magnetic interaction, namely inter-molecular SOC, where the delocalized π electrons of PFO matrix can enter into the large magnetic field generated by the orbital current of $Ir(mppy)_3$ molecules in the $Ir(mppy)_3$:PFO composite. In addition, it has been already found that the dispersed $Ir(mppy)_3$ molecules do not emit phosphorescence because the dispersed $Ir(mppy)_3$ molecules can transfer the triplet excitons to the PFO matrix through efficient Dexter process in the $Ir(mppy)_3$:PFO composite. Nevertheless, the PFO matrix can exhibit dual electro-fluorescence and electro-phosphorescence due to (i) high-density of triplet excitons transferred from the charge trapping $Ir(mppy)_3$ molecules and (ii) the introduced inter-molecular SOC between the $Ir(mppy)_3$ molecules and the PFO chains. More importantly, in the PFO-alone OLED the electro-fluorescence peaked at 420 nm only shows positive MFE_{EL} through magnetic field-sensitive ISC in polaron-pair states. But, in the $Ir(mppy)_3$:PFO composite OLED the electro-fluorescence exhibits a clear negative component in the MFE_{EL} from the PFO matrix. Clearly, this negative MFE_{EL} component is generated by the increased triplet density in the PFO matrix upon dispersing the $Ir(mppy)_3$ molecules. In particular, we should note the following two consequences in the $Ir(mppy)_3$:PFO composite. First, the triplet excitons are largely located in the PFO matrix due to the efficient Dexter transfer from the $Ir(mppy)_3$ molecules to the PFO chains while the excessive charges are confined in the $Ir(mppy)_3$ molecules due to the potential-well effects. Second, the PFO chains and $Ir(mppy)_3$ molecules have close-interfacial contacts confirmed by the efficient Dexter transfer. As a result, the triplet excitons can Coulombically interact with the excessive charges at the $Ir(mppy)_3$/PFO interfaces,

generating TCA in the $Ir(mppy)_3$:PFO composite. In principle, when organic molecules are dispersed in a semiconducting polymer matrix with band offsets, the molecule/chain interfaces can generate potential wells for charge and exciton traps[84,85]. We should further note that the chain/molecule interfaces can often function as effective trapping locations to initiate the TCA because interfacial Coulomb interactions due to their different electron negativities can Coulombically trap the triplets and charges (schematically shown in Figure 4.2 (d)). As a consequence, the chain/molecule interfaces can facilitate the TCA in the $Ir(mppy)_3$:PFO composite.

As the comparation, we also investigate the magnetic field effect on the fluorescence emission of PFO when fluorescent dye Alq_3 is dispersed in PFO system. In Figure 4.3 (a), 1% Alq_3 doping in PFO matrix exhibits a positive electro-fluorescence based MFE_{EL} from PFO emission, which is the same as the pure PFO system. Although the value of positive MFE_{EL} decrease from 4% to 1.5% after 1% Alq_3 doping, insignificant MFE_{EL} decrease component could be observed even further increasing the Alq_3 doping concentration up to 5%. The distinct MFE_{EL} difference between $Ir(mppy)_3$ and Alq_3 can be attributed to different properties and excitonic processes involved in two composite systems. First, it should be noted that phosphorescent $Ir(mppy)_3$ dye have much stronger spin orbital coupling strength than fluorescent Alq_3 material. As a result, the inter-molecular SOC between the Alq_3 molecules and the PFO chains should be weaker. Second, the different triplet energy level between $Ir(mppy)_3$ and Alq_3 will lead to different energy processes in host-guest system.

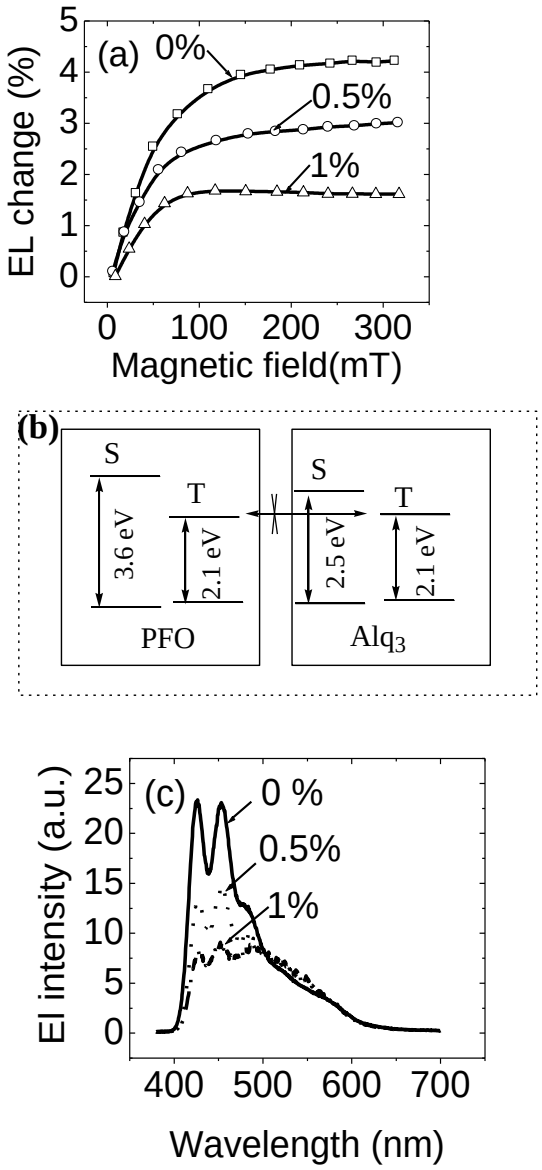

Figure 4.3 (a) MFE_{EL} for electro-fluorescence observed from the PFO matrix in ITO/PFO+Alq_3 (x wt%)/Al OLED. (b) Schematic energy-transfer processes between dispersed Alq_3 molecules and PFO matrix in Alq_3:PFO composite. (c) EL spectra from ITO/PFO/Al and ITO/PFO+ Alq_3 (0.5, 1wt%)/Al OLEDs.

As shown in Figure 4.3 (b), the triplet level of dopant Alq_3 is comparable to the triplet level of matrix PFO. The triplet exciton located on the Alq_3 can not be efficiently back transferred to the host PFO due to energy unfavorable. Due to the weak SOC and insufficient energy transfer between PFO and Alq_3 molecules, we cannot sufficiently increase the triplet densities in the PFO matrix as in the $Ir(mppy)_3$: PFO system. It can be further supported by Figure 4.3 (c) that electro-fluorescence spectra from the Alq_3:PFO composite only show the short-wavelength portion peaked at 420 nm. No phosphorescence emission peaked at 590 nm can be observed.

In general, there are two possibilities that can change the singlet/triplet ratio in the generation of electro-fluorescence and electro-phosphorescence based MFE_{EL} in the $Ir(mppy)_3$:PFO composite. First, applied magnetic field can increase the singlet exciton ratio in the PFO matrix by enhancing the ISC in the polaron-pair states of PFO matrix. Second, applied magnetic field can reduce the TCA rate constant, leading to a decrease component in the singlet exciton ratio and an increase component in the triplet exciton ratio in the PFO matrix. Therefore, the electro-fluorescence and electro-phosphorescence based MFE_{EL} can be given by the changes in singlet and triplet densities as shown in Equation 4.1 and 4.2

$$MFE_{FEL} = \frac{(\Delta S_{P-ISC} - \Delta S_{TCA})}{S_{P0}} \qquad \text{(Equation 4.1)}$$

$$MFE_{PEL} = \frac{(-\Delta T_{P-ISC} + \Delta T_{TCA})}{(T_{P0} + T_{M0})} \qquad \text{(Equation 4.2)}$$

where the MFE_{FEL} and MFE_{PEL} are electro-fluorescence and electro-phosphorescence based magnetic field effects, the S_{P0} and T_{P0} are the singlet and triplet densities formed at

polymer matrix, the T_{M0} is the triplet density formed in dispersed molecules, the $\Delta S_{P\text{-}ISC}$ and ΔS_{TCA} are the changes in singlet density caused by B-dependent ISC and B-dependent TCA rate constant, the $\Delta T_{P\text{-}ISC}$ and ΔT_{TCA} are the changes in triplet density caused by B-dependent ISC and B-dependent TCA rate constant. It can be seen in Equation 4.1 that the $\Delta S_{P\text{-}ISC}$ and ΔS_{TCA} can generate positive and negative MFE_{EL} in electro-fluorescence. Clearly, based on the assumption that (i) the TCA dissociates triplet excitons and (ii) the dissociated charge carriers recombine to form both singlets and triplets, a negative component in the electro-fluorescence-based MFE_{FEL} can be expected when applied magnetic field reduces the TCA rate constant. It should be pointed out that the triplets (T_{M0}) in the dispersed $Ir(mppy)_3$ molecules are formed with largely high density due to charge trapping effects. Especially, the high-density triplets formed in the dispersed $Ir(mppy)_3$ molecules can transfer to the PFO matrix through Dexter process. As a consequence, the singlets and triplets in the PFO matrix have very-low and very-high densities, respectively. Furthermore, the change in triplet density $\frac{(-\Delta T_{P-ISC} + \Delta T_{TCA})}{(T_{P0} + T_{M0})}$ reflected in the Equation 4.2 becomes negligible as compared to the change in singlet density $\frac{(\Delta S_{P-ISC} - \Delta S_{TCA})}{S_{P0}}$ reflected in Equation 4.1 upon applying magnetic field. Therefore, we can theoretically argue that the electro-fluorescence and electro-phosphorescence from the PFO matrix have appreciable and negligible MFE_{EL} values in the $Ir(mppy)_3$:PFO composite. Experimentally, we can see from the Figure 4.2 (a) that the electro-fluorescence peaked at 420 nm and electro-phosphorescence peaked at 590 nm from the PFO matrix show appreciable and un-appreciable MFE_{FEL} and MFE_{PEL} in the

$Ir(mppy)_3$:PFO composite, respectively. It should be further noted that the electro-phosphorescence from heavy-metal complexes does not exhibit appreciable MFE_{EL} in a low field (< 1 T)[53,79]. This is because heavy-metal complex molecules can have a very strong SOC (~100 μeV[86]) with almost 100 % ISC and a low magnetic field (< 1 T) can not disturb SOC-assisted spin momentum conservation involved in the ISC. As a result, the strong SOC can significantly quench the electro-phosphorescence based MFE_{PEL} in heavy-metal complex molecules. However, the early published results indicate that electro-phosphorescence can exhibit a positive MFE_{PEL} in heavy-metal complex molecules dispersed in fluorescent polymer matrices[87]. We found that this positive MFE_{PEL} based on electro-phosphorescence is indeed caused by the Förster energy transfer[79]. Specifically, a magnetic field can increase the singlet ratio in the fluorescent polymer matrix by increasing the ISC in polaron-pair states. The increase of singlet ratio in the fluorescent matrix can be transferred to the singlet states in the phosphorescent molecules through efficient Förster transfer. Eventually, the increase of singlet ratio in the phosphorescent molecules can lead to an increase in triplet ratio through efficient ISC generated by the strong SOC of heavy-metal complex, generating a positive MFE_{PEL} in electro-phosphorescence. Nevertheless, the MFE_{EL} observed in electro-fluorescence and electro-phosphorescence from the PFO matrix reflect the changes in singlet and triplet densities that are essentially determined by the magnetic field-dependent ISC in polaron-pair states, magnetic field-dependent TCA, and Förster and Dexter transfer in the $Ir(mppy)_3$:PFO composite.

4.4.2 Introducing the triplet charge reaction by confining the charge at interface

Now we further investigate the negative MFE_{EL} component by using charge confinement at film-interface in OLEDs. It is known that the interface in multilayer OLEDs can confine injected charge carriers and excitons, which are essential to initiate the TCA. Here, we use the PFO as a common light-emitting layer with two different charge-transport layers to form double-layer OLEDs with significant and negligible confinement, respectively. The charge-transporting materials are 4,4'-N, N' -dicarbazole-biphenyl (CBP) (LUMO=2.0 eV and HOMO=5.5eV [88]) and 2,9-dimethyl-4,7-diphenyl-1,10-phenanthroline (BCP) (LUMO=3.2 eV and HOMO=6.7 eV[89]). It can be seen from the band diagrams in Figure 4.4 (a) that the PFO/CBP interface can largely confine injected charge carriers and excitons due to the band offsets in the ITO/PFO/CBP/Al OLED. On contrast, the PFO/BCP interface does not exhibit a confinement to trap injected charge carriers and formed excitons in the ITO/PFO/BCP/Al OLED due to the absence of band offsets. Figure 4.4 (b) shows that the interfacial confinement generates a clear negative component in the MFE_{EL} from the PFO in the ITO/PFO/BCP/Al OLED. The magnitude of negative MFE_{EL} is around - 2 % at the constant current density of 20 mA/cm^2. In contrast, the MFE_{EL} does not show negative component in the ITO/PFO/CBP/Al OLED where the interfacial confinement is absent.

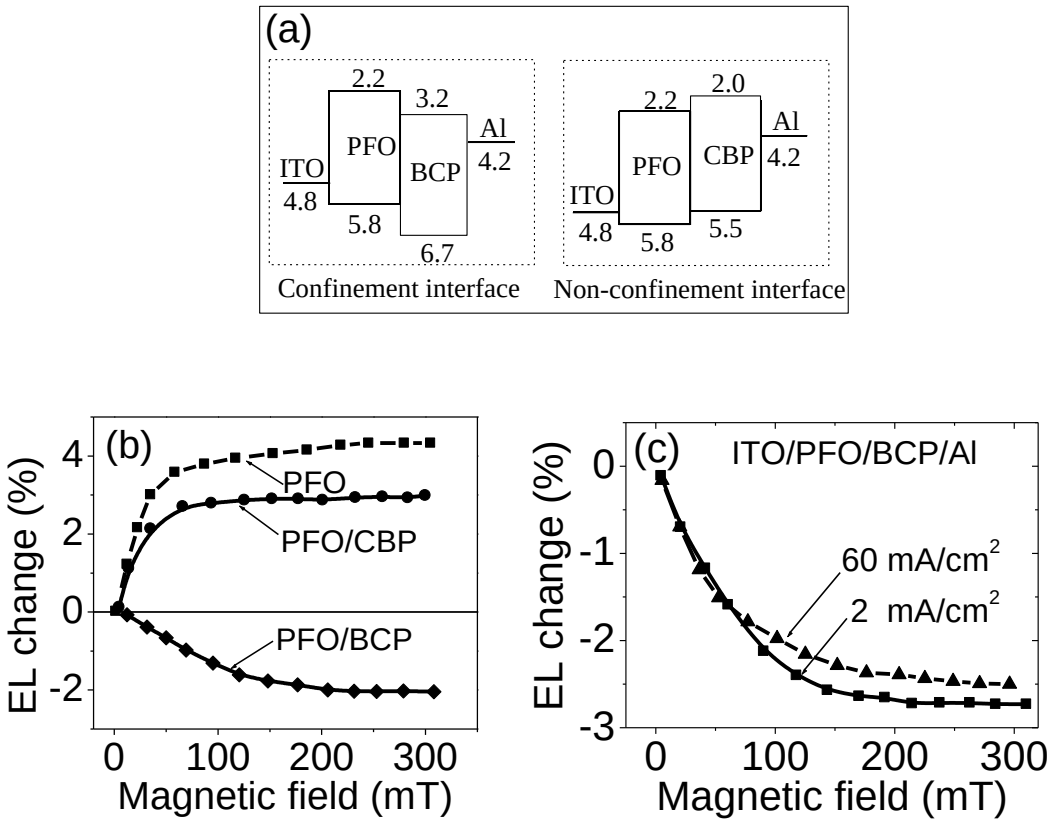

Figure 4.4 (a) Band diagrams for double-layer PFO/BCP and PFO/CBP OLEDs with ITO and Al electrodes. (b) Positive and negative MFE_{EL} for double-layer PFO/CBP and PFO/BCP OLEDs, respectively. (c) Negative MFE_{EL} from double-layer PFO/BCP OLED at different injection current densities.

Clearly, our experimental results (Figure 4.4 (b)) indicate that interfacial confinement can lead to a negative component in the MFE_{EL}. In principle, the PFO/BCP interfacial confinement can generate both TCA and TTA based on confinement effects. Here, we further studied these two possibilities for negative MFE_{EL}. We know that the TTA is a bi-molecular reaction initiated by Coulomb interaction. Therefore, changing injection

current density can largely change the TTA by modifying triplet density in the ITO/PFO/BCP/Al OLED where interfacial traps exist. If the TTA is a dominate process accountable for negative MFE_{EL}, we would observe that changing injection current can essentially determine whether the MFE_{EL} shows a negative component. However, we can see in Figure 4.4 (c) that increasing the injection current from 2 mA/cm^2 to 60 mA/cm^2 does not appreciably change the negative MFE_{EL}. The MFE_{EL} amplitudes are -2.8 % and -2.5 % for the injection current densities of 2 mA/cm^2 and 60 mA/cm^2. Therefore, the injection current dependence of MFE_{EL} does not suggest that the TTA is a dominate process accountable for the negative component in the MFE_{EL}.

4.4.3 Bipolar injection effect on triplet charge reaction

Now we further confirm that the TCA is a dominant process in the generation of negative MFE_{EL}. It is known that the TCA can be generated when triplets and charges exist within close proximity in organic materials. The charge injection can, in principle, generate large amount of triplets with the singlet/triplet ratio of 1:3 in OLEDs through spin-random capture. However, the TCA requires excessive charges available within close proximity with triplets. Therefore, excessive charges are a necessary condition to generate TCA in OLEDs. We know that injected electrons and holes can be maximally paired up to form excitons when they are balanced. On the other hand, un-balanced electron and hole injection can produce excessive charges with reduced exciton formation. The spatial confinement of excessive charges and triplet excitons can then generate TCA. As a result, balanced bipolar injection can increase the electron-hole

pairing ratio and therefore suppress the TCA[90]. However, unbalanced bipolar injection reduces the electron-hole pairing ratio and thereby enhances the TCA when spatial confinement exists. Here, we use insulating thin film of poly(methyl methacrylate) (PMMA) to introduce both spatial confinement and un-balanced bipolar injection in the double-layer ITO/PFO/PMMA/Al OLED (Figure 4.5 (a)). We can then expect TCA and negative MFE_{EL} at the PFO/PMMA interface when the PMMA film introduces un-balanced electrons and holes by reducing electron injection. It can be seen in Figure 4.5 (b) that increasing the PMMA film thickness from 7 nm to 14 nm can clearly generate negative MFE_{EL} in the ITO/PFO/PMMA/Al OLED at the constant current of 20 mA/cm^2. Figure 4.5 (c) shows that the EL intensity increasing rate with injection current largely decreases as the PMMA film thickness increases. This decrease in EL/current rate indicates that increasing PMMA film thickness can indeed lead to un-balanced electron and hole injection and consequently generates excessive carriers available for TCA. As a result, the un-balanced charge injection confirms that the TCA is a dominant process accountable for negative MFE_{EL} in OLEDs.

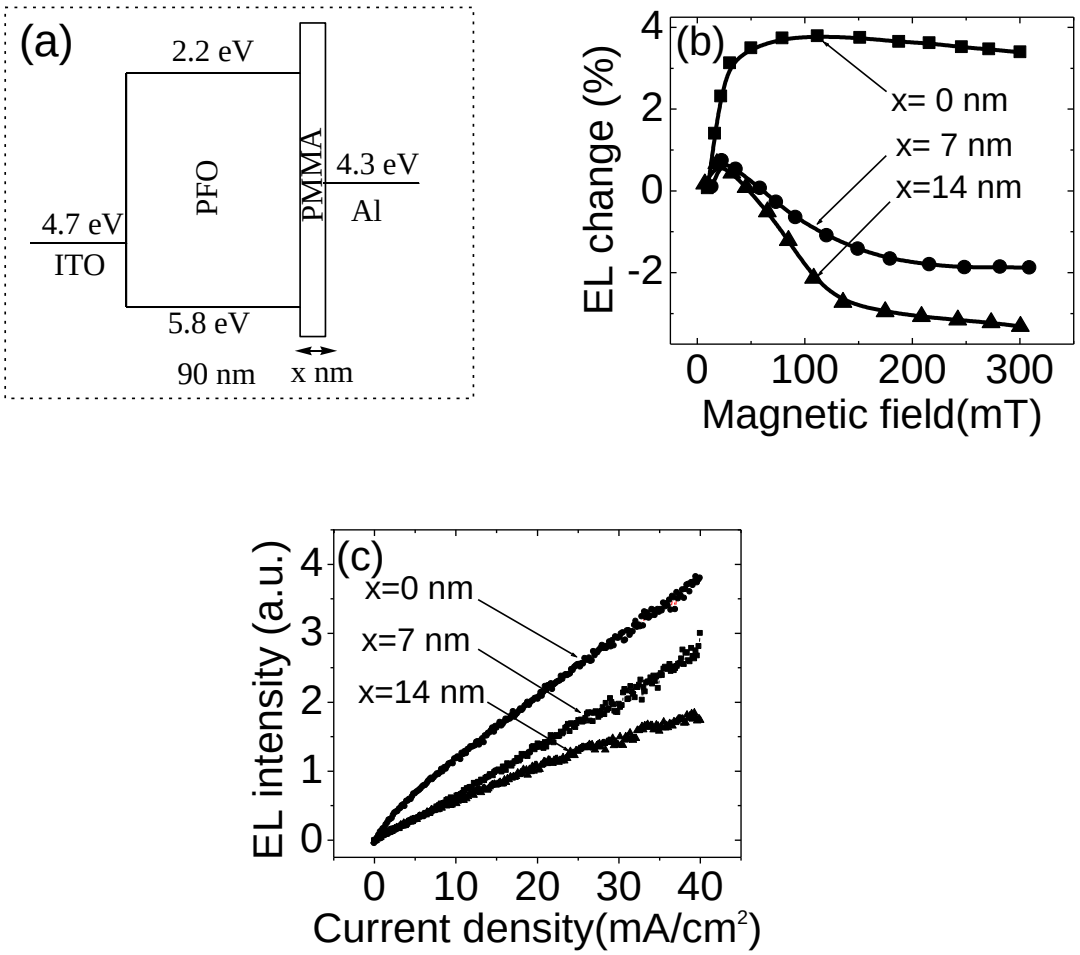

Figure 4.5 (a) Band diagram for double-layer PFO/PMMA OLED with ITO and Al electrode. (b) Changing positive MFE_{EL} to negative MFE_{EL} by increasing the PMMA film thickness to 7 nm and 14 nm in ITO/PFO/PMMA/Al OLED. (c) EL-current characteristics for double-layer ITO/PFO/PMMA (x nm)/Al OLEDs with different PMMA film thicknesses.

Now we discuss why the TCA is a dominant process in the generation of negative MFE_{EL} as compared to the TTA in organic materials reflected. We know that both TCA and TTA occur through Coulomb interaction. Specifically, when a triplet and charge Coulombically interact with a nearby triplet to generate TTA and TCA, this nearby triplet must be located within the Coulomb-interaction radii of a triplet and a charge, respectively. Here, we consider the electric fields generated by a triplet and a charge required for TTA and TCA (Figure 4.6 (a)). When a triplet exciton is treated as a dipole in a simplified two-dimensional x-y system, its electric field E_{Dx} at x axis can be expressed by Equation 4.3. Integrating the E_{Dx} from $\theta = 0$ to $\theta = 2\pi$ gives the average electric field $\overline{E}_{Dx}$ at x axis for a triplet exciton (Equation 4.4).

$$E_{Dx} = \varepsilon_{hx} + \varepsilon_{ex} = \frac{+q}{4\pi\varepsilon x^2} + \frac{-q}{4\pi\varepsilon(x^2 + d^2 - 2xd\cos\theta)} \bullet \cos\alpha \qquad \text{(Equation 4.3)}$$

$$\overline{E}_{Dx} = \frac{1}{2\pi} \bullet \int_0^{2\pi} \frac{q}{4\pi\varepsilon x^2}[-2\frac{d}{x}\cos\theta - \frac{(9\cos^2\theta - 3)}{2}\left(\frac{d}{x}\right)^2]d\theta = -\frac{3qd^2}{16\pi\varepsilon x^4} \qquad \text{(Equation 4.4)}$$

Figure 4.6 (b) shows the electric field generated by a triplet as compared to the electric field generated by a charge. It can be seen that a triplet and a charge have substantially different Coulomb-interaction scales: small and large interaction radii, respectively, with a nearby triplet. It has been determined that the TTA interaction radius is about 0.5 nm[91]. Eq. (4) indicates that the electric field generated by a triplet at 0.5 nm is equivalent to the electric field generated by a charge at 2.9 nm (Figure 4.6 (b)).

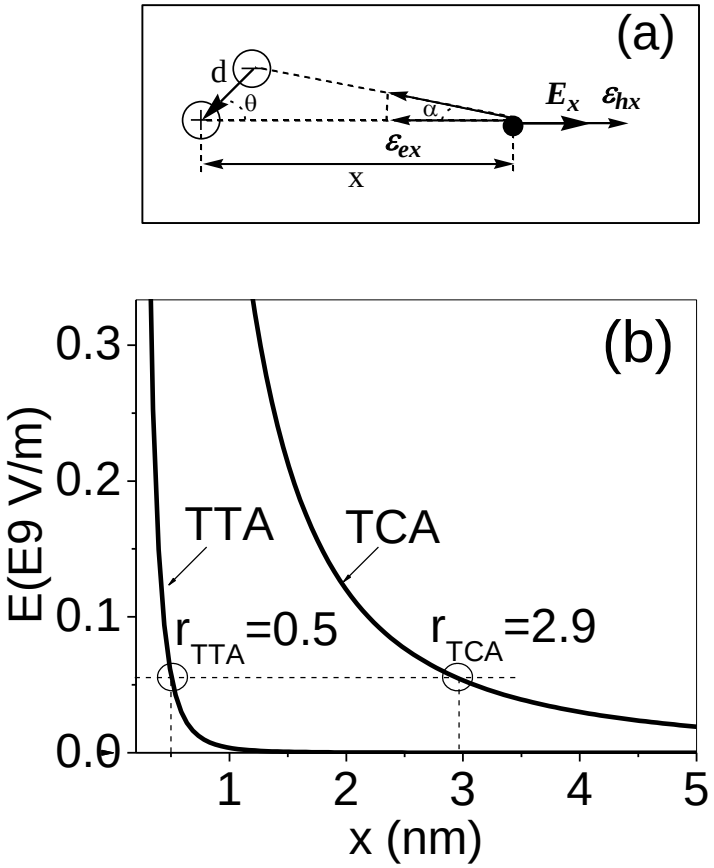

Figure 4.6 (a) Schematic to show electrical field at x axis generated by an electrical dipole assumed from a triplet exciton. ε_{ex} and ε_{hx} are the electric fields at x axis generated by electron and hole in an dipole. (b) Electric fields for triplet and charge as a function of distance. The effective field-interaction radii (r_{TTA} and r_{TCA}) are 0.5 nm and 2.9 nm for a triplet and a charge, respectively

This means that the TCA can occur at a longer distance as compared to the TTA. The experimental studies on fluorescence quenching have also found that an exciton can Coulombically react with a charge in an ultra-long distance of about 14 nm in a single

polymer chain[92]. As a result, the TCA becomes a dominate process in organic light-emitting and photovoltaic systems when excessive charges are available within close proximity from charge injection or exciton dissociation. This TCA is accountable for negative MFE_{EL} in organic semiconducting materials. It should be also noted that the TTA can be a dominant process in photoluminescence generated by Frankel excitons when triplets are confined within close proximity. This is because the photoluminescence lacks excessive carriers in light-emitting materials under photoexcitation. The time-resolved PL measurement indicates that this TTA-induced delay fluorescence can generate a negative component in magnetic field effects on photoluminescence (MFE_{PL}). However, the steady-state fluorescence only shows negligible MFE_{PL} in organic materials under photoexcitation because this delayed fluorescence is only a limited component as compared to prompt fluorescence from excitonic states. We should also note that, when prompt fluorescence is removed by directly exciting triplets, the TTA can be observed in steady-state from delayed fluorescence with negative MFE_{PL} under photoexcitation. Nevertheless, our experimental studies indicate that the TCA is a dominate process in organic light-emitting and photovoltaic systems where excessive charge carriers are available. Combining magnetic field-dependent ISC and TCA can lead to both positive and negative MFE_{EL} as schematically shown in Figure 4.7.

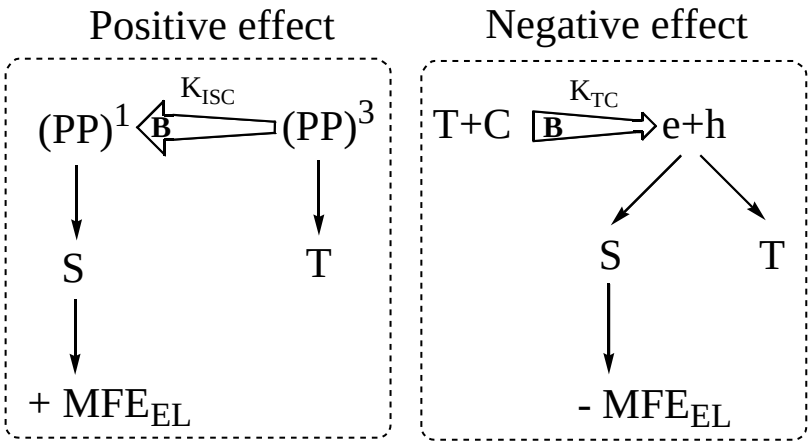

Figure 4.7 Schematic diagrams to show positive and negative MFE_{EL} generated by magnetic field-increasing ISC and magnetic field-decreasing TCA.

4.5 Conclusion

In summary, we studied negative MFE_{EL} at low filed (< 300 mT) based on electro-fluorescence and electro-phosphorescence through adjusting triplet density by using Dexter transfer, charge confinement by using band offsets, and exciton/charge ratio by un-balancing bipolar injection in OLEDs. We discussed two possible mechanisms: TCA and TTA in the generation of negative MFE_{EL} based on the light-emitting $Ir(mppy)_3$:PFO composite with inter-molecular SOC and dual electro-fluorescence and electro-phosphorescence. We found that increasing triplet exciton density can lead to a negative MFE_{EL} in electro-fluorescence in the PFO matrix by transferring the high-density triplets formed in the charge-trapping $Ir(mppy)_3$ molecules to the PFO matrix through Dexter

process. In addition, confining triplet excitons and charges by using double-layer structure can clearly generate a negative MFE_{EL} in electro-fluorescence. However, increasing triplet exciton density by increasing injection current density does not appreciably change the negative MFE_{EL} in electro-fluorescence. Finally, we adjusted balancing degree between injected electrons and holes to change the exciton/charge ratio to enhance the TCA. We found that enhancing the TCA can directly generate negative MFE_{EL} in the ITO/PFO/PMMA/Al OLED. We can therefore conclude that the TCA is a dominant process as compared to the TTA in organic semiconducting materials. In particular, the TCA generates a negative component in MFE_{EL} in organic electroluminescence. As a result, the negative MFE_{EL} form a principle to experimentally reveal triplet-related useful and non-useful processes in organic light-emitting and photovoltaic devices.

CHAPTER 5

SPIN-SPIN INTERACTION IN ORGANIC SEMICONDUCTORS

5.1 Abstract

In this chapter, we report that both significant magnetic field effect on the electroluminescence (MFE_{EL}) and current (MC) were induced in strong spin orbital coupling iridium complex based OLED device after introducing the non-magnetic insulating blocking PVA layer. This experimental result indicates the importance of interface in generating magnetic responses. Capacitance-voltage studies indicate that sufficient charge accumulation at the interface can generate the short distance carrier capture to initiate spin-spin interaction of charge carriers, leading to capture based MFE_{EL} and MC. Moreover, MC and MFE_{EL} can be tuned between positive and negative values by changing the interplay of spin-spin interaction. As a result, changing spin-spin interaction of inter-charge carriers presents a new pathway to tune magnetic field effects in organic semiconductors.

5.2 Introduction

In organic semiconductor devices, it has been found that external magnetic field can generate significant magnetic responses in electroluminescence, photoluminescence, photocurrent and electric current[29,30,32,33]. These magnetic responses are caused by the change of singlet/triplet ratio in intermolecular electron-hole pairs. It is generally accepted that based on the statistics of spin multiplicities, the theoretical limit of singlet ratio is 25% under the electrical excitation, although this ratio may be higher in some conjugated polymers. The external magnetic field can affect the spin-dependent processes

during electron-hole pairs and consequently change the singlet/triplet ratio. In organic semiconductors, two important spin-dependent processes can be affected by external magnetic field, intersystem crossing (ISC)[29,32,37,38] in intermolecular electron-hole pair states and short range inter-charge spin-spin interaction[42,43,44,93]. The intermolecular electron-hole pairs are loosely bonded, with relatively longer distance compared to intramolecular electron-hole pairs. The relative long separation distance will lead to small exchange energy between singlet and triplet states. This makes the magnetic interaction possible to affect the spin-dependent process in intermolecular electron-hole pairs. It should be noted that spin-dependent processes must require both energy and spin momentum conservation to occur. The spin-momentum conservation can be satisfied by internal magnetic interaction, such as hyperfine interaction and spin-orbital coupling. When an external magnetic field is comparable to internal magnetic interaction, the spin-momentum conservation can be partially broken. Breaking the spin-momentum conservation can essentially affect the spin-dependent processes of intermolecular electron-hole pairs and change the singlet/triplet ratio of intermolecular electron-hole pairs. Due to the different dissociation[19,32]and recombination properties of singlet and triplet electron-hole pairs, it consequently generates those magnetic responses. Spin-spin interaction can generate the magnetic response in either in excited states or in charge transport process. In excited states, strong spin-spin interaction prefers the formation of singlet excited states at short electron-hole capture distance[94]. An external magnetic field can disturb the spin-spin interaction and consequently change the singlet to triplet excited states ratio. In charge transport process, inter-charge spin-spin interaction also favor

singlet spin configuration to triplet spin configuration due to strong on-site exchange energy. Because anti-parallel singlet states and spin parallel triplet states have different magnetic dipole moment, triplet states experience stronger magnetic scattering and thus have lower mobility than the singlet states. External magnetic field can perturb this inter-charge spin-spin interaction and generate more triplet states, leading to a change in charge mobility and a mobility based MC.

In this letter, we selected a heavy metal iridium complex, bis [2-(2'-benzothienyl)-pyridinato-N,C3'] iridium (III) (acetylacetonatonate) [$Btp_2Ir(acac)$], which shows negligible magnetic response in bulk material because of its strong spin orbital coupling (SOC) strength, to study spin-spin interaction at the organic layer interface. In order to enhance the spin-spin interaction, the double layer architecture of organic light emitting devices (OLEDs), ITO/light emitting layer/blocking layer/Al, was employed to confine the charge carriers at the interface. Both organic insulating and semiconducting materials are tested as blocking layers. We found that the remarkable magnetic field effects on the electrical current (MC) and electroluminescence (MFE_{EL}) were induced by the interface between non-magnetic organic semiconducting light emitting layer and non-magnetic organic insulating blocking layer. In contrast, insignificant magnetic field response was observed in the device with the interface between non-magnetic organic semiconducting light emitting layer and non-magnetic organic semiconducting blocking layer. Moreover, the MC and MFE_{EL} could be tuned by adjusting the thickness of blocking layer to control the spin-spin interaction through changing the electron hole capture distance. As a result,

changing the inter-charge spin-spin interaction provide a new methodology to control the magnetic responses in organic semiconducting materials.

5.3 Experimental

The organic phosphorescent material, $Btp_2Ir(acac)$ (Ir67), was purchased from American Dye Source, and poly(methyl methacrylate) (PMMA), poly(vinyl alcohol) (PVA), 2,9-Dimethyl-4,7-diphenyl-1,10-phenanthroline (BCP), 4,4′-Bis(9-carbazolyl) -1,1′-biphenyl (CBP), and Copper(II) phthalocyanine (CuPc) were purchased from Sigma-Aldrich. All materials are used as received. The molecular structure of materials used in this experiment is shown in Figure 5.1

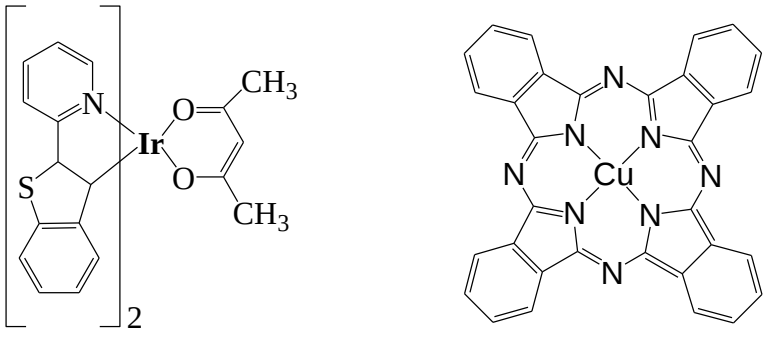

$Btp_2Ir(acac)$ CuPc

Figure 5.1 Chemical structures of $Btp_2Ir(acac)$ and CuPc

The Ir67 molecules were dissolved with the inert polymer matrix PMMA by a weight ratio of 4:2.5 in chloroform. The 80 nm thick films of the Ir67:PMMA composite were spin casted on the pre-cleaned indium tin oxide (ITO) glass substrates from the above

chloroform solution as the light emitting layer. And different concentration of PVA aqueous solution were spin cast on the top of already formed Ir67/PMMA composite layer as thin insulating blocking layers. All of these organic films were prepared under the nitrogen atmosphere protection. The double layer Ir67:PMMA/CBP, Ir67:PMMA /BCP and Ir67:PMMA/CuPc OLEDs were formed by spin coating Ir67:PMMA composite underlayer followed with thermal evaporation of CBP, BCP, CuPc at a high vacuum of no less than 2×10^{-6} torr. Finally, 50 nm Al electrode was thermal deposited at the vacuum of 2×10^{-6} torr. The thickness of the films was measured by a Veeco AFM profiler. The magnetic field effects were measured by positioning the OLEDs in the gap of two poles of an electromagnet. The electroluminescence was characterized by a Jobin Yvon Fluorolog-3 spectrometer with an optical fiber connection. The magnetocurrent was targeted to the injection current of 20 mA/cm^2 for the OLED. The magnetocurrent (MC) refers to the current change $(I_B - I_0)/I_0$ caused by the magnetic field, where I_B and I_0 are the injection current with and without an applied magnetic field. The magnetic effect on electroluminescence (MFE_{EL}) is defined as the electroluminescence change $(EL_B - EL_0)/EL_0$ under the influence of a magnetic field. The EL_B and EL_0 are the electroluminescence with and without an applied magnetic field, respectively. The capacitance-voltage (C-V) characteristics were measured by an Agilent E4980A LCR meter. A 50 mV alternating current (AC) signal superimposed on direct current (DC) bias was used to measure the device capacitance at low frequency 300 Hz.

5.4 Results and Discussion

In Figure 5.2, negligible MC was observed from the single layer Ir67:PMMA composite device within our measurement accuracy. However, it is interesting to observe a clear MC after spin casting a second insulating PVA blocking layer. It should be noted that the aqueous PVA solution does not dissolve the Ir67/ PMMA underlayer, it only adds an interface between PVA and Ir67:PMMA composite without changing electrical and optical properties in the bulk. This result clearly indicates that the interface between Ir67:PMMA composite layer and PVA layer is correspondent to the observed MC because the Ir67:PMMA composite itself doesn't show clear MC in bulk. It has been experimentally showed that pure iridium complexes do not show appreciable magnetic field response because of its strong spin orbital coupling (SOC) strength. An external magnetic field cannot compete with the strong internal magnetic interaction generated by the spin orbital coupling, and subsequently cannot effectively change the singlet/triplet ratio through ISC or spin-spin interaction. Therefore, negligible magnetic field response would be observed in the single layer Ir67: PMMA composite.

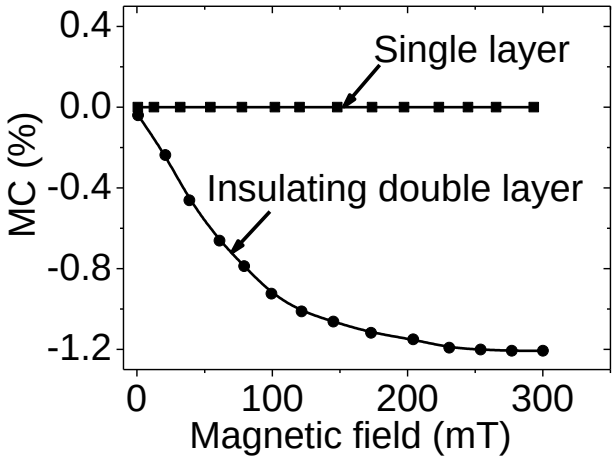

Figure 5.2 MC of single layer device and double layer device with insulating blocking layer.

In Figure 5.3 (a), we found the increasing thickness of second insulating layer PVA can further tune the MC from positive to negative value. The MC is about +0.2 % for a 1 nm thin PVA second layer. The MC gradually changes to around -0.5 % when the PVA thickness increases up to 3 nm. Further increasing the PVA film thickness to 5 nm can increase the negative MC up to -1.2 %. It is known that inserting the insulating blocking layer PVA will yield a large injection potential barrier due to large energy band gap of insulating material. At a low forward bias, electron carriers are difficult to be injected from the cathode and majority holes injected from ITO side will be accumulated at the interface between Ir67: PMMA composite and PVA. When more and more charge carries are confined at a small region of the interface, the inter-charge distance become smaller due to the spatial proximity. As a result, spin-spin interaction would be likely occur at

short inter-charge capture distance. Here, we propose the observed MC may be due to the change of singlet and triplet ratio through magnetically perturbing spin-spin interaction at the interface between strong spin orbital coupling organic semiconductor Ir67 and organic insulating material PVA.

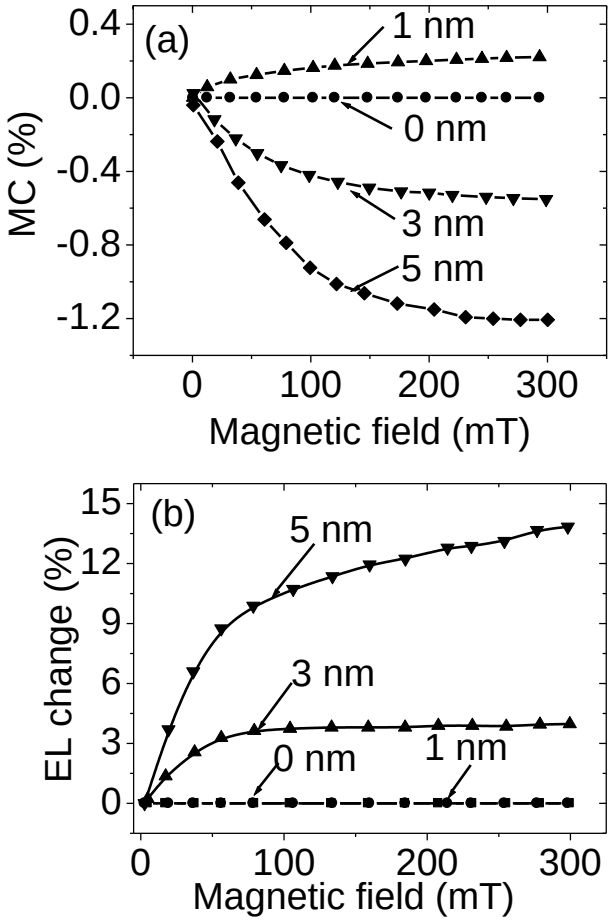

Figure 5.3 (a) MC and (b) MFE_{EL} of ITO/Ir67: PMMA/PVA (x nm)/Al at different PVA thickness.

Specifically, an external magnetic field will reduce the singlet formation and increase the triplet formation. The MC generated by spin-spin interaction can be further confirmed by examining the MFE_{EL} as shown in Figure 5.3 (b). Similarly with MC result, a significant positive MFE_{EL} from the triplet emission of Ir67 is induced after inserting the PVA layer. The positive phosphorescence MFE_{EL} increases with the thickness of PVA layer. The maximum MFE_{EL} is around 14% for the double layer device with 5 nm PVA. The positive phosphorescence MFE_{EL} result clearly reflects the increased formation of triplet excited states under an external magnetic field, which is in good accordance with the prediction by magnetically perturbing spin-spin interaction of intermolecular electron-hole pairs.

In order to probe what has happened at the double layer interface, we carried out the capacitance–voltage (C-V) measurement for the single layer devices and PVA based double layer devices with different PVA thickness, as shown in Figure 5.4. In the single layer Ir67:PMMA composite device, the capacitance of device almost remains constant at low voltage which is equal to the geometrical capacitance followed by a sharp decrease at relative high voltage regime. The capacitance essentially reflects the capability of charge storage in the device. Thus, the decrease of the capacitance is attributed to the recombination of injected electrons and holes[95], which consequently reduces the amount of charge stored in the device. In contrast, the capacitance of double layer device shows a significant increase regime before the capacitance decrease dramatically with the applied voltage. The increase of the capacitance provides a clear evidence for the presence of interfacial charge at the IR67: PMMA/PVA organic-organic interface. It should be also

noted that the C-V peak position goes to higher voltage with increasing the PVA thickness.

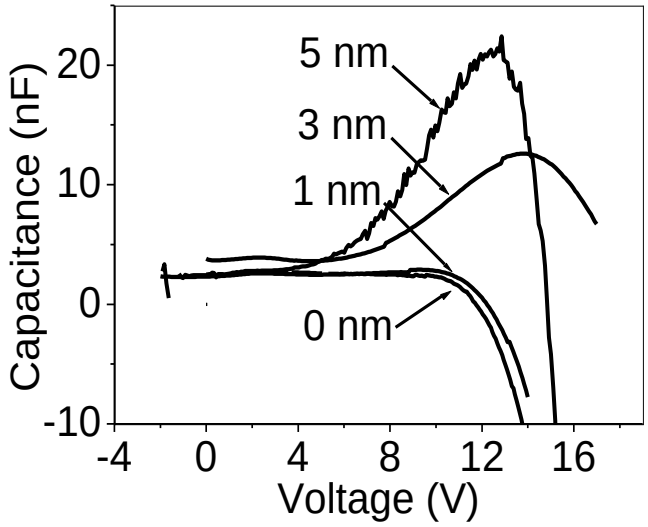

Figure 5.4 Thickness dependent C-V measurement of ITO/Ir67:PMMA/PVA (x nm)/Al

C-V curve of the double layer device with 1 nm PVA shows a small but apparent increase compared with the single layer device. Further increasing the PVA thickness up to 3 nm, the capacitance can increase almost seven times as much as the geometrical capacitance. This result indicates that a number of charge carriers are accumulated at the Ir67/PVA interface, which is consistent with the theoretical predication. Increasing the PVA thickness increases the injection barrier of electron. More and more pre-injected holes are confined at the interface near the cathode.

We now discuss the possible explanations for these interface induced MC and MFE_{EL}.

In general, an external magnetic field can modulate the electrical current either by changing the charge mobility μ or charge carriers density *n*, generating mobility based

MC and density based MC. The reason is that the current density J through the device could be simply expressed by $J = n\mu qE$, where n is the charge density, μ is the carrier mobility, n is the electron charge and E is the applied electric field. In the mobility based MC, the charge mobility is sensitive to magnetic field when the inter-charge spin-spin interaction exists at short inter-charge distance. It is known that singlet and triplet experience different spin scattering strength during charge transport and consequently have different mobility. Spin-spin interaction favors the singlet formation at short inter-charge capture distance. An external magnetic field can perturb the inter-charge spin interaction and subsequently changes the spin configuration of inter-charge, leading to a change in charge mobility and a mobility based MC. In the density based MC, an external magnetic field can modify the singlet and triplet excited states ratio through magnetic field sensitive intersystem crossing (ISC) in the intermolecular electron-hole pairs (polaron pairs) or interrupt the spin-spin interaction in short range intermolecular electron-hole pairs. Specifically, the increasing singlet ratio through ISC leads to an increase in the charge density due to the relatively larger dissociation rate of singlet intermolecular electron-hole pair states. It should be noted that the molecular environment and electronic properties of the interface are distinct from the case in the bulk. It is likely that the interface might modify the magnetic interaction at the interface and thus contributes to the different magnetic response. Three possible mechanisms are discussed as below: (1) Intermolecular spin orbital coupling, (2) Spin-spin interaction, (3) Hyperfine interaction.

First, the SOC interaction is strong in the bulk due to the heavy metal effect of iridium

atom. An external magnetic field cannot compete with the strong internal magnetic field caused by spin orbital coupling and hyperfine interaction, leading to negligible MC and MFE_{EL}[38,53,66,79]. However, the PVA used as the second layer only contains light atoms and consequently has the weak SOC strength. The intermolecular spin-orbital coupling formed between Ir67 and PVA can weaken the effective spin orbital coupling strength at the interface and this may open the channel for the intersystem crossing based MC and MFE_{EL}. Specifically, an external magnetic field can increase the singlet but decrease the triplet formation at the polaron pair states by enhancing the intersystem crossing through spin momentum conservation. The increase of the singlet formation essentially leads to a positive MC（+MC） because the singlet has relatively large dissociation rate than the triplet due to its ionic nature. Second, we have already shown that a large amount of charge carriers are accumulated at the interface of Ir67:PMMA/PVA. At the interface, the electrons and holes capture at very short distance and experience the spin-spin interaction. The spin-spin interaction favors the singlet formation. An external magnetic field can perturb the spin-spin interaction and consequently reduce the singlet ratio and increase triplet ratio during electron-hole capture. As a consequence, a negative MC can be observed because singlets and triplets have high and low dissociation rate, respectively. It should be noted that at the Ir67:PMMA/PVA interface the spin-spin interaction between same polar charge carriers is also possible, because a large amount of charge carriers accumulated at the interface. Inter-charge spin-spin interaction favors the singlet formation at short inter-charge capture distance. An external magnetic field can perturb the inter-charge spin interaction and subsequently increase the triplet spin configuration

of inter-charge, leading to a decrease in charge mobility and causing mobility based negative MC due to that triplet experience stronger spin scattering during charge transport and consequently have lower mobility than singlet. Third, it has been recently reported that hyperfine interaction (HFI)[96,97,98] between the spin of charge carrier and spin of nuclear can generate the magnetic response in organic semiconductor by affecting the spin mixing of the singlet and triplet states. It is believed that strong hyperfine interaction is a prerequisite for the observation of MC. Therefore, it is reasonable to consider whether the distinct MC response from the interface is due to the different hyperfine interaction strength between the bulk and interface. Since we consider that the observed MC and MFE_{EL} are closely related to the interface, we can further examine this proposition by modifying interface to identify the origin of MC. Figure 5.5 (a) shows the MC and MFE_{EL} from the ITO/Ir67:PMMA/Semiconducting layer/Al devices by evaporating different organic semiconductor materials as the blocking layer instead of insulating PVA layer. BCP, CBP and CuPc were selected because they can form different band offsets relative to bulk material Ir67 as shown inset of Figure 5.5 (a). As seen from the energy diagram, the HOMO of BCP is higher than the Ir67 while the LUMO keeps the same with Ir67. This type of band diagram can block the hole injection from the Ir67 side. Ir67: PMMA/CBP structure can confine both injected electrons and holes at the interface, which is in analog to the energy structure of Ir67:PMMA/PVA.

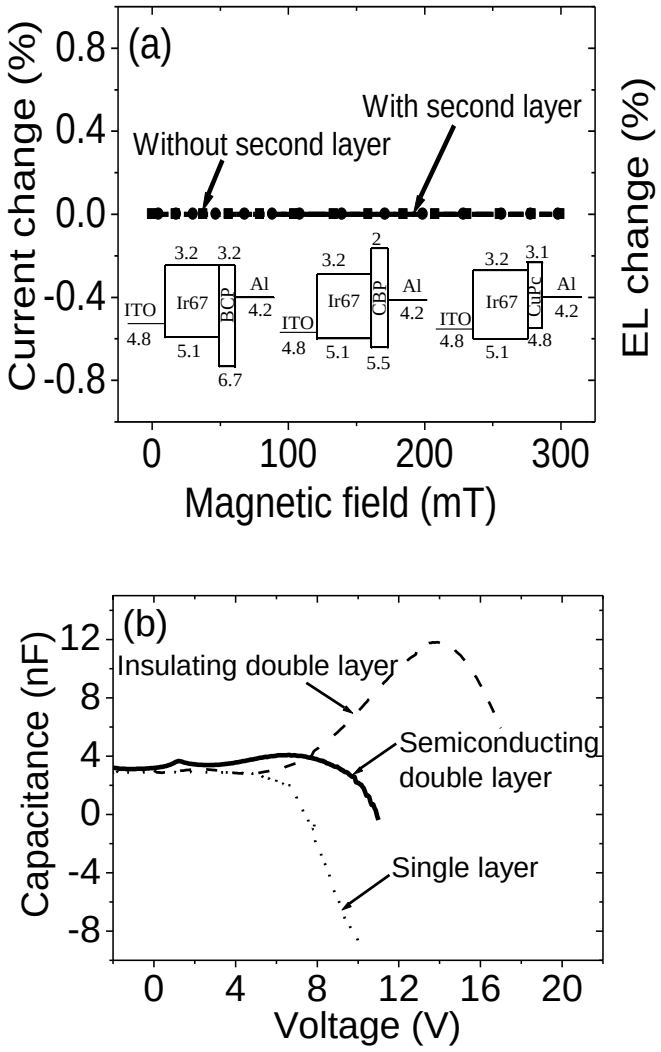

Figure 5.5 (a) MC and (b) C-V measurement of single layer device and double layer device with semiconducting blocking layer, BCP, CBP, and CuPC, the inset in (a) is the energy band diagram.

In Ir67:PMMA/CuPc device, negligible charge will be accumulated at the interface due to its favorable energy level. Surprisingly, none of three types of devices with different

energy diagram exhibits the clear MC, which is distinct from the case in insulating material based-double layer device. First, it should be noted that both organic semiconducting material and organic insulating material used as the blocking layer contain the hydrogen atoms in which have strong hyperfine coupling strength. In comparison of different MC behaviors between semiconducting based-double layer and insulating based-double layer, we can exclude the possibility that the observed interface induced-MC originated from the hyperfine interaction. Second, it is known that magnetic field response can be tuned by changing the balance degree of bipolar injection for the bulk material[37]. By introducing the insulating layer PVA, the balance degree of bipolar injection of the device could be greatly changed because PVA can reduce the minority electron injection from the cathode due to its wide energy bandgap. Nevertheless, we observe the negligible magnetic field response no matter how we adjust the bipolar injection by using different device structures as shown in Figure 5.5 (a). Upon further consideration, modification of the balancing degree of bipolar injection can be also excluded as the reason of the MC. Furthermore, we consider the major difference between organic insulating material and semiconductor material. One significant difference should be particularly noted that organic insulating material and semiconductor material have different conduction mechanisms. In organic semiconductor, the charge carriers are transported through hopping process among organic semiconductor molecules. However, the charge carriers are conducted through one step or multi-step tunneling process in organic insulating materials. It is generally accepted that insulating material PVA cannot hold the charge carriers injected from the cathode as

well as organic semiconductors. Therefore, the charge carries confined at the interface of insulating-based double layer device are spatially closer in proximity than in semiconducting-based double layer device. In this case, the spin-spin interaction between same polar or opposite polar charge carriers is more likely to occur. To probe the charge accumulation and possible spin-spin interaction at the interface, we also carried the C-V measurements for the organic semiconducting based double layer device. Figure 5.5 (b) compares the C-V curve for three devices: single layer device ITO/Ir67:PMMA/Al, insulating based-double layer device ITO/Ir67:PMMA/PVA (5nm)/Al and semiconducting based-double layer device ITO/Ir67:PMMA/BCP (5nm)/Al. It should be also noted that the increase of the capacitance of insulating based double layer device is more pronounced than semiconducting based double layer device. This results indicates that more injected charge carriers are confined at Ir67:PMMA/PVA interface. Due to strong confinement effect, the accumulated charge carriers at the insulating interface are more closed to each other and the electron-hole pairs are also in short capture distance. At very short inter-charge distance or capture distance, the spin-spin interaction becomes dominant, which facilitates the formation of singlet states. When applying external magnetic field, the spin-spin interaction would be disturbed to generate fewer singlet but more triplet excited states. This could be directly supported by the positive MFE_{EL} of the triplet emission from Ir67. Thus, the spin-spin interaction of electron-hole pair is more likely respond to the observed magnetic responses while the spin-spin interaction of same polar charge pair is also possible. However, when we introduce semiconducting material as the second layer, there is no strong confinement for the charge carrier at organic

hetero-layer interface and corresponding inter-charge distance or capture distance becomes larger. In this case, the short range spin-spin interaction could be ignored. The absence of spin-spin interaction would lead to negligible magnetic response in semiconducting based double layer device.

At last, we give the possible explanation for the observed MC and MFE_{EL} in the PVA based double layer device based on electron-hole pair mechanism. In general, the external magnetic field can change the singlet and triplet ratios either by perturbing electron-hole pair spin-spin interaction during the short distance electron-hole capture or by changing the intersystem crossing after electron-hole capture, generating capture based MFE and intersystem-crossing based MFE. The capture-based MFEs require short-distance electron-hole capture through charge confinement to introduce spin-spin interaction. The intersystem crossing-based MFEs occur when the electrons and holes are captured at long distances without experiencing inter-charge spin-spin interaction. The observed MC is the sum of positive and negative component: -MC from the spin-spin interaction and +MC from the intersystem crossing. Therefore, we can tune the MC by adjusting the relative contributions from the spin-spin interaction and intersystem crossing in organic semiconductors. As shown in Figure 5.3, MC and MFE_{EL} can be tuned by changing the thickness of second insulating PVA layer. It is known that changing the thickness of PVA layer can affect the confinement of charge carriers at the electrode interface and subsequently change the electron-hole distance. The double layer device with 1nm thin PVA second layer cannot effectively accumulate the appreciable charge carriers at the interface. The charge density at the interface is low and thus the electron-hole capture

distance is comparable large. Therefore, capture based MFE is negligible and the intersystem crossing based MFE is dominant, leading to positive MC. However, thick PVA layer, such as 3nm and 5nm, can spatially confine a large amount of charge carriers at short distance range and may greatly enhance the spin-spin interaction, yielding negative MC and positive $MFE_{EL.}$

5.5 Conclusion

In conclusion, we found that both MC and MFE_{EL} were observed from the strong spin orbital coupling iridium complex after introducing the insulating blocking layer PVA. This result indicates the importance of interface in generating magnetic responses (MFE and MC). However, introducing organic semiconductor/semiconductor interface did not show any appreciable magnetic response. The reason is explained as only semiconductor/insulating interface can provide efficient charge accumulation to generate the short distance carrier capture to initiate spin-spin interaction of charge carriers. It should be noted that spin-spin interaction is responsible to the observed magnetic response but spin-spin interaction happens between same polar charges carriers or electron-hole pairs is not clear at this moment. Furthermore, we found that MC and MFE can be tuned between positive and negative values by changing the interplay of spin-spin interaction. As a consequence, controlling the spin-spin interaction at the interface opens us a new way to generate the magnetic responses in organic semiconductors.

CHAPTER 6

ELECTRICAL DIPOLE-DIPOLE INTERACTION EFFECTS ON MAGNETOCURRENT IN ORGANIC PHOSPHORESCENT MATERIALS

6.1 Abstract

This chapter reports the experimental studies on electrical dipole-dipole interaction effects on magnetocurrent (MC) and magneto-electroluminescence (MFE_{EL}) based on two phosphorescent dyes: heavy-metal complex $Ir(ppy)_3$ and $Ir(ppy)_2(acac)$ with strong spin-orbital coupling but different electrical dipole moments. We find that the $Ir(ppy)_3$ with strong electrical dipole moment shows negligible MC and MFE_{EL}. However, the $Ir(ppy)_2(acac)$ with weak dipole moment exhibits appreciable MC and MFE_{EL}. The experimental results suggest that the electrical dipole-dipole interaction can change the MC and MFE_{EL} from capture-based regime, where charge carriers are captured through spin-dependent process at short distance, to intersystem crossing-based regime, where charge carriers are captured through spin random process at long distance. As a result, changing electrical dipole-dipole interaction presents a new pathway to tune magnetic field effects in organic semiconductors.

6.2 Introduction

It has been experimentally discovered that an external magnetic field can change the electrical injection current, generating magnetocurrent (MC)[32,33,38,39,66], in the organic semiconducting materials. In essence, the MC originates from magnetic field-dependent singlet and triplet ratios. This is because the singlets and triplets have different contributions to the generation of charge carriers through dissociation and charge reaction

due to their different ionic natures and lifetimes. In general, the singlets and triplets can dominate dissociation and charge reaction, respectively, in the generation of charge carriers. Therefore, changing the singlet and triplet ratios can affect the electrical injection current through dissociation[32,38] and charge-reaction[37,39,40]channels. In principle, an external magnetic field can change the singlet and triplet ratios through two different ways either by perturbing the inter-charge spin-spin interaction[42,43,93] during electron-hole capture at short distance, or by modifying the intersystem crossing (ISC)[32,36,37,38,40] after electron-hole capture at long distance. As a result, the MC can generally consist of capture-based and ISC-based components. Specifically, in capture-based MC, the electron-hole capture experiences inter-charge spin-spin interaction at short distance. When this spin-spin interaction exists, the electron-hole capture favors the formation of singlet states due to exchange energy[94]. An external magnetic field can perturb this spin-spin interaction and consequently changes the inter-charge spin configuration, leading to a decrease in singlet formation and an increase in triplet formation during the capture at short distance. On contrast, in ISC-based MC, the electron-hole capture experiences negligible spin interaction at long distance and undergoes a spin-random formation of singlet and triplet states with the ratio of 1:3. An external magnetic field can not affect the capture but can change the ISC with the consequence of increasing the singlet ratio and decreasing triplet ratio in polaron-pair states after the capture at long distance. More importantly, the inter-molecular dipole-dipole interaction can change the inter-charge capture distance, switching charge capture between spin-dependent and spin-random regimes. Specifically, increasing the inter-molecular dipole-dipole interaction can enlarge

the capture distance and changes the MC from capture-based regime occurring at short capture distance to ISC-based regime occurring at long capture distance. It is noted that, in ISC-based regime, spin-orbital coupling (SOC) is accountable for the spin momentum conservation necessarily required for ISC. When an external magnetic field is stronger than SOC, the spin momentum conservation involved in ISC can be modified, changing the singlet and triplet ratios in polaron-pair states. The change in singlet and triplet ratios in polaron-pair states can be essentially reflected as the change in singlet and triplet ratios in excitonic states when polarons are evolved into excitons, leading to MFE_{EL} and MC in ISC-based regime. However, for the heavy-metal complex molecules with the strong SOC strength, an external magnetic field has little influence on the ISC in polaron-pair states and consequently generates un-appreciable change in singlet and triplet ratios through ISC. As a result, phosphorescent materials with strong SOC can usually show negligible ISC-based MC[38,66,79]. However, when the spin–spin interaction exists in the organic phosphorescent materials, an external magnetic field can change the singlet and triplet ratio during spin-dependent capture at short distance by perturbing the inter-charge spin-spin interaction. It should be noted that changing the singlet and triplet ratios can lead to MC through two different channels: dissociation dominated by singlet excitons[32,45] and charge reaction dominated by triplet excitons[37,39,40]. The dissociation can directly separate excitons into free charge carriers through Onsager process[99,100]. The charge reaction can break excitons through Coulomb interaction when an exciton Coulombically interact with a charge in close proximity. Although both singlet and triplet excitons can involve in dissociation and charge reaction, the singlet and triplet excitons

can dominate dissociation and charge reaction, respectively, in the generation of charge carriers. This is because singlet excitons have stronger ionic natures in their wavefunctions and can largely dissociate into polaron pairs and then free charge carriers[19,32,45]. Triplet excitons can have sufficient Coulomb contact-time with charges due to their long lifetimes and largely contribute to charge reaction to generate free charge carriers. Therefore, decreasing singlet ratio can yield a negative MC through dissociation but increasing triplet ratio can lead to a positive MC through charge reaction. In this letter, we report the effects of inter-molecular dipole-dipole interaction on MC and MFE_{EL} by using select two phosphorescent dyes: fac-tris(2-phenylpyridine)iridium [$Ir(ppy)_3$] and bis(2-phenylpyridine)iridium acetylacetonate [$Ir(ppy)_2(acac)$] with strong and weak electrical dipole moments.

6.3 Experimental

The $Ir(ppy)_3$ and $Ir(ppy)_2(acac)$ are used as the emitting layers (EML) with the thickness of 30 nm in the multilayer OLEDs with indium-tin-oxide (ITO) as anode and aluminum (Al) as cathode. The device structure is ITO/HIL/HTL/EML/ ETL/EIL/Al. The HTL is the hole transport layer of N,N'-diphenyl-N,N'-bis(1-naphthylphenyl)-1,1'-biphenyl-4,4'-diamine (NPB) with the film thickness 40 nm. The ETL is the electron transport layer of 1, 3, 5-tris(N-phenylbenzimidazole-2-yl)benzene (TPBI) with the film thickness 20 nm. The HIL and EIL are hole and electron injection layers, respectively, from Molybdenum trioxide (MoO_3) with the film thickness of 8 nm and LiF with the film thickness of 1 nm to facilitate the hole and electron injection from corresponding

electrodes. This structure allows the excitons well confined in the iridium-complex based emitting layer. The chemical structures of material used in the experiment are listed in Figure 6.1

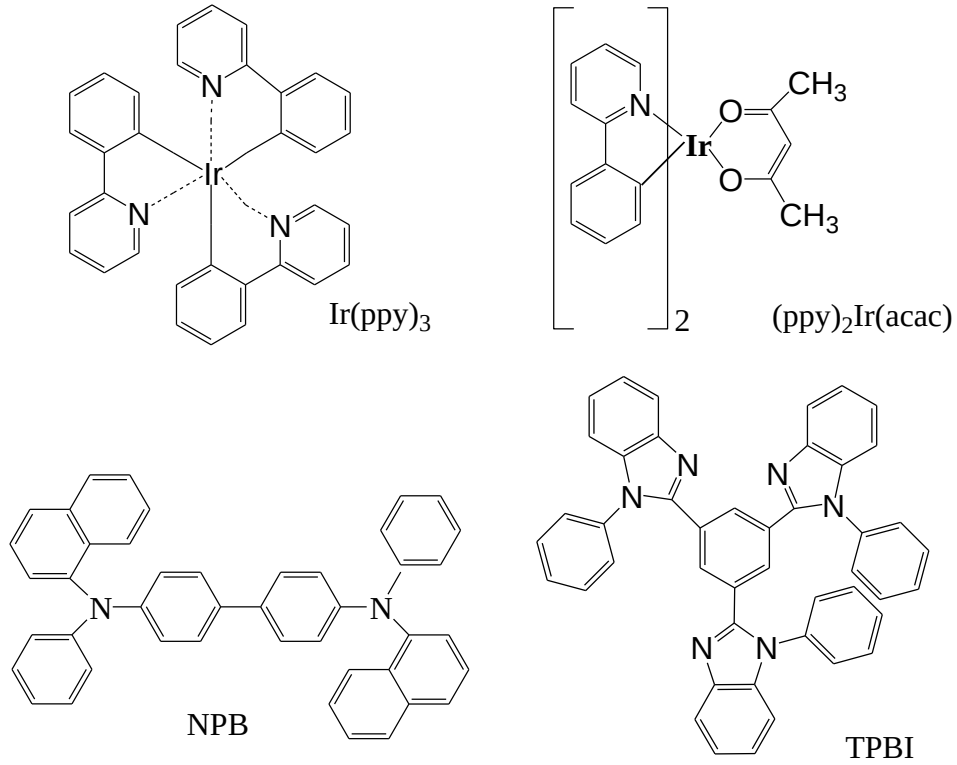

Figure 6.1 Chemical structures of $Ir(ppy)_3$, $(ppy)_2Ir(acac)$, NPB and TPBI

The devices were prepared on pre-cleaned ITO substrates. All molecular layers and Al electrodes were thermally evaporated in a high vacuum of 5×10^{-4} Pa. The current-voltage characteristics were measured by using a Keithley 2400 source meter. The electroluminescence was characterized by a Jobin Yvon Fluorolog-3 spectrometer with an optical fiber connection to the OLED placed in a magnetic field generated by an electromagnet. The MC was measured at constant voltage condition with the injection

current of 20 mA/cm^2. The MFE_{EL} was measured at constant current condition. The experimental errors for MC and MFE_{EL} are within 0.02 % and 0.2 %, respectively.

6.4 Results and Discussion

Figure 6.2 shows MC characteristics for the $Ir(ppy)_3$ and $Ir(ppy)_2(acac)$ based OLEDs. A clear positive MC is observed from the $Ir(ppy)_2(acac)$ based OLED with weak electric dipole moment (1.91D)[101]. The magnitude of MC is around 0.1 % measured at constant voltage 7 V. However, the $Ir(ppy)_3$ based OLED with large electric dipole moment (6.26 D)[101] exhibits a negligible MC. Because both $Ir(ppy)_3$ and $Ir(ppy)_2(acac)$ have strong SOC, the different MC characteristics can be attributed to the different electrical dipole moments of these two iridium-complex molecules. Specifically, inter-molecular dipole-dipole interaction can form an effective dielectric background and thus influences the charge-capture distance through electric screening effect[102]. Photochemistry studies have found that varying the dielectric constant of solvents can modify the average distance between the radical ions within radical pairs, and consequently change the magnetic effect on fluorescence intensity[62,64].

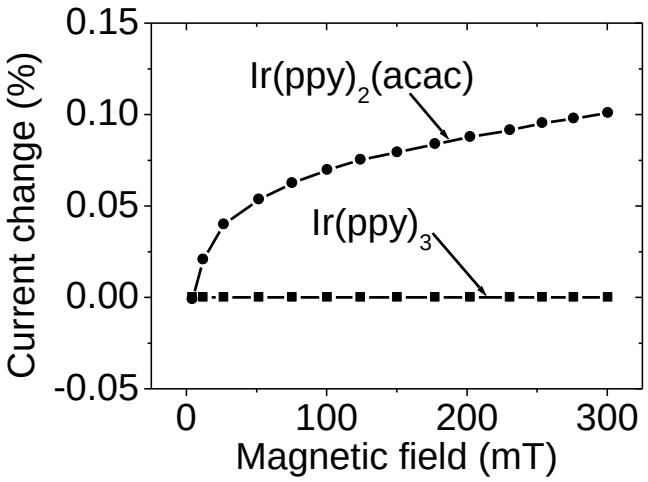

Figure 6.2 MC characteristics are shown for $Ir(ppy)_2(acac)$ based OLED with weak electric dipole moment (1.91 D) and $Ir(ppy)_3$ based OLED with strong electric dipole moment (6.26 D).

Here, we suggest that strong electrical dipole-dipole interaction between $Ir(ppy)_3$ molecules can enlarge the charge-capture distance and consequently leads to negligible inter-charge spin-spin interaction. We should note that negligible spin-spin interaction at long distance removes capture-based MC. In addition, strong SOC can make ISC-based MC un-appreciable. Clearly, capture-based MC is a possible channel to develop MC for phosphorescent materials with strong SOC. Therefore, whether inter-molecular dipole-dipole interaction can induce inter-charge spin-spin interaction during capture can essentially determine whether MC can be observed in iridium-complex molecules. For the $Ir(ppy)_3$ with strong electrical dipole moment, the overall MC becomes negligible (Figure 6.2) because of absence of inter-charge spin-spin interaction. In contrast, the

$Ir(ppy)_2(acac)$ has weak electric dipole-dipole interaction in ground states. The weak dipole-dipole interaction in ground states forms a weak dielectric background for the excited states in the $Ir(ppy)_2(acac)$. Therefore, the weak dipole-dipole interaction can lead to a short distance for electron-hole capture and consequently generates inter-charge spin-spin interaction during capture. This can enable capture-based MC through inter-charge spin-spin interaction. In capture-based MC it should be further pointed out that the spin-spin interaction favors the singlet formation in polaron pairs during charge capture. An external magnetic field can decrease singlet formation but increase triplet formation in polaron pairs by disturbing this spin-spin interaction during capture. Again, the decrease in singlets and the increase in triplets in polaron pairs can eventually reflect as the decrease in singlets and the increase in triplets in excitonic states when polaron pairs are relaxed into excitons. It should be noted that the decrease in singlets and increase in triplets in excitonic states should correspond to negative and positive MC through singlet dominated dissociation and triplet-dominated charge reaction, respectively. Therefore, the observed positive MC from the $Ir(ppy)_2(acac)$ clearly indicates that the triplet-dominated charge reaction is a main mechanism to generate MC in capture-based regime for phosphorescent materials.

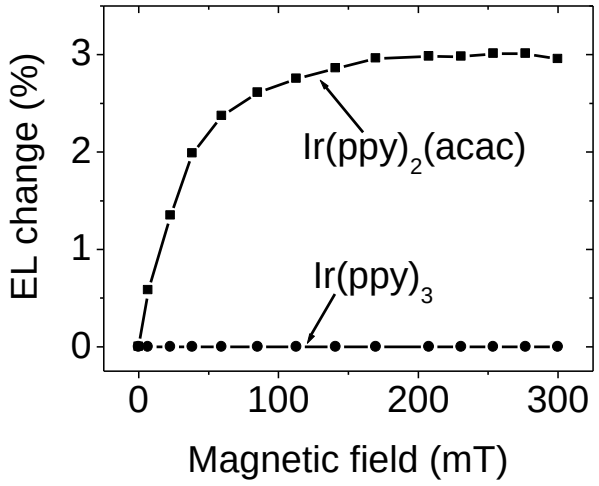

Figure 6.3 MFE_{EL} characteristics are shown at constant current density 20 mA/cm^2 for $Ir(ppy)_2(acac)$ and $Ir(ppy)_3$ based OLEDs.

To further confirm capture-based MC through inter-charge spin-spin interaction, we investigate the MFE_{EL} from both $Ir(ppy)_3$ and $Ir(ppy)_2(acac)$-based OLEDs. It can be seen in Figure 6.3 that the $Ir(ppy)_3$ based-phosphorescent OLED with strong electrical dipole moment shows un-appreciable MFE_{EL}. On contrast, the $Ir(ppy)_2(acac)$-based phosphorescent OLED with weak electrical dipole moment shows a clear positive MFE_{EL}. The magnitude of MFE_{EL} is about 3% measured at constant current density of 20 mA/cm^2 in the ITO/$Ir(ppy)_2(acac)$/Al OLED. Obviously, this positive MFE_{EL} indicates that an external magnetic field increases the triplet ratio in excitonic states in the phosphorescent $Ir(ppy)_2(acac)$. It is known that in heavy-metal complex materials an applied magnetic field less than 1 T is much weaker than internal SOC[86]. As a consequence, an applied external magnetic field cannot compete with internal strong SOC to affect the ISC. This

means that the ISC becomes insensitive to applied magnetic field in strong SOC materials, leading to negligible ISC-based MFE_{EL}. Therefore, our observed positive MFE_{EL} from the $Ir(ppy)_2(acac)$ must come from capture-based channel. This confirms that with weaker electrical dipole-dipole interaction an applied magnetic field can still change the singlet and triplet ratios in phosphorescent materials by disturbing the spin-spin interaction during electron-hole capture at short distance. Specifically, an applied magnetic field perturbs the spin-spin interaction during electron-hole capture and essentially decreases the singlet formation but increases the triplet formation, leading to positive MFE_{EL} in the $Ir(ppy)_2(acac)$ with weaker electrical dipole-dipole interaction. On contrast, a stronger electrical dipole-dipole interaction can correspond to a long electron-hole capture distance without inter-charge spin-spin interaction, removing spin-spin interaction and capture-based MFE_{EL}. Therefore, changing electrical dipole-dipole interaction presents a convenient methodology to generate capture-based MFE_{EL} in organic phosphorescent materials with strong SOC.

Furthermore, we use an external electrical field to modify the electron-hole capture distance in $Ir(ppy)_2(acac)$ based OLED with weak electric dipole moment. Figure 6.4 (a) shows the MFE_{EL} at different applied voltages for ITO/$Ir(ppy)_2(acac)$/Al OLED. The MFE_{EL} amplitude decreases with the increasing of applied voltage. At a low voltage of 3 V, the maximum MFE_{EL} is around 6 %. When the applied voltage increases up to 11 V, the magnitude of MFE_{EL} drops to 1.5 %. Further increasing the voltage will diminish the $MFE_{EL.}$ The experimental studies on electric field-modulated photoluminescence quenching have suggested that excitons can be converted into polaron pairs at 1MV/cm[103].

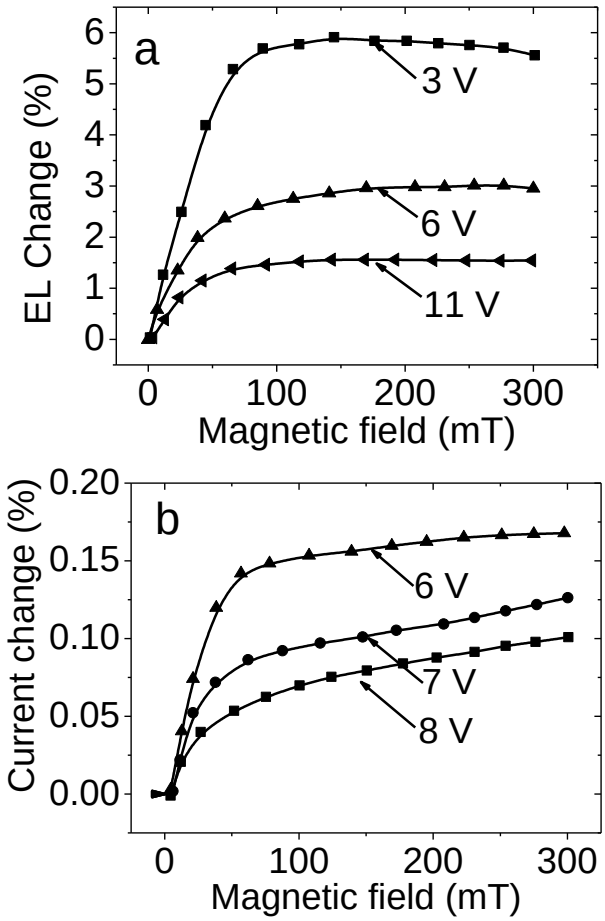

Figure 6.4 MFE_{EL} (a) and MC (b) characteristics are shown for $Ir(ppy)_2(acac)$ based OLED at different voltages.

This result indicates that the electron-hole capture distance can be enlarged by applying strong electrical field. As the electron-hole capture distance enlarges, the electron-hole pairs can dissociate into free charge carriers through Onsager process[99,104]. This can decrease the MFE_{EL} by reducing the density of polaron pairs with increasing applied voltage. In addition, we should note the following possibility that can also contribute to

the MFE_{EL} reduction upon increasing applied voltage. When the electron-hole capture distance increases with the increasing electrical field, the inter-charge spin interaction can decrease rapidly. This can remove capture-based MFE_{EL} in the $Ir(ppy)_2(acac)$. On the other hand, the strong SOC from the $Ir(ppy)_2(acac)$ molecules inhibits the redistribution of singlet and triplet ratios through ISC. Therefore, the overall MFE_{EL} can gradually decrease upon increasing applied voltage. As a result, we can observe a reduction in MFE_{EL} at higher voltages in the $Ir(ppy)_2(acac)$ based OLED. Moreover, the MC of $Ir(ppy)_2(acac)$ based OLED shows the similar voltage dependence as compared to MFE_{EL}. Clearly, this MC result further suggests that increasing applied voltage can decrease MFE_{EL} and MC through two possible channels: decreasing the density of electron-hole pairs through dissociation and weakening the spin-spin interaction through capture distance in phosphorescent materials.

6.4 Conclusion

In conclusion, our MC and MFE_{EL} studies have shown that the heavy-metal complex $Ir(ppy)_3$ with the strong electric dipole moment exhibits the negligible MC and MFE_{EL}. However, the heavy-metal complex $Ir(ppy)_2(acac)$ with weak electric dipole moment gives both MC and MFE_{EL}. The MFE_{EL} and MC comparison between $Ir(ppy)_3$ and $Ir(ppy)_2(acac)$ suggests that inter-molecular dipole-dipole interaction can be used to tune the magnetic responses in organic phosphorescent materials.

CHAPTER 7

TUNING THE MAGNETIC FIELD EFFECT ON THE FLUORESCENCE AND PHOSPHORESCENCE IN OLED

7.1 Abstract

In this chapter, we simultaneously monitor the magnetic field effect on the electro-fluorescence and electro-phosphorescence in OLED. The sign of fluorescence based MFE_{FEL} and phosphorescence based MFE_{PEL} can be tuned either in the same direction (both positive or both negative) or in opposite direction (one is positive and the other is negative) by controlling the intersystem crossing, energy transfer and spin-spin interaction processes. Theoretically, the opposite MFE_{EL} on the fluorescence and phosphorescence result clearly exclude the formation based MFE_{EL} which claims that magnetic field can increase the formation rate of both singlet and triplet while their spin polarization are conserved. Practically, the fully tuning magnetic field effect on fluorescence and phosphorescence at the same time provide a potential application for novel magnetic field controlled organic optoelectronics devices.

7.2 Introduction

Under electrical excitation, only 25% singlet exciton can be formed in organic semiconductors and subsequently give the radiative emission[1,2]. Almost 75% triplet exicton are wasted through non-radiative emission because the triplet transition to ground state is spin forbidden, which limits the efficiency of organic material based light emitting devices (OLED) . To fully use the rest of 75% triplet, Baldo et al successfully activate the phosphorescence emission channel by introducing the strong spin orbital

coupling heavy metal complex PtOEP into a fluorescent host[20]. After that, most highly efficient OLED are based on the electrophosphorescence emission[105,106]. Magnetic field measurement has been used as a powerful tool to understand the formation and decay of excited states in OLED. Till now, most magnetic field studies focus on the fluorescence emission in OLED.. However, few attentions were paid on the magnetic field effect on the phosphorescence in OLED. Therefore, it is very important to investigate magnetic field effect on electrophosphorescence and relationship between magnetic field dependent fluorescence and phosphorescence. Kalinowski compared the magnetic field effect on the electrophosphorescence of idiridium and plantinum based heavy metal complex and contribute the different value of MFE_{EL} for the two phosphors comes from their different molecular structures[87]. Lupton monitored the magnetic field effect on the fluorescence and phosphorescence in a ladder–type poly(p-phenylene) (PhPPP)[103]. External magnetic field can increase both fluorescence and phosphorescence intensity at the same time, leading to positive fluorescence based MFE_{FEL} and phosphorescence based $MFE_{FEL.}$ Consequently, it was concluded that magnetic field can increase the both singlet and triplet formation rate while the spin polarization was conserved during the carrier recombination. Furthermore, Lupton also exclude the magnetic field dependent intersystem crossing between singlet and triplet during the carrier recombination, which usually predicts the increased singlet exciton formation together with decreased triplet formation. However, we should note that internal energy transfer between polymer segments may exists in this ladder polymer. If the energy transfer processes is involved, the increased phosphorescence may comes from the efficient Forest energy transfer from

the increase of singlet formation in the fluorescent segment followed by intersystem crossing from singlet to triplet on the heavy metal complex site. Our experimental results also showed that both positive MFE on the fluorescence and phosphorescence can be observed in a polymer fluorescent host and phosphorescent guest system where sufficient energy transfer occurs between fluorescent host and phosphorescent dopant[79]. Therefore, we need to re-examine the conclusion proposed by the Lupton that magnetic field increase the singlet and triplet formation at the same time.

7.3 Experimental

The organic phosphorescent material bis [2-(2'-benzothienyl)- pyridinato-N,C3'] iridium (III) (acetylacetonatonate) [$Btp_2Ir(acac)$] (Ir67) and fluorescent polyfluorene (PFO) was purchased from American Dye Source, and poly(9- vinylcarbazole) (PVK), poly(vinyl alcohol) (PVA), 2,9-Dimethyl-4,7-diphenyl-1,10-phenanthroline (BCP), were purchased from Sigma-Aldrich. All materials are used as received. Low weight concentration 1% $Btp_2Ir(acac)$ were mixed with PVK and PFO in chloroform, forming PVK: $Btp_2Ir(acac)$ and PFO: $Btp_2Ir(acac)$ composite solution. The composite films around 80 nm were spin cast on the pre-cleaned ITO substrates from the respective chloroform solution. PVA was first dissolved in deionized water facilitated by the heating solution at 70 ℃. To built double layer device, the PVA water solution were spin cast on the composite film with high spin coating speed 4000 rpm/sec to form thin second layer. PVA water solution cannot dissolve the PVK: $Btp_2Ir(acac)$ and PFO: $Btp_2Ir(acac)$ composite underlayer. The

aluminum (Al) electrode was prepared by thermal evaporation at a vacuum of 2×10^{-6} Torr. The magnetic field effect on the fluorescence and phosphorescence was measured at constant current mode (current density 20 mA/cm^2) for the OLED in liquid nitrogen temperature.

7.4 Results and Discussion

Before investigating the magnetic field effect on fluorescence and phosphorescence emission at the same time, we need to construct the fluorescence and phosphorescence coexisting system. One convenient method is to dope the appropriate concentration phosphorescent dye into fluorescent host matrix. If the concentration of phosphorescent dye is too high, most of exciton formed in the host matrix will be transferred to the dopant and thus we can only observe the fluorescence emission from the host. Otherwise, If the doping concentration of phosphorescent dye is too low, we cannot get the sufficient phosphorescence emission from the heavy metal complex. Here, we dope 1 wt % phosphorescent dye $Btp_2Ir(acac)$ into fluorescent polymer matrix PVK and PFO, from which we can observe decent the fluorescence from the host and phosphorescence from the dopant.

7.4.1 Both positive fluorescence and phosphorescence MFE

Figure 7. 1 (a) shows the electroluminescence spectrum from ITO/PVK+ $Btp_2Ir(acac)$ (1 wt %) /Al OLED. The short wavelength peaked at 400 nm is known as the fluorescence

emission from the PVK matrix. The long wavelength peaked at 617 nm is the characteristic phosphorescence emission from the heavy metal complex $Btp_2Ir(acac)$.

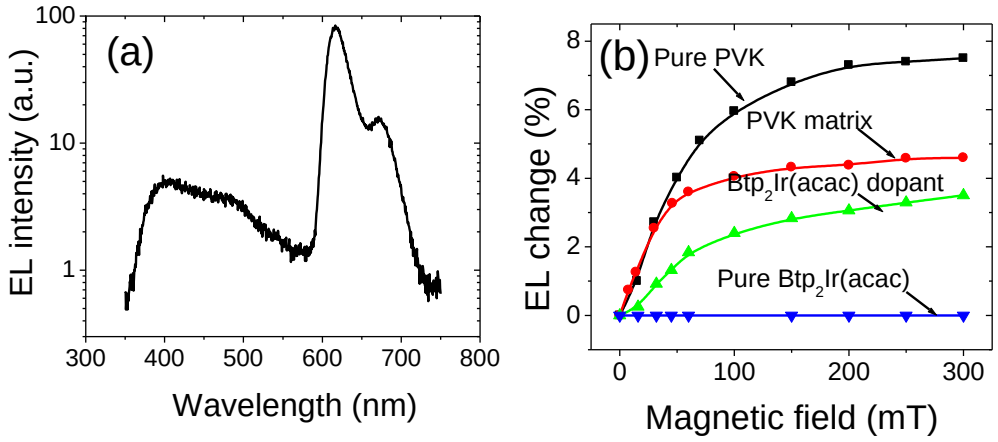

Figure 7.1 (a) Electroluminescence spectrum of ITO/PVK+ $Btp_2Ir(acac)$ (1 wt%)/ Al OLED (b) Fluorescence and phosphorescence based MFE from pure PVK , pure $Btp_2Ir(acac)$ and PVK+ $Btp_2Ir(acac)$ (1 wt%) composite

It can be seen in Figure 7.1 (b) that the fluorescence MFE_{FEL} from the PVK emission decreases from 7.6 % to 4.5 % after dispersing 1 wt % $Btp_2Ir(acac)$ into PVK polymer. This experimental result suggests that heavy metal complex $Btp_2Ir(acac)$ can enhance the spin orbital coupling of PVK: $Btp_2Ir(acac)$ composite. Subsequently, the enhanced spin orbital coupling can reduce the magnetic field sensitive ISC and cause the reduction of fluorescence based MFE_{FEL} from the PVK matrix. It is known that pure $Btp_2Ir(acac)$ complex doesn't show any magnetic field effect on the phosphorescence emission due to its strong spin orbital coupling. However, when 1 wt % $Btp_2Ir(acac)$ are dispersed into PVK matrix, a clear positive MFE_{PEL} about 3 % can be observed from the $Btp_2Ir(acac)$

dopant. This positive MFE_{PEL} indicates that magnetic field increased triplet exciton in the $Btp_2Ir(acac)$ dopant comes from the magnetic field increased singlet in the PVK matrix through long range Forster energy transfer process.

7.4.2 Positive fluorescence and negative phosphorescence MFE

We built a double layer ITO/PFO+$Btp_2Ir(acac)$ (1 wt%)/PVA (x nm)/Al device by inserting a second PVA layer between organic semiconductor layer and Al cathode. Figure 7.2 shows the magnetic field effect on the fluorescence from PFO matrix in double layer with different PVA thickness. After inserting a ultra-thin PVA layer x= 0.5 nm, the MFE_{FEL} on the fluorescence shows a significant increase from the 2.6% to 4.3 % compared to the single layer device. Further increasing the PVA thickness to 1 nm can enhance the MFE_{FEL} to a maximum value 8 %, which is almost three times as large as the MFE_{FEL} from single layer device. Next, we discuss the possibility for this observed large MFE. On one hand, the use of PVA layer can effectively reduce the heavy metal electrode effects on the spin orbital coupling strength near the cathode interface. As a result, external Zeeman splitting can overwhelm the internal magnetic interaction raised by spin orbital coupling and consequently facilitate the ISC from triplet states to singlet states, leading to a enhanced positive $MFE_{FEL.}$ Another possibility for this sharp increase of MFE_{FEL} maybe come from the increased electron-hole pair radius caused by inserting this thin PVA layer. Inserting a ultrathin PVA layer will modify the morphology near the electrode interface and hence tune the local electronic structure around the interface[107]. It is highly possible ulta-thin PVA can separate the correlated electron and hole as the spacer, and therefore enlarge the average electron-hole pair radius.

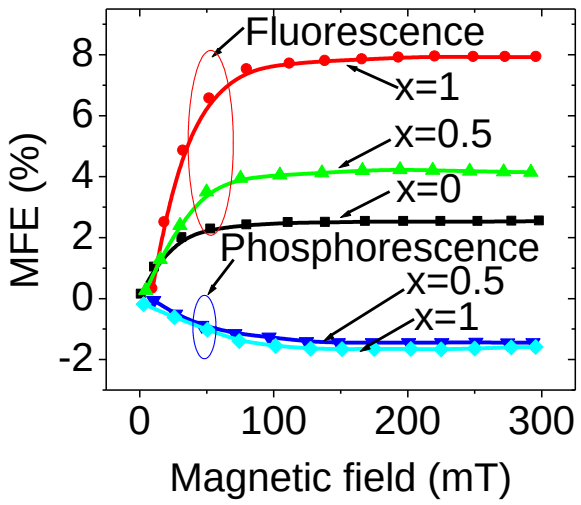

Figure 7.2 Magnetic field effect on the fluorescence (MFE_{FEL}) and the phosphorescence (MFE_{PEL}) from double layer ITO/PFO+ $Btp_2Ir(acac)$ (1 wt%)/ PVA (x nm)/Al devices with ultra-thin PVA film thickness.

When the average electron-hole pair radius is enlarged by the insertion of thin PVA, the exchange energy J will decrease dramatically with the increasing average radius, and promote the spin conversion from triplet to singlet excited states, and thus increase the singlet excited states population, leading to a increased positive $MFE_{FEL.}$ Meanwhile, we monitor the magnetic field effect on the phosphorescence emission shown in Figure 7.2. Compared with $MFE_{FEL,}$ magnetic field effect on the phosphorescence shows a negative MFE_{PEL} when the PVA thickness is 0.5 nm and 1 nm. This opposite sign of MFE_{FEL} and MFE_{PEL} is against the formation based MFE_{EL} theory which anticipate that magnetic field increase both the single and triplet formation rate. Nevertheless, the positive

MFE_{FEL} and negative MFE_{FEL} seems in a good accordance with magnetic field dependent ISC which predicts the magnetic field increase the singlet and decrease the triplet formation.

7.4.3 Negative fluorescence and positive phosphorescence MFE

In order to get the negative fluorescence and positive phosphorescence, we fabricate the multi-layer device with the structure ITO/PFO (60 nm)/BCP (15 nm)/$Btp_2Ir(acac)$ (30 nm)/PVA (3 nm)/ Al. In this type of device structure, we use 15 nm BCP layer to separate the PFO fluorescence emission with $Btp_2Ir(acac)$ phosphorescence emission. The interaction distance of Forster energy transfer is typical less than 10nm. Thus, 15 nm BCP is thick enough to remove the energy transfer influence between PFO layer and $Btp_2Ir(acac)$. Figure 7.3 (a) shows the electroluminescence spectrum in which the short wavelength regime from 400 nm to 600 nm is the fluorescence emission from PFO layer and longer wavelength peaked at 617 nm is the phosphorescence emission from $Btp_2Ir(acac)$ layer. We observe a negative fluorescence MFE_{FEL} and positive phosphorescence MFE_{PEL} measured at the constant current density 20 mA/cm^2 shown in Figure 7.3 (b). It should be noted that two emission layer PFO and $Btp_2Ir(acac)$ have different emission zone. The emission zone of PFO is close to the PFO/BCP interface, while the emission zone of $Btp_2Ir(acac)$ is located at $Btp_2Ir(acac)$/PVA interface.

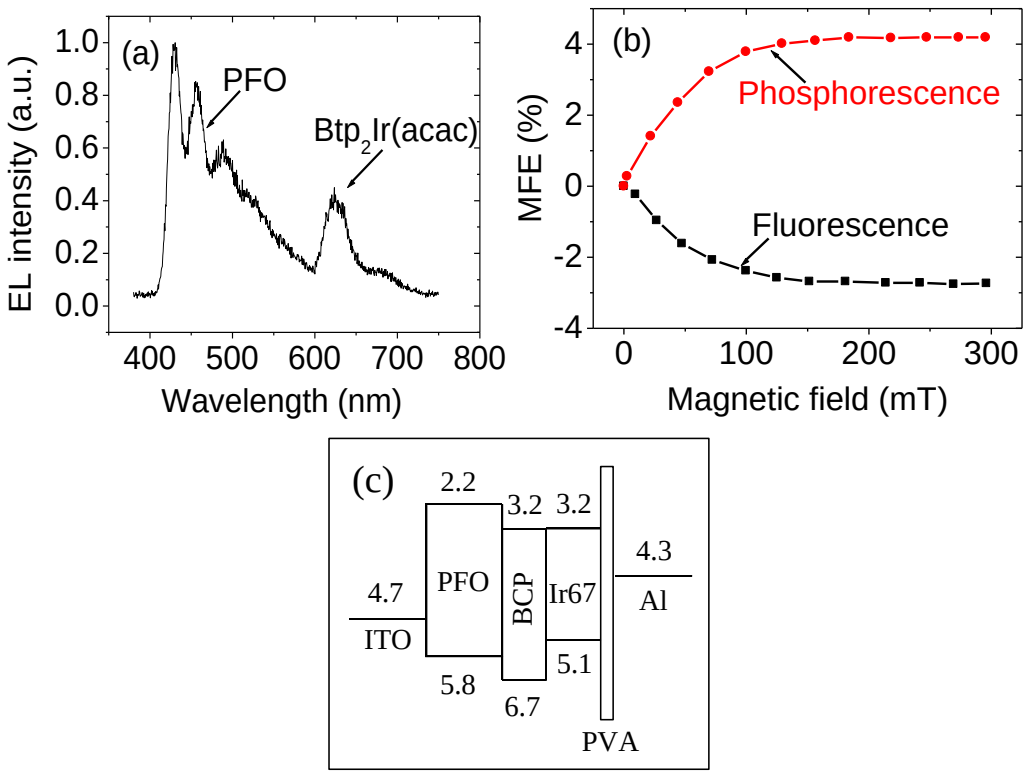

Figure 7.3 (a) Electroluminescence spectrum of multilayer ITO/PFO (60 nm)/BCP (15 nm)/$Btp_2Ir(acac)$ (30 nm)/PVA (3 nm)/Al device (b) Magnetic field effect on the fluorescence MFE_{FEL} and phosphorescence MFE_{PEL} from multi-layer device (c) Band diagram of ITO/PFO (60 nm)/BCP (15 nm)/$Btp_2Ir(acac)$ (30 nm)/PVA (3 nm)/Al

As seen from the band diagram shown in Figure 7.3 (c), there is a large energy offset between the HOMO of PFO and BCP. A large amount of holes will be confined at the PFO/BCP interface. As we discussed in previous Chapter 4, charge confinement at the interface will initiate significant triplet charge reaction. It is known that triplet charge reaction can dissociate the triplet excitons through Coulomb scattering and generate

secondary free charge carriers. The dissociated charge carriers can recombine into singlet and triplet through random capture. An external magnetic field can reduce the triplet charge reaction rate and subsequently reduce the singlet ratio, generating negative fluorescence MFE_{PEL}. However, the positive phosphorescence MFE_{PEL} may originate from the interface induced spin-spin interaction, which was discussed in Chapter 5. The inter-charge carriers spin-spin interaction at the short capture distance is in favor of the singlet spin configuration formation due to strong on site exchange energy. An external magnetic field can disturb the spin-spin interaction and generate more triplet excited states, leading to positive phosphorescence MFE_{PEL}.

7.4.4 Both negative fluorescence and phosphorescence MFE

In Figure 7.2, we have found that the insertion of a very thin insulating PVA layer can generate a positive MFE_{FEL} and negative MFE_{PEL} from the double layer device ITO/PFO+$Btp_2Ir(acac)$ (1 wt%)/PVA (x nm)/Al. It is interesting to find that both MFE_{FEL} and MFE_{PEL} will become negative after increasing PVA thickness up to 3 nm and 5 nm in Figure 7.4. This is the first time to observe both negative MFE for fluorescence and phosphorescence. Now, we discuss possible explanations for this dual negative MFE_{FEL} and MFE_{PEL}. Insulating PVA layer with wide energy bandgap can effectively act as a large energy barrier at the cathode interface and reduce the minority carrier injection. Increasing the PVA layer thickness will increase the injection potential barrier, which turn the bipolar injection toward a more unbalanced injection condition.

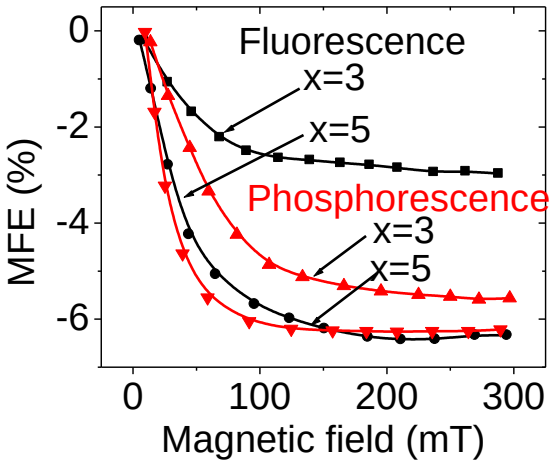

Figure 7.4 Magnetic field effect on the fluorescence (MFE_{FEL}) and the phosphorescence (MFE_{PEL}) from double layer ITO/PFO+ $Btp_2Ir(acac)$ (1 wt%)/ PVA (x nm)/Al devices at thicker PVA film thickness.

Unbalanced bipolar injection will facilitate the triplet charge reaction. Correspondingly, an external magnetic field can reduce the triplet charge reaction rate and redistribute the singlet and triplet ratio, leading to negative fluorescence based $MFE_{FEL.}$ Similarly, the negative fluorescence based MFE_{FEL} can be then reflected as a negative phosphorescence based in the $Btp_2Ir(acac)$ dopant through dominant Forester energy transfer from PFO matrix to the $Btp_2Ir(acac)$ molecules. Another possible explanation for both negative MFE_{FEL} and MFE_{PEL} is that an external magnetic field can increase the population of quenchers such as polaron or bipolaron which essentially contribute to the nonradiative quenching of fluorescence and phosphorescence emission. As a result, increased quenchers population can leads to the reduction of overall electroluminescence, leading

to both negative MFE_{FEL} and $MFE_{PEL.}$

7.5 Conclusion

In conclusion, we investigated the magnetic field effect on the fluorescence and phosphorescence emission by constructing the OLEDs which emit the fluorescence and phosphorescence at the same time. The fluorescence based MFE_{FEL} and phosphorescence based MFE_{PEL} can show the same sign or the opposite sign depending on the device structure. It was found that energy transfer and interface induced spin-spin interaction play an important role in tuning the sign of MFE_{FEL} and $MFE_{PEL.}$ Nevertheless, different sign of MFE_{FEL} and MFE_{PEL} are clearly against the formation based MFE that both singlet and triplet formation increases with the applied magnetic field. The simultaneously tuning fluorescence based MFE_{FEL} and phosphorescence based MFE_{PEL} provide the feasibility of magnetic field controllable high efficient optoelectronic devices.

CHAPTER 8

GIANT MAGNETIC FIELD EFFECTS ON ELECTROLUMINESCENCE IN ELECTROCHEMICAL CELLS

8.1 Abstract

Magnetic field effects occurring in functional materials are important experimental phenomena. Using magnetic field effects can lead to the development of magnetically controllable electronic, optic, and optoelectronic materials and devices. Here we report the giant magnetic field effects on the electroluminescence (MFE_{EL}) (> 400 %) in liquid states by using the triplet tris(2, 2'-bipyridyl) ruthenium(II)–tripropylamine based electrogenerated chemiluminescence system based on facile-controllable electrochemical co-reaction. We find that Lorentz force effects is, as a primary mechanism, mainly accountable for the observed giant MFE_{EL} through magnetic field-sensitive ion transport and magnetic field-sensitive diffusion-layer thickness based on angle, voltage, and concentration dependences. Furthermore, our experimental results suggest that magnetic body force due to magnetization of paramagnetic radicals and triplet-charge reaction due to interaction between triplet excited states and radicals are counted as a secondary mechanism in the observed giant MFE_{EL}. Clearly, our experimental results present a new methodology to develop giant magnetic field effects in liquid states by combining Lorentz force effects and electrochemical reaction.

8.2 Introduction

Recently, there has been growing interests to the magnetic field effects that an external magnetic field can substantially change photoluminescence[31], electroluminescence[32], photocurrent[29,30], and electrical current[32,33]in nonmagnetic organic semiconducting

materials with potential applications for magneto-electronics, magneto-optics, and magneto-optoelectronics. In general, three types of magnetic field effects can be observed based on inter-charge spin-spin interaction, spin-dependent excited processes, and Lorentz force effects. First, when inter-charge spin-spin interaction occurs, an external magnetic field can perturb the spin-spin interaction and consequently changes singlet and triplet formation ratios in excited states [61]and carrier mobilities[42,44]in charge transport. Second, an external magnetic field can affect spin-dependent excited processes such as singlet-triplet intersystem crossing, triplet-charge reaction, and triplet-triplet annihilation after the formation of excited states by involving in spin moment conservation required for those excited processes and essentially changes both singlet and triplet ratios in excited states and carrier densities in charge transport. Third, an external magnetic field can introduce a Lorentz force exerted on moving charged species and changes charge transport and consequently generates magnetocurrent (MC)[108,109]. In principle, magnetic field effects can occur in both solid and liquid states. In liquid states early experimental studies have found that electrochemical reaction can show considerable magnetic field effect on the electroluminescent intensity (MFE_{EL}) with the amplitude less than 30 % [110]with suggested mechanism of triplet-charge reaction and triplet-triplet annihilation[111-114]. In this paper, we report giant MFE_{EL} with the magnitude larger than 400 % in liquid states by using conveniently controllable electrochemical co-reaction in aqueous solution based on Lorentz force effects.

8.3 Experimental

The cyclic voltammograms measurements were performed by using a Basi Epsilon electrochemical work station with three-electrode configuration. The two planar platinum (Pt) foil plates with the area of 7 mm×10 mm were used as working and auxiliary electrodes. The working and counter electrodes are glassy carbon electrodes. The Ag/AgCl was used as the reference electrode. The chemicals including Tris(2-2'-bipyridly) dichlororuthenium(II) hexahydrate ($Ru(bpy)_3Cl_2 \cdot 6H_2O$), Rubrene, and coreactant tripropylamine (TPrA) used in this work were purchased from Aldrich. $Ru(bpy)_3$ based energy-deficient electrochemical system contains $Ru(bpy)_3^{2+}$ (1mM), TPrA (0.1 M), and phosphate buffer solution (0.2 M) dissovled in deionized water. Rubrene based energy-sufficient electrochemical system contains Rubrene (1mM), TPrA (0.1 M), and (0.1 M) $TBAPF_6$ as the working electrolyte dissolved in DMF solution. The liquid solutions were degassed by using nitrogen gas before the measurements. The magnetic field effects were measured with two planar-electrode configuration for convenient angle dependence studies. Specifically, the electrochemical cell was placed in a magnetic field generated by an electrical magnet. The MFE_{EL} and MC are defined as a relative change in intensity in electroluminescence and current caused by applied magnetic field. The magnitude of magnetic field effects is given by the relative change in percentage: $MFE=\frac{S_B - S_0}{S_0} \times 100\%$, where S_B and S_0 are the signal intensities with and without the magnetic field. The electroluminescence and electrical current were recorded by using Jobin Yvon Fluorolog III spectrometer equipped with an optical fiber connection and electrometer Keithley 2400. It should be noted that the Lorentz force-driven convection effects can be accumulated in the measurements of magnetic field

effects, which can significantly enhance the MFE_{EL}. In this work, the MFE_{EL} and MC were measured within the initial stable period with the corresponding experimental errors of about 10 % and 1 % for MFE_{EL} and MC, respectively.

8.4 Results and discussion

Figure 8.1 (a) shows the electrogenerated chemiluminescence spectrum based on the triplet emission from the tris(2-2'-bipyridyl) ruthenium(II) ($Ru(bpy)_3^{2+}$) molecules. The spectral peak at 610nm is the characteristic of phosphorescence from the triplet states of the $Ru(bpy)_3^{2+}$ through electrochemical reaction[115] shown in Equation 8.1.

$$Ru(bpy)_3^{3+} + TPrA^{\bullet} \longrightarrow Ru(bpy)_3^{2+*} + products \qquad \text{(Equation 8.1)}$$

The $Ru(bpy)_3^{2+}$ metal chelate complex has been widely studied for electrogenerated chemiluminescence due to its high luminescence efficiency and electrochemical stability in aqueous solvents[116,117]. The tripropylamine (TPrA) works as an efficient coreactant with $Ru(bpy)_3^{2+}$ upon electrochemical oxidation via a catalytic route. In general, the electrogenerated chemiluminescence can be divided into energy-deficient and energy-sufficient systems through triplet and singlet route emission[118], respectively. The early studies have indicated that the oxidation of TPrA by electrogenerated $Ru(bpy)_3^{3+}$ is the dominant process in the generation of chemiluminescence[119]. The free energy released from ion annihilation is insufficient to generate singlet excited states but enough to populate the triplet excited states of the $Ru(bpy)_3^{2+*}$, which is so called energy-deficient system.[118]

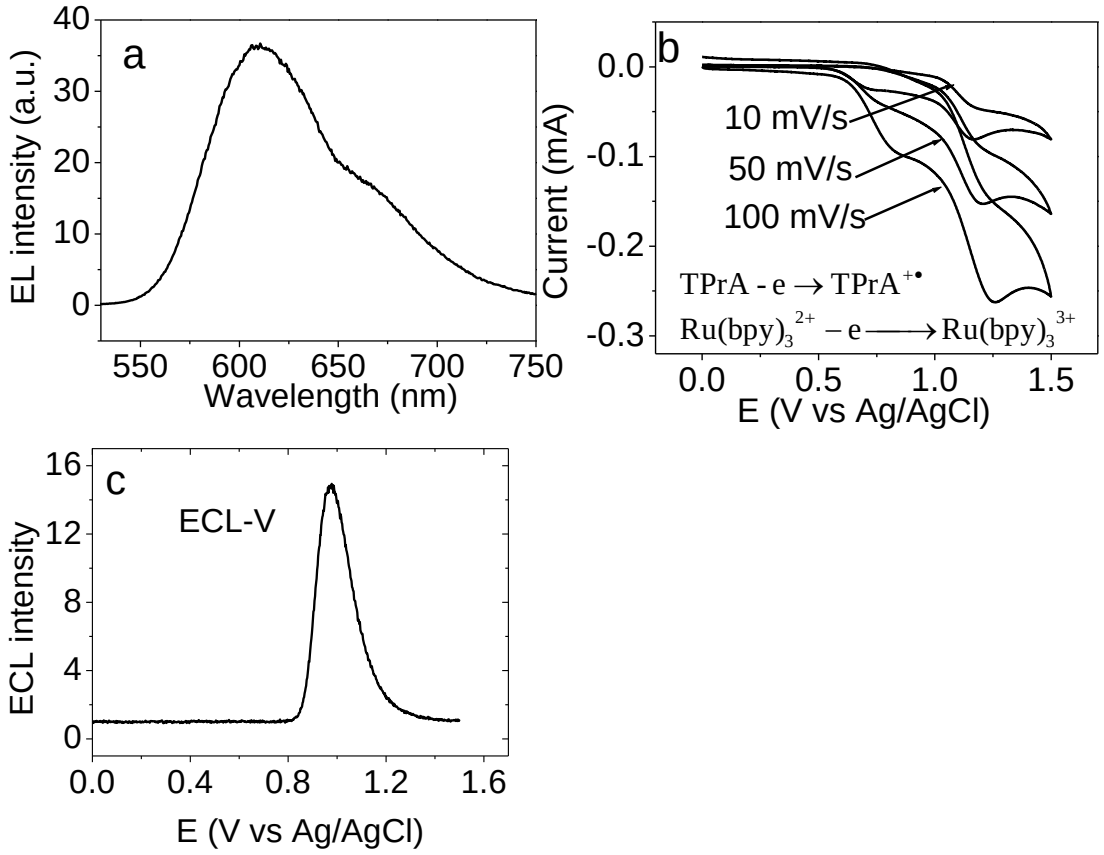

Figure 8.1 Electrogenerated chemiluminescence (ECL) characteristics for triplet $Ru(bpy)_3$ based energy-deficient electrochemical system with three-electrode configuration. a: ECL spectrum. b: Cyclic voltammograms at different scan rates. c: ECL intensity-voltage characteristic.

On contrast, when the free energy through the electron transfer is available to directly generate the singlet excited states, the system is named as energy-sufficient system.

It should be noted that the radical ions are effective quenchers to the generated excited states through triplet-charge reaction in electrochemical reaction.[120] Therefore, the triplet excited states of $Ru(bpy)_3^{2+*}$ can be quenched through triplet-charge reaction due to the long lifetime to generate non-radiative emission instead of the radiative emission as described in Equation 8.2.

$$Ru(bpy)_3^{2+*} + ion \xrightarrow{Quenching} Ru(bpy)_3^{2+} \qquad \text{(Equation 8.2)}$$

The cyclic voltammograms measurements indicate two separated oxidation peaks at different scan rates with three-electrode configuration as shown in Figure 8.1 (b), which confirms the required electrochemical reaction occurring in the electrogenerated chemiluminescence. The first peak corresponds to the direct oxidation of TPrA at the electrode at a potential of about 0.75 V vs the reference electrode: Ag/AgCl. The second peak has a potential of 1.15 V where $Ru(bpy)_3^{2+}$ is oxidized at the electrode at a scan rate of 10 mV/s. As the scan rate increases, both oxidation current and cyclic voltammogram peaks increase to higher values. It has been also found that the increase in scan rate can reduce the diffusion-layer thickness and subsequently increases the electrical current[121]. It can be seen from the voltage-electroluminescence characteristics (Figure 8.1 (c)) that the electroluminescence intensity clearly increases and then decreases with increasing the electrical potential voltage. This result implies that the generation of electroluminescence is a mass transport-limited process in the electrochemical reaction. In mass transport-limited process the reaction species are required to diffuse to the reaction interface around the positive electrode to produce the precursors for the generation of electrogenerated chemiluminescence. These precursors subsequently react in a spatially

restricted emission zone within the diffusion layer near the electrode. The observed electroluminescence intensity is essentially determined by mass transport of reactive species at given reaction rate to produce the light. Therefore, the electroluminescence intensity increases when mass transport can provide enough reaction species for light generation near the electrode. However, the electroluminescence intensity drops down when the mass transport is limited. With the two-electrode electrochemical configuration in an external magnetic field (Figure 8.2 a), the $Ru(bpy)_3$ based electrochemical reaction generates giant MFE_{EL} at different electrical biases. The MFE_{EL} reaches 400 % at 3.3 V in the magnetic field of 700 mT (Figure 8.2 b), which is the largest MFE_{EL} so far for any electroluminescent system. No significant magnetic response appears below 100 mT. We can see that the sign and magnitude of MFE_{EL} depend on the applied potential bias. At the 2.2 V bias, the electroluminescence intensity is monotonically quenched by an external magnetic field and no clear saturation was found at the higher magnetic field. The magnitude of MFE_{EL} drops down to a negative value of - 17% at external magnetic fields of 700 mT. We should note that the two-electrode setup, specially designed to conveniently measure magnetic field effects, requires the turn-voltage of 1.9 V to initiate the electrochemiluminescence while the three-electrode setup needs the turn-on voltage of 0.8 V. However, this difference should not affect the mechanisms of magnetic field effects in the electrochemical co-reaction.

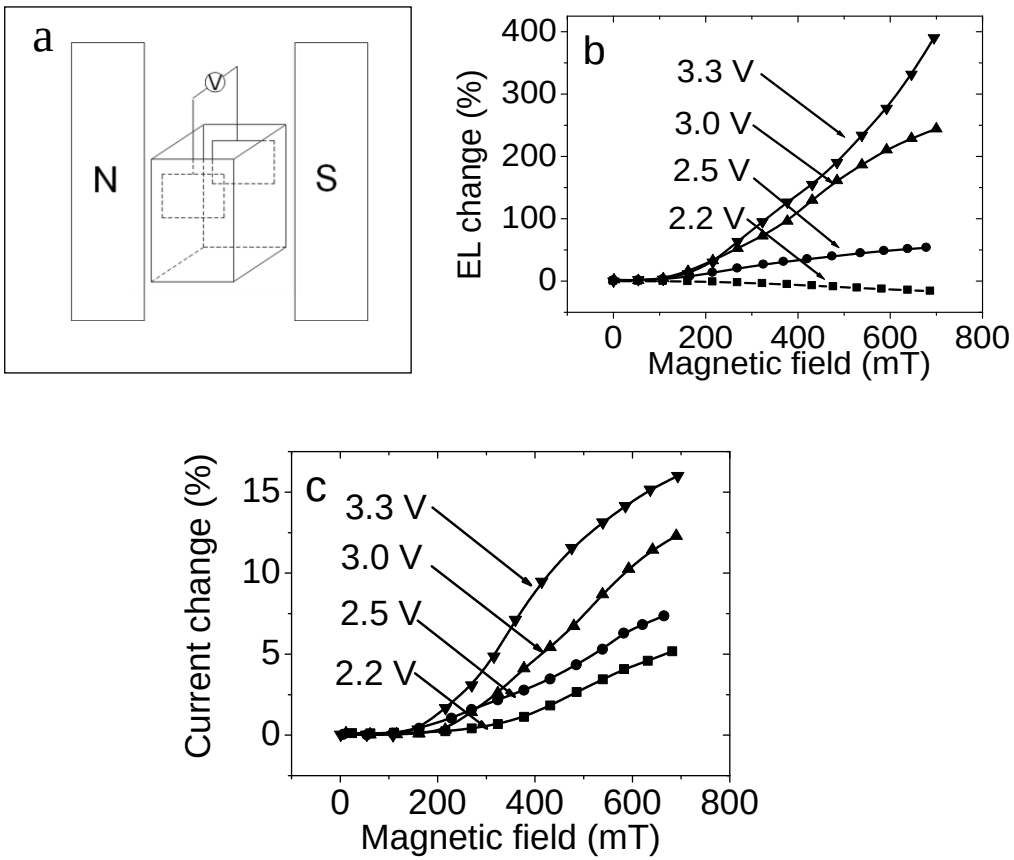

Figure 7.2 Electrogenerated chemiluminescence (ECL) characteristics for singlet $Ru(bpy)_3$-based energy-deficient electrochemical system. a: Experimental setup with two-electrode configuration for electrochemical cell placed in magnetic field. b: MFE_{EL} at different voltages. c: MC at different voltages.

Now we discuss the origin of the observed MFE_{EL} in electrogenerated chemiluminescence. Early studies have found that an external magnetic field can increase

the electroluminescence intensity in electrochemical reaction[110,111] and this positive MFE_{EL} was attributed to the magnetic field-sensitive triplet-charge reaction[112,114]. The spin physics in solid states indicates that an external magnetic field can perturb the spin interaction between a triplet excited state and a charge, and consequently reduce the triplet-charge reaction-rate constant. In the absence of magnetic field, the triplet excited states: $Ru(bpy)_3^{2+*}$ are partially quenched by the excess radical ions through triplet-charge reaction. With applied magnetic field, this quenching process is reduced by decreasing the reaction-rate constant[47,49], and subsequently increases the triplet light emission in the electrochemical reaction. As a result, a positive MFE_{EL} can be observed in triplet energy-deficient electrochemical system based on triplet-charge reaction. However, magnetic field-sensitive triplet-charge reaction only contributes to a few tenth of a percent MFE_{EL}[110,112] in liquid states, as reported previously. In addition, it has been also observed in solid states that an external magnetic field can only change triplet-charge reaction by a few percents indicated by the studies of magnetic field effects of photocurrent[68,122]. Clearly, the triplet-charge reaction is not sufficient to generate the giant MFE_{EL} observed from our $Ru(bpy)_3^{2+}$ system. Here, we suggest that Lorentz force effects to be a dominant process accountable for the observed giant positive and negative MFE_{EL}. It is known that the liquid solution flux containing charged species can experience the Lorentz force, which is given by the cross product of current and magnetic field: $\mathbf{F} = \mathbf{I} \times \mathbf{B}$. This Lorentz force can result in a convection for reactive species around the diffusion layer in the liquid solution through momentum transfer between reactive ions and solvent molecules[123,124], as shown in Figure 8.3 a. As a consequence, the Lorentz

force can generate two effects through convection: increasing ion penetration through diffusion layer and decreasing the diffusion-layer thickness in the electrochemical reaction. On one hand, increasing ion penetration can enhance the electrochemical reaction and thus increase the electroluminescence intensity, leading to a positive MFE_{EL}, namely transport-based positive MFE_{EL}. On the other hand, decreasing the diffusion-layer thickness can reduce the entire electrochemical reaction volume. Since the light-emitting zone occurs within the diffusion layer, the reduction of diffusion-layer thickness can decrease the electroluminescence intensity and essentially generate a negative MFE_{EL}, namely volume-based negative MFE_{EL}. At high voltage, the high density of reactive species generates a thicker diffusion layer. With a thicker diffusion layer, the reduction in diffusion-layer thickness due to Lorentz force effects can be limited as compared to the entire diffusion-layer thickness, minimizing volume-based negative MFE_{EL}. On the other hand, at high voltage with higher ion concentration the increase in ion penetration caused by Lorentz force through mass transport can be more significant (as suggested by larger MC at high voltage), which leads to a dominant transport-based positive MFE_{EL}. As a result, a high voltage can generate an overall positive MFE_{EL} (Figure 8.2 b). At low voltage, the low density of reactive species produces a thinner diffusion layer. With a thinner diffusion layer, the reduction in diffusion-layer thickness due to Lorentz force effects can be significant relative to entire diffusion-layer thickness, maximizing volume-based negative MFE_{EL}. On the other hand, at low voltage with lower ion concentration the increase in ion penetration caused by Lorentz force trough mass transport is less significant (as suggested by lower MC at low voltage), which minimizes

transport-based positive MFE_{EL}. Therefore, a low voltage can lead to an overall giant negative MFE_{EL} (Figure 8.2 b). Furthermore, it should be noted that the mass transport driven by Lorentz force can generate magnetocurrent (MC) in electrochemical reaction. This is because, when a magnetic field is applied, the Lorentz force (**I**×**B**) exerting on the charged reaction species yields a momentum transfer to the solvent molecules and enhances the charge transport and the electrical current in the electrochemical reaction. It should be further noted that changing electrical potential can affect the density of reactive ions and consequently changes the total mass transport based on Lorentz force effects, leading to a modification on MC amplitude. At high voltage, high-density reactive ions can more significantly increase electrical current, as compared to low-density reactive ions at low voltage, due to Lorentz force-driven mass transport. It can be clearly seen in Figure 8.2 c that the MC reaches 16 % at 3.3 V and 5 % at 2.2 V in the magnetic field of 700 mT. This voltage dependence of MC further suggests that the Lorentz force effects are mainly accountable for the observed magnetic field effects. To verify Lorentz force effects in observed MFE_{EL}, we investigate the angle dependence of MFE_{EL} in the electrochemical reaction with two-planar electrodes by changing the angle from $\theta = 0^{\circ}$, where the **I** and **B** are parallel, to $\theta = 180^{\circ}$, where the **I** and **B** are anti-parallel. Figure 8.3 b shows a significant angle dependence of MFE_{EL} when the current direction is changed relevant to the orientation of applied magnetic field. Clearly, the maximal positive MFE_{EL} is observed at $\theta = 90^{\circ}$. The maximal MC is also shown at $\theta = 90^{\circ}$. In general, angle dependence of magnetic field effects can be attributed to Lorentz force effects. It is clear that the Lorentz force ($\mathbf{I} \times \mathbf{B}$) can largely changes its value at different angles (θ)

and therefore affects the ion transport in the generation of electroluminescence through convection in the electrochemical reaction cell (Figure 8.3 a). As a result, applied magnetic field can cause different responses in electroluminescence and electrical current as the angle θ changes. This phenomenon has been observed in the magnetic field dependence of electrical current in electrochemical reaction reported in early publications. To further confirm the Lorentz effects, we studied the effects of concentration of reactive species on the MFE_{EL} in the electrochemical co-reaction. Figure 8.3 c shows the MFE_{EL} from triplet $Ru(bpy)^{2+*}$ emission as a function of co-reactant TPrA concentration from 0.01 M to 0.3 M. We can see that the MFE_{EL} largely increases with increasing the co-reactant TPrA concentration. In addition, increasing TPrA concentration can also enhance the electrogenerated chemiluminescence intensity (inset in Figure 8.3 c). These concentration results indicate that the Lorentz force can generate larger mass transport through convection and consequently enhances the MFE_{EL} as the reactive mass increases. As a result, the experimental results from voltage, angle, and concentration dependences indicate that the Lorentz force effects can generate giant MFE_{EL} in liquid states based on electrochemical reaction. In addition, we should note that, if applied magnetic field is considerably non uniform within electrochemical cell, the magnetic field gradient associated with this non-uniformity can generate magnetic field effects on electrochemical reaction and consequently change electrochemiluminescence intensity.

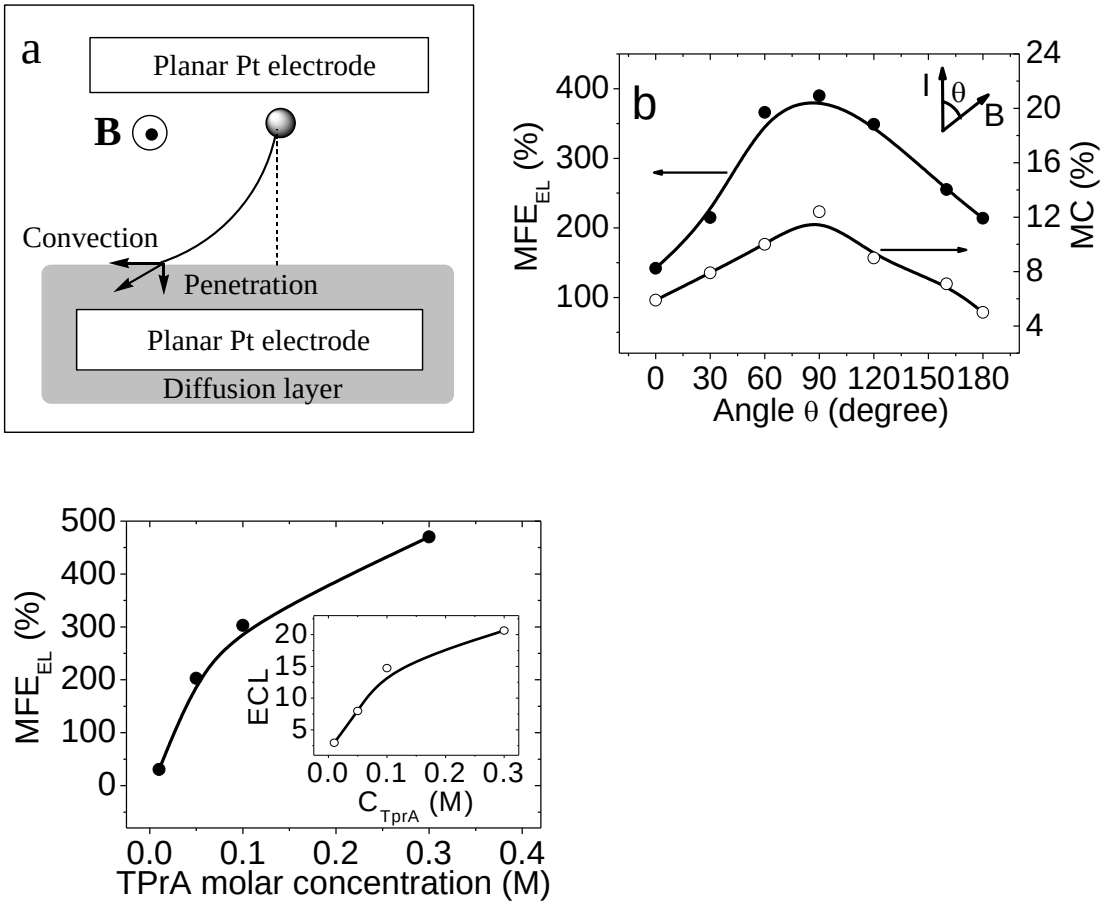

Figure 8.3 Schematic for Lorentz force effects and angle dependence results for magnetic field effects. a: Schematic for Lorentz force effects: liquid convection and ion penetration in electrochemical cell placed in a magnetic field (700 mT). b: Angle dependence of MFE_{EL} and MC in triplet $Ru(bpy)_3$ based electrochemical system c: MFE_{EL} at different TPrA molar concentrations for $\theta = 90^{\circ}$. Inset shows ECL intensity versus TPrA molar concentration.

We have examined this issue by manually changing the non-uniformity through adjusting the distances (2 mm and 5 mm) between two platinum electrodes with our setup (two magnetic poles with diameter of 65 mm and distance of 20 mm; two platinum electrodes with size of 7 mm x10 mm and adjustable distance from 2 mm to 5 mm). We observed that changing the distance between two platinum electrodes does not appreciably change the angle dependence of magnetic field effects. This means that the non-uniformity of magnetic field does not have considerable contribution to the observed magnetic field effects.

Now we discuss the remaining MFE_{EL} at $\theta = 0^{\circ}$ and 180°. It is noted that considerable MFE_{EL} remains when **I** and **B** are parallel or anti-parallel (Figure 8.3 b). In principle, this remaining MFE_{EL} can be due to two different possibilities: magnetic body force due to magnetization of paramagnetic ions [125] and triplet-charge reaction due to interaction between triplet excited states and radicals. First, applied magnetic field can magnetize paramagnetic radicals and generate magnetic body force at $\theta = 0^{\circ}$ and 180°. This magnetic body force can contribute to mass transport through momentum transfer between solvent molecules and paramagnetic radicals, leading to a remaining MFE_{EL} at $\theta = 0^{\circ}$ and 180°. In particular, this magnetic body force can push paramagnetic radicals away and toward the diffusion layer when the **I** and **B** are parallel and anti-parallel, respectively, generating a relatively smaller and larger remaining MFE_{EL} at $\theta = 0^{\circ}$ and 180°, as supported by the experimental results shown in Figure 3 b. Second, triplet excited states can react with radicals to produce triplet-charge reaction with the consequence of quenching light emission from triplet excited states. This triplet-charge

reaction can lead to a positive MFE_{EL} on triplet emission at $\theta = 0^{\circ}$ and 180° when applied magnetic field reduces the triplet-charge reaction. Early studies have suggested that the triplet-charge reaction can generate a positive MFE_{EL} with the amplitude less than 30 %. As a result, it can be suggested that magnetic body force-based mass transport and triplet-charge reaction can generate the remaining MFE_{EL} at $\theta = 0°$ and 180°. It should be further noted that magnetic force-based mass transport and triplet-charge reaction can also generate the remaining MC at $\theta = 0°$ and 180°. This is because magnetic force-driven mass transport and triplet-charge reaction can increase ion transport within diffusion layer and generate a positive MC. Nevertheless, our experimental studies indicate that the Lorentz force effects function as a main mechanism to generate giant positive and negative MFE_{EL} in electrochemical reaction. The magnetic body force and triplet-charge reaction play a secondary role in the generation of giant MFE_{EL}.

Besides the energy-deficient system containing triplet $Ru(bpy)_3$ and TPrA, we also expanded the MEF_{EL} study to a singlet electrochemical system, namely energy-sufficient system based on Rubrene and coreactant TPrA to further investigate the origin of MFE_{EL} in the electroluminescence generated by electrochemical reaction. Figure 4 a shows the electroluminescence spectrum of singlet Rubrene-based system. The electroluminescence peak at 572 nm was observed, which is the characteristic fluorescence from the singlet excited states of Rubrene[126]. The cyclic voltammograms measured with three electrode configuration are shown as an inset in Figure 8.4 a.

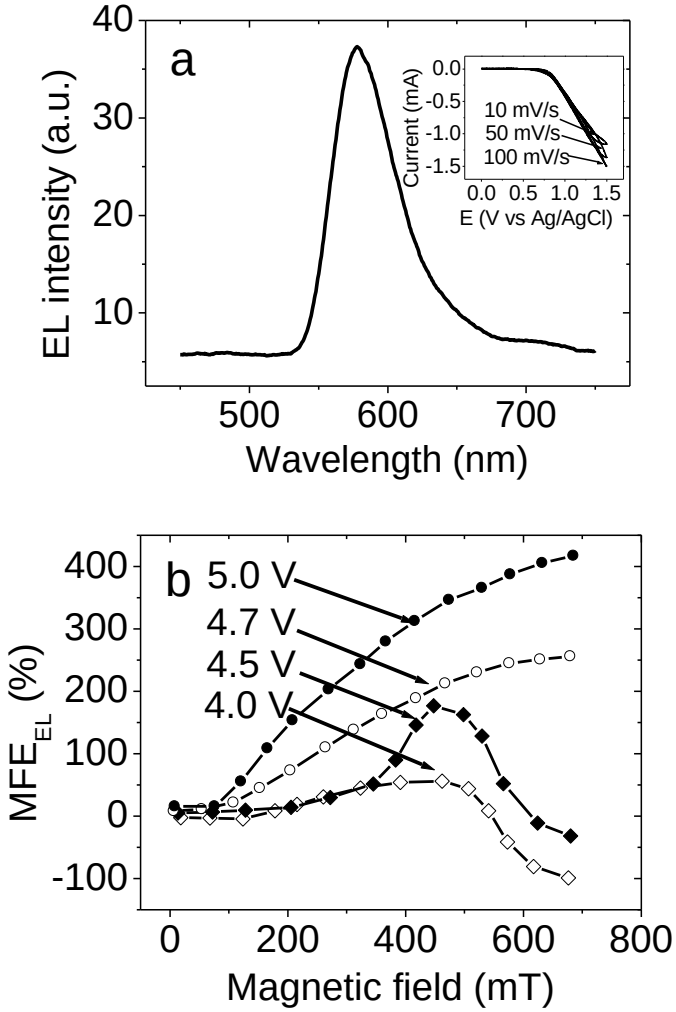

Figure 8.4 Electrogenerated chemiluminescence (ECL) characteristics for singlet Rubrene-based energy-sufficient electrochemical system. a: ECL spectrum (inset: Cyclic voltammograms). b: MFE_{EL} at different voltages.

Similar to the $Ru(bpy)_3$ system, the reaction in the Rubrene system comes from the charge transfer between oxidized rubrene$^+$ and neutral TPrA$^{\cdot}$ radicals. Unlike the excited states of $Ru(bpy)_3$ generated through the T route, the potential of TPrA$^{\cdot}$ radical is

sufficient to generate the singlet states of the Rubrene and produce the fluorescence via the S route. Early studies have indicated that negligible magnetic field effects should be observed through S route in the energy-sufficient system because of lacking significant triplet-charge reaction and triplet-triplet annihilation in singlet systems. Surprisingly, our singlet Rubrene-based system shows a giant MFE_{EL} in the electroluminescence generated by electrochemical reaction with two planar-electrode electrochemical configuration (Figure 8.4 b). At 5 V, the electroluminescence intensity monotonically increases with applied magnetic field, leading to giant MFE_{EL} of about 400% at the magnetic field of 700 mT. This result indicates that the transport-based positive MFE_{EL} is a dominant mechanism in the overall magnetic field effects at relative higher voltage (5 V) with higher ion concentration and thicker diffusion layer. At a lower voltage (4 V), the electroluminescence intensity slightly increases from 100 mT to 450 mT and then rapidly decreases. The maximal negative MFE_{EL} reaches - 100 % at 700 mT where the electroluminescence intensity is completely quenched by applied magnetic field. This result implies that the volume-based negative MFE_{EL} is a major mechanism in the overall magnetic field effects at relatively low voltage with lower ion concentration and thinner diffusion layer. In general, the observed MFE_{EL} can reflect the combination of transport-based positive MFE_{EL} and volume-based negative MFE_{EL} components based on Lorentz force-driven convection in electrochemical reaction. Because liquid viscosity can also affect the convection and then changes the interplay between transport-based positive MFE_{EL} and volume-based negative MFE_{EL}, singlet and triplet systems may exhibit slightly different behavior in MFE_{EL}. Here, we note that the singlet MFE_{EL} from the

Rubrene (Figure 8.4 b) follows a similar trend in voltage dependence as compared to the triplet MFE_{EL} from the $Ru(bpy)_3$ (Figure 8.2 b). Therefore, this giant singlet MFE_{EL} can exclude the possibility that the triplet-charge reaction and triplet-triplet annihilation play an important role in the observed MFE_{EL} in the liquid-state electroluminescence generated by electrochemical reaction.

8.5 Conclusion

In summary, we experimentally demonstrate giant magnetic field effects (> 400 %) in electrogenerated chemiluminescence based on co-reaction. The angle, voltage, and concentration dependences of magnetic field effect suggest that the Lorentz force-driven ion transport and the Lorentz force-dependent diffusion-layer thickness through liquid convection are mainly accountable for the observed giant MFE_{EL}, respectively. In addition, we find that the magnetic body force due to magnetization of paramagnetic radicals and the triplet-charge reaction due to interaction between triplet excited states and radicals can also contribute to giant magnetic field effects as a secondary mechanism. Furthermore, our experimental results indicate that the MFE_{EL} observed at different angles, concentrations, and voltages can be used to elucidate magnetic field-dependent mass transport, magnetization of paramagnetic radicals, and magnetic field-dependent triplet-charge reaction in electrochemical reaction. Moreover, rationally adjusting Lorentz force effects presents a new path way to develop giant magnetic field effects in liquid states based on electrochemical reaction.

CHAPTER 9 CONCLUSION

It has been found that an external magnetic field can substantially change the injection current, photoluminescence and electroluminescence intensity in organic semiconductors, leading to MR (MC), MFE_{PL} and MFE_{EL}. However, the origin of magnetic field effects still remains puzzling. Therefore, it requires careful discrimination of existing spin dependent processes in organic semiconductors and discovers the underlying mechanism for MFE_{EL} and MR.

We have investigated MFE_{PL} and MFE_{EL} from TPD:BBOT exciplex, which is one type of intermolecular excited states. Exciplex exhibits a clear positive MFE_{PL}, while MFE_{PL} is usually absent in intramolecular excited states. MFE_{PL} measurement indicates that magnetic field can only influence the intersystem crossing (ISC) at polaron pairs and exciplex state, but cannot affect the ISC in exciton state. The reason is because magnetic field sensitive ISC strongly depends on the electron-hole separation distance, which determine the exchange energy between singlet and triplet excited states. We successfully enhance the magnitude of MFE_{PL} and MFE_{EL} by increasing the electron-hole separation distance through material mixing and introducing electrical dipole-dipole interaction in TPD:BBOT exciplex composite film. These experimental results further support that magnetic field sensitive ISC contribute to the positive MFE_{PL} and $MFE_{EL.}$

The mechanism of negative MFE_{EL} has been studied through modifying the triplet density on PFO matrix by using Dexter energy transfer, charge confinement by using band offsets and exciton charge ratio by unbalanced bipolar injection in OLEDs. Two possible mechanisms TTA and TCR in the generation of negative MFE_{EL} were considered. We found that increasing triplet exciton density can lead to a negative MFE_{EL}

in electro-fluorescence in the PFO matrix by transferring the high-density triplets formed in the charge-trapping $Ir(mppy)_3$ molecules to the PFO matrix through Dexter process. In addition, confining triplet excitons and charges by using double-layer structure can clearly generate a negative MFE_{EL} in electro-fluorescence. Finally, we found that enhancing the TCA can directly generate negative MFE_{EL} by unbalancing the bipolar injection of ITO/PFO/PMMA/Al OLED. Therefore TCA can be attributed to a dominant process for negative MFE_{EL} in organic semiconducting materials.

We found that both MC and MFE_{EL} were observed from the strong spin orbital coupling iridium complex after introducing the insulating blocking layer PVA. However, introducing organic semiconductor/semiconductor interface didn't show any appreciable magnetic response. This interface induced MC and MFE_{EL} can be attributed to magnetic field perturbed spin-spin interaction of inter-charge carriers confined at semiconductor/insulating interface.

We compared the MC and MFE_{EL} from two similar heavy metal dyes: $Ir(ppy)_3$ and $Ir(ppy)_2(acac)$ with strong spin-orbital coupling but different electrical dipole moments. $Ir(ppy)_3$ with strong electrical dipole moment shows negligible MC and MFE_{EL}. However, $Ir(ppy)_2(acac)$ with weak dipole moment exhibits appreciate MC and MFE_{EL}. The experimental results suggest that the electrical dipole-dipole interaction can change the MC and MFE_{EL} from capture-based regime, where charge carriers are captured through spin-dependent process at short distance, to intersystem crossing-based regime, where charge carriers are captured through spin random process at long distance.

Not limited to the studies of magnetic effect on fluorescence (MFE_{PEL}), we also extend our investigation to magnetic effect on the phosphorescence (MFE_{FEL}) in OLED at the same time. The sign of MFE_{FEL} and MFE_{PEL} can be tuned either in the same direction or in opposite direction by controlling the intersystem crossing, energy transfer, triplet charge reaction and spin-spin interaction. The opposite MFE_{EL} on the fluorescence and phosphorescence result clearly exclude the formation based MFE_{EL} which claims that magnetic field can increase the formation rate of both singlet and triplet while their spin polarization are conserved. Fully tuning MFE_{PEL} and MFE_{FEL} provide the feasibility of novel high efficient magneto-optoelectronic devices.

At last, we discovered the giant MFE_{EL} (over 400 %) in electrochemical cells. The Lorentz force is mainly accountable for the observed giant MFE_{EL} through magnetic field-sensitive ion transport and magnetic field-sensitive diffusion-layer thickness based on angle, voltage, and concentration dependences. Furthermore, our experimental results suggest that magnetic body force due to magnetization of paramagnetic radicals and triplet-charge reaction due to interaction between triplet excited states and radicals are counted as a secondary mechanism in the observed giant MFE_{EL}.

Therefore, our research works elucidate the underlying mechanism of MFE_{EL} and MR in organic semiconductors. Theoretical understanding of these magnetic field effects can provide us a powerful tool to reveal critical spin-dependent useful and non-useful progresses in organic light emitting and photovoltaic systems, leading to the development of high efficient organic light emitting diode and photovoltaics. Practically, we successfully realized the complete tuning of both sign and amplitude of MFE_{EL} and MR,

leading to the development of novel multifunctional organic magneto-optoelectronics devices.

REFERENCE

[1] R. H. Friend , R. W. Gymer, A. B. Holmes, J. H. Burroughes, R. N. Marks, C. Taliani, D. D. C. Bradley, D. A. Dos Santos, J. L. Brédas, M. Lögdlund, and W. R. Salaneck. Electroluminescence in conjugated polymers. *Nature* **397**, 121-128 (1999).

[2] M. Pope, C. E. Swenberg, Electronic processes in Organic Crystals, 2nd edition, Oxford University Press, Oxford 1999.

[3] C. W. Tang and S. A. Van Slyke, Organic electroluminescent diodes. *Appl. Phys. Lett.* **51**, 913-915 (1987).

[4] L. S. Hung, C. H. Chen, Recent progress of molecular organic electroluminescent materials and devices. *Materials Science and Engineering R* **39,** 143-222 (2002).

[5] C. W. Tang, Two-layer organic photovoltaic cell. *Appl. Phys. Lett.* **48,** 183-185(1986).

[6] G. Yu, J. Cao, J. C. Hummelen, F. Wudl, & A. J. Heeger, Polymer Photovoltaic cells: Enhanced Efficiencies via a Network of Internal Donor-Acceptor Heterojunctions. *Science* **270**, 1789-1791 (1995) .

[7] H. Koezuka, A. Tsumura and T. Ando, Field-effect Tansistor with polythiphoene thin film. *Synth. Met.* **18**, 699-704(1987).

[8] Y. M. Sun, Y. Q. Liu and D. B. Zhu, Advances in organic field-effect transistors, *J. Mater. Chem.* **15**, 53-65 (2005).

[9] J. H. Burroughes, D. D. C. Bradley, A. R. Brown, R. N. Marks, K. Mackay, R. H. Friend, P. L. Burns and A. B. Holmes, Light-emitting diodes based on conjugated polymers, *Nature* **347**, 539-541(1990).

[10] D. Braun and A. J. Heeger, Visible light emission from semiconducting polymer diodes, *Appl. Phys. Lett.* **58**, 1982-1984(1991).

[11] S. M. Sze , Physics of Semiconductor Devices, Wiley, New York, 1981.

[12] A. J. Campbell, D. D. C. Bradley, and D. G. Lidzey, Space-charge limited conduction with trips in poly(phenylene vinylene) light emitting diodes. J. Appl. Phys. **82,**6326-6342(1997).

[13] V. C. Sudar, J. Zaumseil, V. Podzorov, E. Menard, R. L. Willett, T. Someya, M. E. Gershenson, J. A. Rogers, Elastomeric Transistor Stamps: Reversible Probing of Charge Transport in Organic Crystals. *Science* **303**, 1644-1646 (2004).

[14] V. Coropceanu, J. Cornil, D. A. S. Filho, Y. Olivier, R. Silbey and J. L. Bredas

Charge Transport in Organic Semiconductors. *Chem. Rev.* **107**, 926-952 (2007).

[15] M. A. Baldo, D. F. O'Brien, M. E. Thompson, and S. R. Forrest, Excitonic singlet-triplet ratio in a semiconducting organic thin film. *Phys. Rev. B* **60**, 14422 -14428 (1999).

[16] Y. Cao, I. D. Parker, G. Yu, C. Zhang, and A. J. Heeger, Improved quantum efficiency for electroluminescence in semiconducting polymers, *Nature* **397**, 414-417(1999).

[17] Z. Shuai, D. Beljonne, R. J. Silbey and J. L. Bredas, Singlet and Triplet Exciton Formation Rates in Conjugated Polymer Light-Emitting Diodes, *Phys. Rev. Lett.* 84, 131-134 (2000).

[18] J. S. Wilson, A. S. Dhoot, A. J. A. B. Seeley, M. S. Khan, A. Köhler and R. H. Friend, Spin-dependent exciton formation in π-conjugated compounds, *Nature* **413**, 828-831(2001).

[19] M. Wohlgenannt, K. Tandom, S. Mazumdar, S. Ramasesha, and Z. V. Vardeny, Formation cross-sections of singlet and triplet excitons in π conjugated polymers, *Nature* 409, 494-497(2001).

[20] M. A. Baldo, D. F. O'Brien, Y. You, A. Shoustikov, S. Sibley, M. E. Thompson and S. R. Forrest, Highly efficient phosphorescent emission from organic electroluminescent devices. *Nature* **395**, 151-154 (1998).

[21] C. Adachi, M. A. Baldo, M. E. Thompson and S. R. Forrest, Nearly 100% internal phosphorescence efficiency in an organic light emitting device. *J. Appl. Phys.* **90**, 5048-5051 (2001).

[22] Y. Kawamura, K. Goushi, J. Brooks, J. J. Brown, H. Sasabe and C. Adachi, 100% phosphorescence quantum efficiency of Ir(III) complexes in organic semiconductor films. *Appl. Phys. Lett.* **86**, 071104 (2005).

[23] I. Bergenti, V. Dediu, E. Arisi, T. Mertelj, M. Murgia, A. Riminucci, G. Ruani, M. Solzi, C. Taliani, Spin polarized electrodes for organic light emittind diodes, Org. Electron. **5**, 309(2004).

[24] W. J. M. Naber and W. G. V. D. Wiel, Organic spintronics. *J. Phys. D: Appl. Phys.* **40,** R205-R228 (2007).

[25] A. R. Rocha, V. M. Garcia-Suarez, S. W. Bailey, C. J. Lambert, J. Ferrer, and S. Sanvito, Towards molecular spintronics. *Nat Mater* **4**, 335-339 (2005).

[26] Z. H. Xiong, D. Wu, Z. V. Vardeny and J. Shi, Giant magnetoresistance in organic spin-valves. *Nature* **427**, 821 (2004).

[27] U. E. Steiner and T. Ulrich, Magnetic-field effects in chemical-kinetics and related phenomena.*Chem. Rev.* **89**, 51-147 (1989).

[28] I. V. Khudyakov, Y. A. Serebrennikov, and N. J. Turro, Spin-orbit coupling in free-radical reactions: on the way to heavy elements. *Chem. Rev.* **93**, 537-570(1993).

[29] E. L. Frankevich, A. A. Lymarev, I. Sokolik, F. E. Karasz, S. Blumstengel, R. H. Baughman, and H. H. Horhold, Polaron-pair generation in poly(phenylene vinylenes) *Phys. Rev. B* **46**, 9320-9324 (1992).

[30] E. Frankevich, A. Zakhidov, K.Yoshino, Y. Maruyama, and K.Yakushi, Photoconductivity of poly (2,5-diheptyloxy-p-phenylene vinylene) in the air atmosphere: Magnetic-field effect and mechanism of generation and recombination of charge carriers. *Phys. Rev. B* **53**, 4498 (1996).

[31] F. Ito, T. Ikoma, K. Akiyama, A. Watanabe, S. Tero-Kubota, Carrier Generation Process on Photoconductive Polymer Films as Studied by Magnetic Field Effects on the Charge-Transfer Fluorescence and Photocurrent. *J. Physic. Chem B* **109**, 8707-8717 (2005).

[32] J. Kalinowski, M. Cocchi, D. Virgili, P. Di Marco, and V. Fattori, Magnetic field effects on emission and current in Alq_3-based electroluminescent diodes. *Chem. Phys. Lett.* **380**, 710-715 (2003).

[33] T. L. Francis, O. Mermer, G. Veeraraghavan, and M. Wohlgenannt, Large magnetoresistance at room temperature in semiconducting polymer sandwich devices. New J. Phys. **6**, 8 (2004).

[34] O. Mermer, G. Veeraraghavan, T. L. Francis, Y. Sheng, D. T. Nguyen, M. Wohlgenannt, A. Kohler, M. K. Al-Suti, and M. S. Khan, Large magnetoresistance in nonmagnetic pi-conjugated semiconductor thin film devices. *Phys. Rev. B* **72**, 12 (2005).

[35] O. Mermer, G. Veeraraghavan, T. L. Francis, and M. Wohlgenannt, Large magnetoresistance at room-temperature in small-molecular-weight organic semiconductor sandwich devices. *Solid State Commun.* **134**, 631 (2005).

[36] J. D. Bergeson, V. N. Prigodin, D. M. Lincoln, and A. J. Epstein, Inversion of magnetoresistance in organic semiconductors. *Phys. Rev. Lett.* **100,** 067201 (2008).

[37] B. Hu and Y. Wu, Tuning magnetoresistance between positive and negative values in organic semiconductors. *Nat. Mater.* **6**, 985-991(2007)

[38] V. N. Prigodin, J. D. Bergeson, D. M. Lincoln, and A. J. Epstein, Anomalous room temperature magnetoresistance in organic semiconductors. *Synth. Met.* **156**, 757-761

(2006).

[39] P. Desai, P. Shakya, T. Kreouzis, and W. P. Gillin, Magnetoresistance and efficiency measurements of Alq_3-based OLEDs. *Phys. Rev. B* **75**, 094423 (2007).

[40] P. Desai, P. Shakya, T. Kreouzis, and W. P. Gillin, The role of magnetic fields on the transport and efficiency of aluminum tris(8-hydroxyquinoline) based organic light emitting diodes. J. Appl. Phys. **102**, 073710 (2007).

[41] P. Desai, P. Shakya, T. Kreouzis, and W. P. Gillin, Magnetoresistance in organic light-emitting diode structures under illumination. *Phys. Rev. B* **76,** 235202 (2007).

[42] P. A. Bobbert, T. D. Nguyen, F. W. A. van Oost, B. Koopmans, and M. Wohlgenannt, Bipolaron mechanism for organic magnetoresistance. Phys. Rev. Lett. **99**, 216801 (2007).

[43] W. Wagemans, F. L. Bloom, and P. A. Bobbert, A two- bipolaron model for organic magnetoresistance. J. Appl. Phys. 103, 07F303 (2008).

[44] F. L. Bloom, M. Kemerink, W. Wagemans, and B. Koopmans, Sign Inversion of Magnetoresistance in Space-Charge Limited Organic Devices. *Phys. Rev. Lett.* **103**, 066601 (2009).

[45] M. Wohlgenannt, Z. V. Vardeny, Spin-dependent exciton formation rates in π-conjugated materials. *J. Phys. Conden. Matter* **15**, R83-R107 (2003).

[46] R. C. Johnson, R. E. Merrifield, P. Avakian, and R. B. Flippen, Effects of Magnetic Fields on the Mutual Annihilation of Triplet Excitons in Molecular Crystals. *Phys. Rev. Lett.* **19**, 285-287 (1967).

[47] V. Ern and R. E. Merrifield, Phys. Rev. Lett. **21**, 609 (1968). Magnetic field effect on triplet exciton quenching in organic crystals. *Phys. Rev. Lett.* **21**, 609-611 (1968).

[48] R. C. Johnson and R. E. Merrifield, Effects of Magnetic Fields on the Mutual Annihilation of Triplet Excitons in Anthracene Crystals. *Phys. Rev. B* **1**, 896-902 (1970).

[49] M.Wittmer and I. Zschokkegranacher, Exciton-charge carrier interactions in the electroluminescence of crystalline anthracence. *J. Chem. Phys.* **63**, 4187-4194 (1975).

[50] R. Belaid, T. Barhoumi, L. Hachani, L. Hassine, and H. Bouchriha, Magnetic field effect on recombination light in anthracene crystal. *Synth. Met.* **131**, 23-30 (2002).

[51] R. Liu, Y. Zhang, Y. L. Lei, P. Chen, and Z. H. Xiong, Magnetic field dependent triplet-triplet annihilation in Alq(3)-based organic light emitting diodes at different temperatures. *J. Appl. Phys.* **105** , 093719 (2009).

[52] F. J. Wang, H. Bassler, and Z. V. Vardeny, Magnetic Field Effects in pi -Conjugated Polymer-Fullerene Blends: Evidence for Multiple Components. *Phys. Rev. Lett.* **101**, 236805 (2008).

[53] C. Garditz, A. G. Muckl and M.Colle, Influence of an external magnetic field on the singlet and triplet emissions of tris-(8-hydroxyquinoline)aluminum(III) (Alq_3). *J. Appl. Phys.* **98**, 104507 (2005).

[54] A. R. B. M.Yusoff, W. J. da Silva, J. P. M. Serbena, M. S. Meruvia, I. A. Hummelgen, Very high magnetocurrent in tris-(8-hydroxyquinoline) aluminum-based bipolar charge injection devices. *Appl. Phys. Lett.* **94,** 253305 (2009).

[55] T. D. Nguyen, Y. Sheng, J. Rybicki, M. Wohlgenannt, M. Magnetic field-effects in bipolar, almost hole-only and almost electron-only tris-(8-hydroxyquinoline) aluminum devices. *Phys. Rev. B* **77**, 235209 (2008).

[56] J. Yang, K. C. Gordon, Organic light emitting devices based on exciplex interaction from blends of charge transport molecules. *Chem. Phys. Lett.* **375**, 649-654(2003).

[57] M. Chandross, S. Mazumdar, S. Jeglinski, X. Wei, Z. V. Vardeny, E. W. Kwock, and T. M. Miller, Excitons in poly(para-phenylenevinylene). *Phys. Rev. B* **50**, 14702-14705 (1994).

[58] B. A. Gregg, Toward a Unified Treatment of Electronic Processes in Organic Semiconductors. *J. Phys. Chem.* B **108**, 17285-17289 (2004).

[59] C. Doubleday, N. J.Turro, J. F.Wang, Dynamics of flexible triplet biradicals. *Accounts of Chemical Research **22,*** 199-205(1989).

[60] A. Köhler, J. S. Wilson and R. H. Friend, Fluorescence and Phosphorescence in Organic Materials. *Adv. Mater.* **14**, 701-70, (2002).

[61] B. Hu, L.Yan, and M. Shao, Magnetic-Field Effects in Organic Semiconducting Materials and Devices. *Adv. Mater.* **21**, 1500-1516 (2009).

[62] U. Werner and H. Staerk, Magnetic Field Effect in the Recombination Reaction of Radical Ion Pairs: Dependence on Solvent Dielectric Constant. *J. Phys. Chem.* **99**, 248-254 (1995).

[63] Y. Tanimoto, K. Hasegawa, N. Okada, M. Itoh, K. Iwai, K. Sugioka, F. Takemura, Magnetic Field Effects on the Intra- and Intermolecular Excipiex Fluorescence of Phenanthrene and Dimethylaniline. *J. Phys. Chem.***93**, 3586-3594 (1989).

[64] N. Kh. Petrov, V. N. Borisenko, A. V. Starostin and M. V. Alfimov, Polar Molecular Clusters Produced upon Photoinduced Electron Transfer in an Intermolecular

Exciplex in Binary Solvents. *J. Phys. Chem.* **96**, 2901-2903(1992).

[65] C. F. Madigan, V. Bulovic, Solid State Solvation in Amorphous Organic Thin Films. *Phys. Rev. Lett.* **91**, 247403(2003).

[66] Y. Wu, and B. Hu, Metal electrode effects on spin-orbital coupling and magnetoresistance in organic semiconductor devices. *Appl. Phys. Lett.* **89**, 203510 (2006).

[67] G. Veeraraghavan, T. D. Nguyen, Y. G. Sheng, ö. Mermer and M.Wohlgenannt, An 8 x 8 pixel array pen-input OLED screen based on organic magnetoresistance. *IEEE Trans. Electron Devices* **54**, 1571-1577 (2007).

[68] Z. Xu and B. Hu, Photovoltaic Processes of Singlet and Triplet Excited States in Organic Solar Cells. *Adv. Funct. Mater.* **18**, 2611-2617 (2008).

[69] H. Zang, Z. Xu, B. Hu, Magneto-Optical Investigations on the Formation and Dissociation of Intermolecular Charge-Transfer Complexes at Donor−Acceptor Interfaces in Bulk-Heterojunction Organic Solar Cells. *J. Phys. Chem. B* **114**, 5704-5709 (2010).

[70] Y. Iwasaki, T. Osasa, M. Asahi, & M. Matsumura, Y. Sakaguchi, T. Suzuki, Fractions of singlet and triplet excitons generated in organic light-emitting devices based on a polyphenylenevinylene derivative. *Phys. Rev. B* **74**, 195209 (2006).

[71] R. G. Kepler, J. C. Caris, P. Avakian and E. Abramson, Triplet excitons and Delayed Fluorescence in Anthracene Crystals. *Phys. Rev. Lett.* **10**, 400 (1963).

[72] R. P. Groff, R. E. Merrifield, A. Suna and P. Avakian, Magnetic Hyperfine Modulation of Dye-Sensitized Delayed Fluorescence in an Organic Crystal. *Phys. Rev. Lett.* **29**, 429-431 (1972).

[73] A. H. Davis, K. Bussmann, Large magnetic field effects in organic light emitting diodes based on tris(8-hydroxyquinoline aluminum) (Alq_3)/N, N'-Di(naphthalene-1-yl)-N, N' diphenyl-benzidine (NPB) bilayers. *J. Vac. Sci. Technol. A* **22**, 1885-1891 (2004).

[74] Y. Zhang, R. Liu, Y. L.Lei, and Z. H. Xiong, Low temperature magnetic field effects in Alq_3-based organic light emitting diodes. *Appl. Phys. Lett.* **94**, 083307 (2009)

.

[75] A. Endo, K. Suzuki, T. Yoshihara, S. Tobita, M.Yahiro, C. Adachi, Measurement of photoluminescence efficiency of Ir(III) phenylphridine derivatives in solution and solid-state films. *Chem. Phys. Lett*. **460**, 155-157 (2008).

[76] M. Sudhakar, P. I. Djurovich, T. E. Hogen-Esch, and M. E. Thompson,

Phosphorescence Quenching by Conjugated Polymers. *J. Am. Chem. Soc.* **125**, 7796-7797 (2003).

[77] H. H. Liao, H. F. Meng, S. F. Horng, W. S. Lee, J. M. Yang, C. C. Liu, J. T. Shy, F. C. Chen, C. S. Hsu, Triplet exciton energy transfer in polyfluorene doped with heavy metal complexes studied using photoluminescence and photoinduced absorption. *Phys. Rev. B.* **74**, 245211 (2006).

[78] Z. G. Yu, Spin-Orbit Coupling, Spin Relaxation, and Spin Diffusion in Organic Solids. *Phys. Rev. Lett.* **106**, 106602 (2011).

[79] Y. Wu, Z. H. Xu, B. Hu, J. Howe, Tuning magnetoresistance and magnetic-field-dependent electroluminescence through mixing a strong-spin-orbital-coupling molecule and a weak-spin-orbital-coupling polymer. *Phys. Rev. B* **75**, 035214 (2007).

[80] O. Bolton, K. Lee, H. J. Kim, K. Y. Lin, J. S. Kim, Activating efficient phosphorescence from purely organic materials by crystal design. *Nature chemistry* **3**, 205-210 (2011).

[81] Y. Wu, B. Hu, J. Howe, Morphology-dependent exciton emission and energy transfer in fluorine-polymer-related fluorescent and phosphorescent composite films spin cast from a mixture of two dissimilar organic solvents. *J. Appl. Phys.* **98**, 103510 (2005).

[82] X. Yang, D. Neher, D. Hertel, T. K. Däubler, T. K. Highly Efficient Single-Layer Polymer Electrophosphorescent Devices. *Adv. Mater.* **16**, 161-166 (2004).

[83] F.-C. Chen, S.-C. Chang, G. He, S. Pyo, Y. Yang, M. Kurotaki, J. Kido, Energy transfer and triplet exciton confinement in polymeric electrophosphorescent devices. *Journal of Polymer Science Part B: Polymer Physics* **41**, 2681-2690 (2003).

[84] I. A. Howard, M. Hodgkiss, X. P. Zhang, K. R. Kirov, H. A. Bronstein, C. K. Williams, R. H. Friend, S. Westenhoff, N. C. Greenham, Charge Recombination and Exciton Annihilation Reactions in Conjugated Polymer Blends. *J. Am. Chem. Soc.* **132**, 328-335 (2009).

[85] Y. Luo, H. Aziz, Correlation Between Triplet-Triplet Annihilation and Electroluminescence Efficiency in Doped Fluorescent Organic Light-Emitting Devices. *Adv. Funct. Mater.* **20**, 1285-1293 (2010).

[86] J. B. Birks, Organic Molecular Photophysics (Wiley, London, 1975).

[87] J. Kalinowski, M. Cocchi, D. Virgili, V. Fattori, P. Di. Marco, Magnetic field effects on organic electrophosphorescence. *Phys. Rev. B* **70**, 205303 (2004).

[88] X. J. Xu, S. Y. Chen, G. Yu, C. A. Di, H. You, D. G. Ma, Y. Q. Liu, High-Efficiency Blue Light-Emitting Diodes Based on a Polyphenylphenyl Compound with Strong

Electron-Accepting Groups. *Adv. Mater.* **19**, 1281-1285 (2007).

[89] M. A. Baldo, S. Lamansky, P. E. Burrows, M. E. Thompson, S. R. Forrest, Very high-efficiency green organic light-emitting devices based on electrophosphorescence. *Appl. Phys. Lett.* **75**, 4-6 (1999).

[90] C. Ganzorig, M. Fujihira, A possible mechanism for enhanced electrofluorescence emission through triplet-triplet annihilation in organic electroluminescent devices. *Appl. Phys. Lett.* **81**, 3137-3139 (2002).

[91] A. Köhler, H. Bässler, Triplet states in organic semiconductors. *Materials Science and Engineering: R* ***66***, 71-109 (2009).

[92] J. C. Bolinger, M. C. Traub, T. Adachi, P. F. Barbara, Ultralong-Range Polaron-Induced Quenching of Excitons in Isolated Conjugated Polymers. *Science* **331**, 565-567 (2011).

[93] W. Wagemans, A. J. Schellekens, M. Kemper, F. L. Bloom, P. A. Bobbert, and B. Koopmans, Spin-Spin interaction in Organic Magnetoresistance Probed by Angle-Dependent Measurements. Phys. Rev. Lett. 106, 196802 (2011).

[94] S. Difley, D. Beljonne, and T. Van Voorhis, On the singlet-triplet splitting of geminate electron-hole pairs in organic semiconductors. *J. Am. Chem. Soc.* **130**, 3420-3427(2008).

[95] V. Shrotriya, Y. Yang, Capacitance-voltage characterization of polymer light emitting diodes. J. Appl. Phys. **97**, 054504 (2005).

[96] Y. Sheng, T. D. Nguyen, G. Veeraraghavan, O. Mermer, M. Wohlgenannt, S. Qiu, and U. Scherf, Hyperfine interaction and magnetoresistance in organic semiconductors. *Phys. Rev. B* **74**, 045213 (2006).

[97] T. D. Nguyen, Y. G. Sheng, J. Rybicki, G. Veeraraghavan, and M. Wohlgenannt, Magnetoresistance in pi-conjugated organic sandwich devices with varying hyperfine and spin-orbit coupling strengths, and varying dopant concentrations. *J. Mater. Chem.* **17**, 1995-2001(2007).

[98] T. D. Nguyen, G. H. Markosian, F. J. Wang, L. Wojcik, X. G. Li, E. Ehrenfreund and Z. V. Vardeny, Isotope effect in spin response of π-conjugated polymer films and devices. *Nat Mater* **9**, 345-352(2010).

[99] J. Kalinowski, W. Stampor, J. Szmytkowski, D. Virgili, M. Cocchi, V. Fattori and C. Sabatini. Coexistence of dissociation and annihilation of excitons on charge carriers in organic phosphorescent emitters. *Phys. Rev. B* **74**, 085316(2006).

[100] L. Onsager, Initial Recombination of Ions. *Phys. Rev.* **54**, 554-557(1938).

[101] S. Reineke, T. C. Rosenow, B. Lussem, and K. Leo, Improved High-Brightness Efficiency of Phosphorescent Organic LEDs Comprising Emitter Molecules with Small Permanent Dipole Moments. *Adv. Mater.* **22**, 3189-3193 (2010).

[102] U. Werner, H. Staerk, Estimation of the probability distribution of end-group distances of chain-linked electron donor-acceptor molecules and radical ion pairs: a Monte-Carlo approach. *J. Phys. Chem.* **97**, 9274-9279 (1993).

[103] M. Reufer, M. J. Walter, P. G. Lagoudakis, A. B. Hummel, J. S. Kolb, H. G. Roskos, U. Scherf, and J. M. Lupton, Spin-conserving carrier recombination in conjugated polymers *Nat Mater* **4**, 340-346 (2005).

[104] J. Kalinowski, W. Stampor, J. Mezyk, M. Cocchi, D. Virgili, V. Fattori, and P. D. Marco, Quenching effects in organic electrophosphorescence, *Phys. Rev. B* 66, 235321(2002).

[105] S. J. Su, E. Gonmori, H. Sasabe, J. Kido, Highly Efficient Organic Blue-and White-Light-Emitting Devices Having a Carrier- and Exciton-Confining Structure for Reduced Efficiency Roll-Off. *Advanced Materials* **20**, 4189-4194(2008).

[106] S. Reineke, F. Lindner, G. Schwartz, N. Seidler, K. Walzer, B. Lussem, K. Leo, White organic light-emitting diodes with fluorescent tube efficiency. *Nature* **459**, 234-238(2009).

[107] H. Odaka, Y. Okimoto, T. Yamada, H. Okamoto, M. Kawasaki, Y. Tokura, Control of magnetic-field effect on electroluminescence in Alq_3-based organic light emitting diodes. *Appl. Phys. Lett.* **88**, 123501 (2006).

[108] J. Lee, X. Gao, L. D. A. Hardy, and H. S. White, Influence of Magnetic Fields on the Voltammetric Response of Microelectrodes in Highly Concentrated Organic Redox Solutions. *J. Electrochem. Soc.* **142**, L90 (1995).

[109] S. R. Ragsdale, J. Lee, X. Gao, and H. S.White, Magnetic Field Effects in Electrochemistry. Voltammetric Reduction of Acetophenone at Microdisk Electrodes. *J. Phys. Chem.* **100**, 5913 (1996).

[110] L. R. Faulkner, H. Tachikawa, and A. J. Bard, Electrogenerated Chemiluminescence. VII. The Influence of an External Magnetic Field on Luminescence Intensity. *J. Am. Chem. Soc.* **94,** 691 (1972).

[111] L. R. Faulkner, A. J. Bard, Electrogenerated Chemiluminescence. IV. Magnetic Field Effects on the Electrogenerated Chemiluminescence of Some Anthracenes. *J. Am.*

Chem. Soc. **91**, 209 (1969).

[112] L. R. Faulkner, A. J. Bard, Magnetic Field Effects on Anthracene Triplet-Triplet Annihilation in Fluid Solutions. *J. Am. Chem. Soc.* **91**, 6495 (1969).

[113] H. Tachikawa, A. J. Bard, Effect of Concentration and Magnetic Field on Radical Ion (Wurster's Blue Cation and Benzoquinone Anion) Quenching of Anthracene Triplets in Fluid Solution. *Chem. Phys. Lett.* **26**,10 (1974).

[114] H.Tachikawa, A. J. Bard, , Electrogenerated Chemiluminescence Effect of Solvent and Magnetic Field on ECL of Rubrene Systems. *Chem. Phys. Lett.***26**, 246 (1974).

[115] J. K. Leland, M. J. Powell, Electrogenerated Chemiluminescence: An Oxidative-Reduction Type ECL Reaction Sequence Using Tripropyl Amine. *J. Electrochem. Soc.* **137**, 3127 (1990).

[116] I. Rubinstein, A. J. Bard, Electrogenerated Chemiluminescence. 37. Aqueous Ecl Systems Based on Ru(2,2'-bipyridine)$_3^{2+}$, and Oxalate or Organic Acids. *J. Am. Chem. Soc.* **103**, 512 (1981).

[117] B. A. Gorman, P. S. Francis, N. W. Barnett, Tris(2,2 '-bipyridyl)ruthenium(II) chemiluminescence. Analyst **131**, 616 (2006).

[118] A. J. Bard, *Electrogenerated chemiluminescence*, Marcel Dekker, Inc. New York **2004**.

[119] F. Kanoufi, Y. Zu, A. J. Bard, Homogeneous Oxidation of Trialkylamines by Metal Complexes and Its Impact on Electrogenerated Chemiluminescence in the Trialkylamine/Ru(bpy)$_3^{2+}$ System. *J. Phys. Chem. B* **105,** 210 (2001).

[120] G. J. Hoytink, , Electrochemiluminescence of Aromatic Hydrocarbons. *Discussions Faraday Soc.* **45**, 14 (1968).

[121] M. A. Prasad, M. V.Sangaranarayanna, Analysis of the diffusion layer thickness, equivalent circuit and conductance behaviour for reversible electron transfer processes in linear sweep voltammetry *Electrochimica Acta* **49**, 445 (2004).

[122] I. V.Tolstov, A. V. Belov, M. G. Kaplunov, I. K.Yakuschenko, N. G. Spitsina, M. M.Triebel, E. L. Frankevich, , On the role of magnetic field spin effect in photoconductivity of composite films of MEH-PPV and nanosized particles of PbS. *J. Lumines.* **112**, 368 (2005).

[123] O. Aaboubi, J. P. Chopart, J. Douglade, A. Olivier, C. Gabrielli, B.Tribollet, Magnetic Field Effects on Mass Transport. *J. Electrochem. Soc.* **137**, 1796 (1990).

[124] O. Lioubashevski, E. Katz, I. Willner, Magnetic Field Effects on Electrochemical

Processes: A Theoretical Hydrodynamic Model. *J. Phys. Chem. B***108**, 5778 (2004).

[125] O. Lioubashevshki, E. Katz, I. Willner, Effects of magnetic field directed orthogonally to surfaces on electrochemical processes, *J. Phys. Chem. C* **111**, 6024 (2007).

[126] R. Y. Lai, A. J. Bard, Electrogenerated Chemiluminescence. 70. The Application of ECL to Determine Electrode Potentials of Tri-n-propylamine, Its Radical Cation, and Intermediate Free Radical in MeCN/Benzene Solutions. *J. Phys. Chem. A*, **107**, 3335, (2003).

VITA

Ming Shao was born in Maanshan, Anhui Province, People's Republic of China in April, 1982. He attended the Huazhong University of Science and Technology in 1999, and received his Bachelor's Degree from the Department of Optoelectronic science and Engineering in 2003. After the graduation, he continued his graduate study in Shanghai University, Shanghai, China and earned his Master's Degree in Microelectronics and Solid State Electronics in 2006. His research area was organic electroluminescent devices and driving circuit. In August 2006, he attended the Department of Materials Science and Engineering, University of Tennessee, Knoxville for his Ph. D degree. He has been working on magnetic field controllable organic electronics.